A multinuclear (^{1}H, ^{13}C, ^{31}P and ^{195}Pt) magnetic resonance spectroscopy study of mixed ligand platinum(II) complexes with new *N,N*-dialkyl-*N'*-acyl(aroyl)thioureas as ligands.

by

Sibusiso Mtongana

Thesis presented in partial fulfilment of the requirements for the degree of

Master of Science at the **University of Stellenbosch**.

Supervisor: Professor Klaus R. Koch

December 2002

I, the undersigned, hereby declare that the work contained in this thesis is my own original work and that I have not previously in its entirety or in part submitted it at any university for a degree.

Abstract

Ligands of the type *N,N*-dialkyl-*N'*-acyl(aroyl)thiourea (HL), have been prepared in high yield via a "one-pot" synthesis, in two steps. These ligands were fully characterised by means of melting point measurement, elemental analysis, ^{1}H and $^{13}C\{^{1}H\}$ NMR spectroscopy. The molecular structure of *N,N*-diethyl-*N-4*-nitrobenzoylthiourea was determined by means of X-ray diffraction method. This ligand is monoclinic and crystallises in the space group $P2_1/c$ with a = 6.887(1) Å, b = 19.244(3) Å, c = 10.147(1) Å, β = 93.01(1)° and Z = 4.

The relative donor properties of sulphur and oxygen in these ligands were evaluated by treating *cis*-$[Pt(P^{n}Bu_3)_2Cl_2]$, in $CDCl_3$, directly in an NMR tube with an equimolar quantity of ligand. Until the addition of a base (triethylamine) to the solution, which result in mixed ligand-platinum(II) complexes, *cis*-$[Pt(P^{n}Bu_3)_2(L\text{-}S,O)]^{+}Cl^{-}$, no reaction takes place. The reactions were monitored mainly by means of $^{31}P\{^{1}H\}$ and $^{195}Pt\{^{1}H\}$ NMR spectroscopy. The magnetic equivalence of the ^{31}P atoms in *cis*-$[Pt(P^{n}Bu_3)_2Cl_2]$ is lifted once the ligand coordinates to the platinum(II) ion. The relative donor properties of sulphur and oxygen of the ligands are then indirectly evaluated by observing the $^{1}J(^{195}Pt\text{-}^{31}P)$ and $\delta(^{195}Pt)$ values of the mixed ligand-platinum(II) complexes. It was found that in general, the donicity of the oxygen atom and sulphur atom is enhanced as the ligand is varied from having electron withdrawing groups to having electron donating groups.

Platinum(II) chelates formed from the asymmetrically disubstituted *N,N*-dialkyl-*N'*-acylthioureas were synthesised in good yield and characterised by means of melting point measurement, elemental analysis, ^{1}H, $^{13}C\{^{1}H\}$ and $^{195}Pt\{^{1}H\}$ NMR spectroscopy. It was found that if the starting ligand exists as *E/Z* isomers, this isomerism is carried through to the resultant complexes.

The platinum(II) chelates of *N*-diisopropoxythiophosphoryl thioamide (**I**) and *N*-diisopropoxythiophosphoryl-*N'*-phenylthiourea (**II**) were synthesised in high yield and characterised fully by means of $^{31}P\{^{1}H\}$ NMR spectroscopy besides the usual characterisation methods. It was observed that the complex resulting from **I** is exclusively the *trans*-isomer as revealed by a single ^{31}P peak at 42.6 ppm with a $^{2}J(^{195}Pt\text{-}^{31}P)$ value of 119 Hz and a ^{195}Pt peak at -3923 ppm. The coordination chemistry of **II** significantly differs from that of **I** in that the platinum(II) chelates may either be exclusively *trans* or a mixture of *cis* and *trans*-isomers, depending on the mode of complex preparation. The $^{31}P\{^{1}H\}$ NMR spectrum revealed two ^{31}P peaks at 43.6 ppm with a $^{2}J(^{195}Pt\text{-}^{31}P)$ value of 106 Hz and at 44.5 ppm with a $^{2}J(^{195}Pt\text{-}^{31}P)$ value of 101 Hz for the *trans* and *cis*-isomers respectively. The existence of the two isomers is confirmed by the appearance of two ^{195}Pt peaks at -3964 ppm and -3956 ppm for the *trans* and the *cis*-isomers respectively. The molecular structures of the *trans* chelates resulting from both **I** and **II** were determined by means of X-ray diffraction methods. Both crystals are monoclinic and centrosymmetric with distorted square planarity around the platinum atom. The thiocarbonyl sulphur atoms are relatively strongly coordinated to the platinum(II) ion than the

thiophosphoryl sulphur atoms in both complexes, as revealed by shorter Pt-S(C) bond lengths than the Pt-S(P) bond lengths.

The platinum(II) chelates formed from **II** were also observed to isomerise in solution resulting in a mixture of *cis* and *trans*-isomers. The kinetics of the isomerisation of the *trans*-isomer to a mixture of *trans* and *cis*-isomers, in $CDCl_3$ was followed by means of $^{31}P\{^1H\}$ NMR spectroscopy. Equilibrium is reached in no less than 300 hours with an equilibrium constant of $8.53x10^{-1}$ at 25°C.

Treatment of *cis*-$[Pt(P^nBu_3)_2Cl_2]$, in $CDCl_3$, directly in an NMR tube with equimolar quantities of ligands, **I** and **II** also resulted in mixed ligand-platinum(II) complexes. These reactions afforded the evaluation of the relative sulphur-sulphur donor properties of the ligands. In this case, it was observed that the thiocarbonyl sulphur coordinates relatively stronger than the thiophosphoryl sulphur, which is consistent with the bond lengths obtained for the platinum(II) chelates of these ligands.

Samevatting

Ligande van die tipe *N,N*-dialkiel-*N'*-asiel(aroïel)tioureum (HL), is in hoë opbrengs in 'n twee-stap een-fles sintese berei. Die ligande is volledig deur middel van smeltpunt, elemente analise en ^{1}H en $^{13}C\{^{1}H\}$ kern magnetiese resonans spektroskopie gekarakteriseer. Die molekulêre struktuur van *N,N*-diëtiel-*N'*-*4*-nitrobensoïeltioureum is met behulp van X-straal diffraksie metings bepaal. Hierdie ligand is monoklinies en kristalliseer in 'n $P2_1/c$ puntgroep met a = 6.887(1) Å, b=19,244(3) Å, c=10.147(1) Å, B=93.01(1)° en Z = 4.

Die relatiewe donor eienskappe van swawel en suurstof in hierdie ligande is evalueer deur $CDCl_3$-oplossings van *cis*-$[Pt(P^nBu_3)_2Cl_2]$ in 'n KMR buis te behandel met 'n ekwimolare hoeveelheid ligand. Geen kompleksering vind plaas alvorens die basis tri-etielamien bygevoeg word nie, waarna gemengde ligand-platinum(II) komplekse ontstaan. Die reaksies is hoofsaaklik deur middel van $^{31}P\{^{1}H\}$ en $^{195}Pt\{^{1}H\}$ KMR spektroskopie gemoniteer. Na koordinasie van die ligand aan die platinum(II)-ioon is die ^{31}P atome in die resulterende kompleks nie meer magneties ekwivalent nie. Die waardes van $^{1}J(^{195}Pt\text{-}^{31}P)$ en $\delta(^{195}Pt)$ in die gemengde ligand-platinum(II) komplekse kan dan gebruik word om afleidings te maak in verband met die relatiewe donor eienskappe van die koordinerende swawel en suurstof atome. Daar is oor die algemeen gevind dat die donor eienskappe van die suurstof atoom en die

swawel atoom toeneem soos die ligand gevarieer word van een wat elektron-onttrekkende groepe bevat na een wat elektron-donerende groepe bevat.

Platinum(II) komplekse met asimetries di-gesubstitueerde *N,N*-dialkiel-*N'*-asieltioureums is in hoë opbrengs berei en gekarakteriseer deur middel van smeltpunt, elemente analise en ^{1}H, $^{13}C\{^{1}H\}$ en $^{195}Pt\{^{1}H\}$ KMR spektroskopie. Daar is bevind dat indien die ligand voorkom as *E/Z* isomere, die isomerisme ook in die resulterende komplekse voorkom.

Die platinum(II) komplekse van *N*-di-isopropoksitiofosforieltioamied (**I**) en *N*-di-isopropoksitiofosforiel-*N'*-fenieltioureum (**II**) is ook in hoë opbrengs berei en gekarakteriseer op die gewone manier, asook deur middel van $^{31}P\{^{1}H\}$ KMR spektroskopie. Die platinum(II) kompleks van **I** kom uitsluitlik as die *trans*-isomeer voor soos aangedui deur 'n enkele ^{31}P resonans by 42.6 dpm met 'n $^{2}J(^{195}Pt\text{-}^{31}P)$-waarde van 119 Hz, en 'n ^{195}Pt resonans by -3923 dpm. Die koordinasie chemie van **II** verskil beduidend van dié van **I** deurdat die platinum(II) kompleks van eersgenoemde óf uitsluitlik die *trans*-isomeer is, óf 'n mengsel van *cis*- en *trans*-isomere is, afhangend van die manier waarop die sintese uitgevoer word. In die geval waar beide isomere voorkom dui die $^{31}P\{^{1}H\}$ KMR spektrum twee pieke aan, een by 43.6 dpm met 'n $^{2}J(^{195}Pt\text{-}^{31}P)$-waarde van 106 Hz en een by 44.5 dpm met 'n $^{2}J(^{195}Pt\text{-}^{31}P)$-waarde van 101 Hz, vir die *trans*- en *cis*-isomere respektiewelik. Die voorkoms van twee isomere word verder bevestig deur die teenwoordigheid van twee ^{195}Pt pieke, by -3964 dpm en -3956 dpm vir die *trans*- en *cis*-isomere respektiewelik. Die molekulêre strukture van die *trans*-isomere vir beide **I** en **II** is deur middel van

X-straal diffraksie metings bepaal. Beide komplekse is monoklinies en sentrosimmetries met verwronge vierkantig planêre strukture om die platinum atoom. Korter Pt-S(C) bindingslengtes as Pt-S(P) bindingslengtes dui aan dat die tiokarboniel-swawel-atome sterker koordineer as die tiofosforiel-swawel-atome.

Daar is verder gevind dat die platinum(II) komplekse van **II** in oplossing isomeriseer om 'n mengsel van *cis*- en *trans*-isomere te gee. Die kinetika van isomerisasie van die *trans*-isomeer na 'n mengsel van *trans*- en *cis*-komplekse in $CDCl_3$ is bestudeer deur middel van $^{31}P\{^1H\}$ KMR spektroskopie. Ewewig word in 'n tydsbestek van nie minder as 300 uur nie bereik, met 'n ewewigskonstante van $8.53x10^{-1}$ by 25°C.

Die behandeling van $CDCl_3$-oplossings van *cis*-$[Pt(P^nBu_3)_2Cl_2]$ met ekwimolare hoeveelhede van die ligande **I** en **II**, in 'n KMR buis, het ook aanleiding gegee tot gemengde platinum(II) komplekse. Met behulp van hierdie reaksies is die relatiewe swawel-swawel donor eienskappe van die ligande ondersoek. Bindingslengtes in die komplekse van hierdie ligande dui aan dat die tiokarboniel-swawel sterker koordineer as die tiofosforiel-swawel.

Acknowledgements

I hereby would like to thank the following people and organisations for contributing to the success of my research work.

- Professor Klaus R. Koch for the continued guidance and support as my academic father from the days we were both at the University of Cape Town where I studied my undergraduate and B.Sc. (honours) degrees.
- PGM research group members, who in many ways have had input to my work, with their valuable comments and proof reading.
- Kubazali (to parents), nakusapho ngokubanzi, ndibulela kakhulu ngendima eniyidlalileyo ekundikhuthezeni nasekundixhaseni kwade kwalapha.
- Sasol and the National Research Foundation (NRF) for financial support.

Thank you.

Table of contents

Abbreviations

Me	Methyl group
Et	Ethyl group
^{n}Pr/Pr	Propyl group
^{i}Pr	Isopropyl group
^{n}Bu/Bu	Butyl group
^{t}Bu	Tertiary butyl group
Ph	Phenyl group
R and R'	Alkyl group or Hydrogen
R"	Alkyl group or Aroyl group
py	Pyridine
HL	Uncoordinated ligand with one dissociable proton
H_2L	Uncoordinated ligand with two dissociable protons
Å	Angstrom; 10^{-10} metres
δ	NMR chemical shift in parts per million (ppm)
Δ	Coordination chemical shift ($\delta_{complex} - \delta_{unbound\ ligand}$)
$^{n}J(AB)$	Coupling constant between atoms A and B, n number of bonds apart, measured in hertz (Hz)
$W_{1/2}$	Peak width at half height in hertz
$CDCl_3$	Deuterated chloroform
C_6D_6	Deuterated benzene
DMF-d_7	Deuterated dimethylformamide
DMSO-d_6	Deuterated dimethylsulphoxide
TLC	Thin layer chromatography
R_f	Peak position (mm) divided by solvent front (mm)
K_e	Equilibrium constant

Chapter One

Introduction

1 INTRODUCTION

1.1 BACKGROUND: Why is platinum so important?

The platinum group metals, PGMs (viz: platinum, palladium, rhodium, ruthenium, osmium and iridium) are very rare with economically viable deposits located in only few places around the world. These are now mainly mined in South Africa, Russia and North America.[1, 2, 3] (see **figure 1** from reference 3).

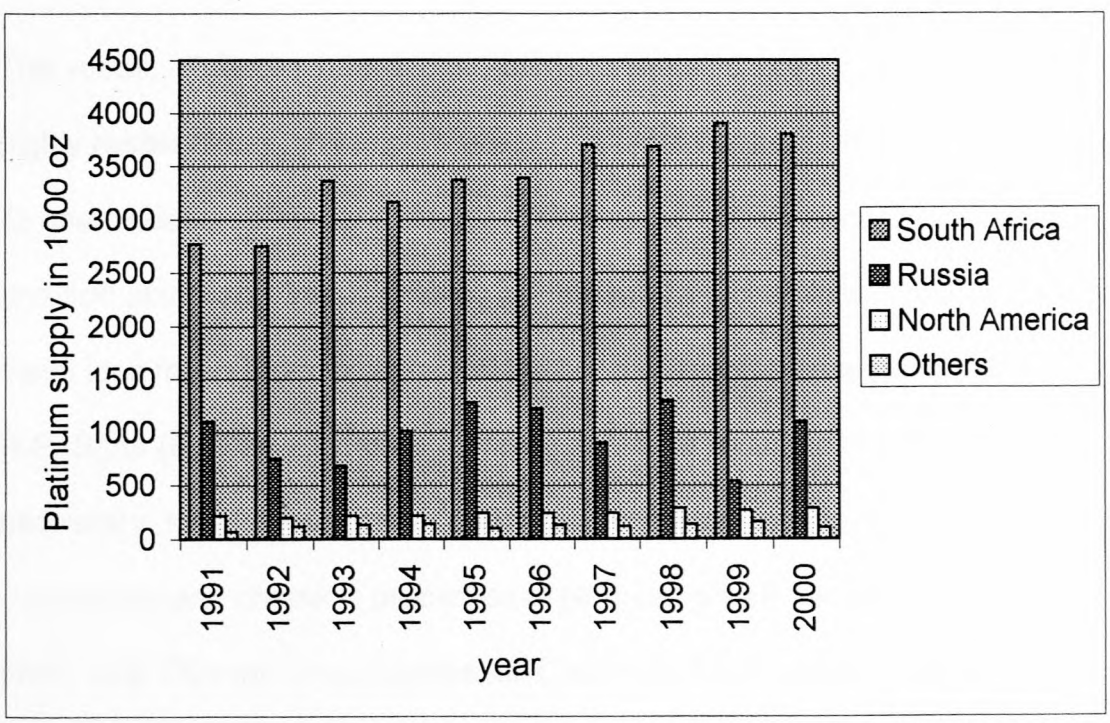

Figure 1: The platinum supply by region in the past decade. This chart shows that world's supply is dominated by the large deposits located in South Africa

Generally, the PGMs can occur naturally as metals, but more often as binary and ternary alloys and mineral sulphides and arsenides as well as other ores.[1] Commonly associated with the PGMs are base metals, cobalt, nickel and copper, which have similar chemistry to PGMs and hence they tend to occur in the same environment on the earth crust.

Platinum occupies the third row and group ten of the transition metal series and was first recognised as an impurity in gold-containing ores, between the years 1500 and 1700. It was a great interference and a nuisance to the early gold miners since it could not dissolve with ease. For this reason it had a derogatory name "*platina da silva*", which could be translated as little silver.

The metal, platinum has a characteristic metallic grey colour, ductile and highly resistant to high temperature corrosion (oxidation) and chemical attack. Its low oxidation state ions are classified as soft acids according to the hard and soft acids and bases (HSAB) principle.[4] This chemical property of these metal ions make them to preferentially bond with soft bases such as R_2S, RS^-, R_3P, R_3As (R is an alkyl or aryl group) and I^- for example. This information is necessary for its refinement and other chemical manipulations. Both the mechanical and chemical properties of platinum give it numerous applications. From Kirk Othmer Encyclopedia of Chemical Technology,[1] **Table 1** shows some principal applications of the PGMs.

Table 1: Applications of the platinum group metals indicated by the + sign.

Application	Pt	Pd	Ru	Rh	Ir
automotive catalysts	+	+		+	
industrial emission catalysts	+				
fuel cell	+				
gas sensor	+	+			
jewellery	+	+			
investment	+				+
biomedical devices	+				+
chemotherapeutic, anticancer	+				
dental materials		+			
electronics	+	+	+		+
electrochemical	+		+		+
chemical*	+	+	+	+	+
petroleum refining	+	+			
glass	+			+	
crucibles	+				+
coatings	+				
spark plugs	+				+

* Osmium is used as a catalyst for the chemical and pharmaceutical industries.

It is evident from the above table that platinum is by far the most widely used and hence its great importance. Besides its many applications, its low natural abundance and intense refinement from ores to 99.99% purity contribute to its

high market value. **Figure 2** (from reference 3) shows the platinum demand by application in the past decade.

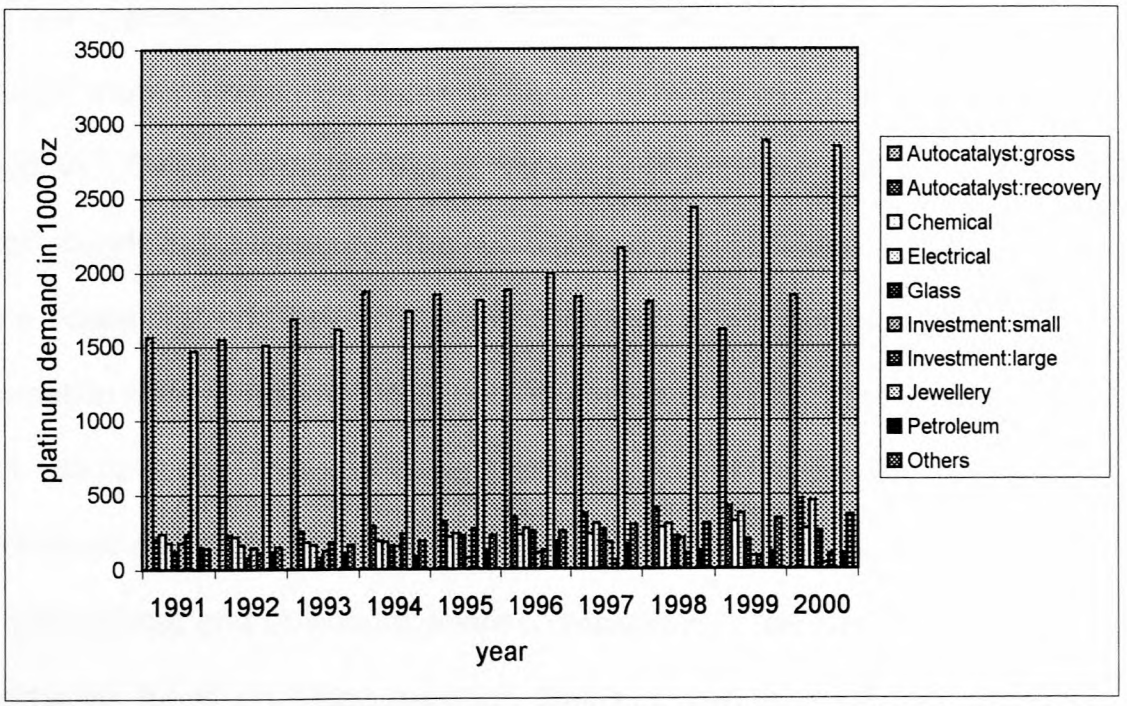

Figure 2: The platinum demand by application in the past decade has been dominated by the autocatalyst and the jewellery market.

By far, platinum has largely been applied to the automotive emission control catalysts, which are important for eliminating hazardous gases such as residual hydrocarbons in fuels and carbon monoxide. With regards to South Africa, the PGMs mining industry plays a pivotal role in the economy as this country is a world's leading supplier of platinum,[3, 4] hence the considerable interest in the chemistry of platinum.

1.2 LITERATURE SURVEY

1.2.1 Platinum(II) general chemistry

In the chemistry of platinum, the metal may be found in various oxidation states, from low oxidation states, 0, I and II to higher oxidation states III, IV, V and VI.[5] Oxidation states V and VI are rare with few examples of fluoro compounds in the literature. The fluoro compounds of oxidation state V and VI are octahedral and have the same coordination number, six. Examples of oxidation state V include $[PtF_5]_4$ and PtF_6^- while oxidation state VI has PtF_6 as an example. For this study, we limit the general discussion to the most dominant oxidation states Pt(II) and Pt(IV), where the metal is orientated in square planar and octahedral shapes, respectively. The other reason for this particular focus on these oxidation states is that in PGM industries, the refinement and separation of PGMs takes place in highly acidic aqueous media, with the initial complexes being chloro species (i.e. $[MCl_4]^{2-}$ and $[MCl_6]^{2-}$, M = PGM metal ion).[6]

1.2.1.1 Platinum(II) tertiary phosphines

Tertiary phosphine ligands, PR_3 (R = H, alkyl group, aryl group or a halogen) are generally classified as π-acid ligands because they usually accept π electrons from the metal, Pt, to which they are bonded.[5] These ligands form numerous stable complexes with Pt(II) and Pt(IV) and have been extensively studied.[7, 8, 9]

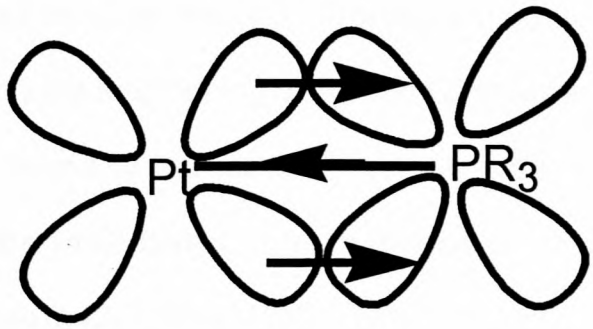

The degree to which the phosphorus atom accepts the π electrons from the metal ion is enhanced by having electron withdrawing R groups, e.g. PF_3 is a good π-acid ligand. Infrared spectroscopy studies have shown that the π-acid nature of PF_3 is very comparable to CO, a well-known π-acid ligand.[10] The trialkyl substituted PR_3 are not strong π-acid ligands and are regarded mainly as σ donors.[6] The σ donor ligands stabilise electron deficient metals such as metals in high oxidation states like IV and VI by donating their electrons to the metal in question. On the other hand, the π-acid ligands stabilise electron rich metals in lower oxidation states like 0 and II by accepting the electrons from the metal. Generally, these ligands coordinate quite strongly to transition metals relative to other ligands, like halide ions (Cl^-, Br^- and I^-) for example. The synergy between a ligand (which is either a good σ donor or a good π acceptor) with a metal ion is depicted above.

1.2.1.2 *Trans effect and trans influence*

As just mentioned, tertiary phosphines coordinate strongly to square planar Pt(II) centres, this has a profound effect on the ligands bonded *trans* to them. *Trans influence* is defined as the extent to which a ligand weakens the bond of the other ligand *trans* to it. This effect is quite prominent with tertiary

phosphines as it will be observed later. The supporting evidence for such an effect is undoubtedly the lengthening of the bond of that particular *trans* ligand to the phosphine bound to the metal centre. An example of this is shown when comparing the Pt-Cl bonds of *trans* and *cis* isomers of $[Pt(PEt_3)_2Cl_2]$, which are 2.32 Å and 2.42 Å respectively.[7] The triethyl phosphine ligand has a stronger *trans* influence than the chloride ion ligand hence the observed bond lengths for the two Pt-Cl's. The knowledge of the *trans influence* can therefore be a useful tool in predicting values for the $^1J(^{195}Pt\text{-}^{31}P)$ coupling constants. The converse argument is also useful in predicting the nature of the ligand that is bonded *trans* to a phosphine ligand in *cis*-platinum(II) complexes.

Trans effect on the other hand refers to the effect a ligand has on the rate of substitution of the ligand in *trans* position to itself. This effect is important in rationalising mechanisms of reactions, and is useful in the synthesis of special complexes. In reference 11, ligands have been ordered in a *trans-directing* series as follows: $CN^- \sim CO \sim NO \sim H^- > CH_3^- \sim SC(NH_2)_2 \sim SR_2 \sim PR_3 > SO_3H^- > NO_2^- \sim I^- \sim SCN^- > Br^- > Cl^- > py > RNH_2 \sim NH_3 > OH^- > H_2O$. This series can give one a good idea about which ligand will be substituted and ultimately which product will be formed in certain substitution reactions. A good example to demonstrate the *trans effect* phenomenon is the exclusive formation of the *cis*-$[Pt(NH_3)_2Cl_2]$ product when two-mole equivalents of NH_3 are added to $[PtCl_4]^{2-}$, as shown in **figure 3**.

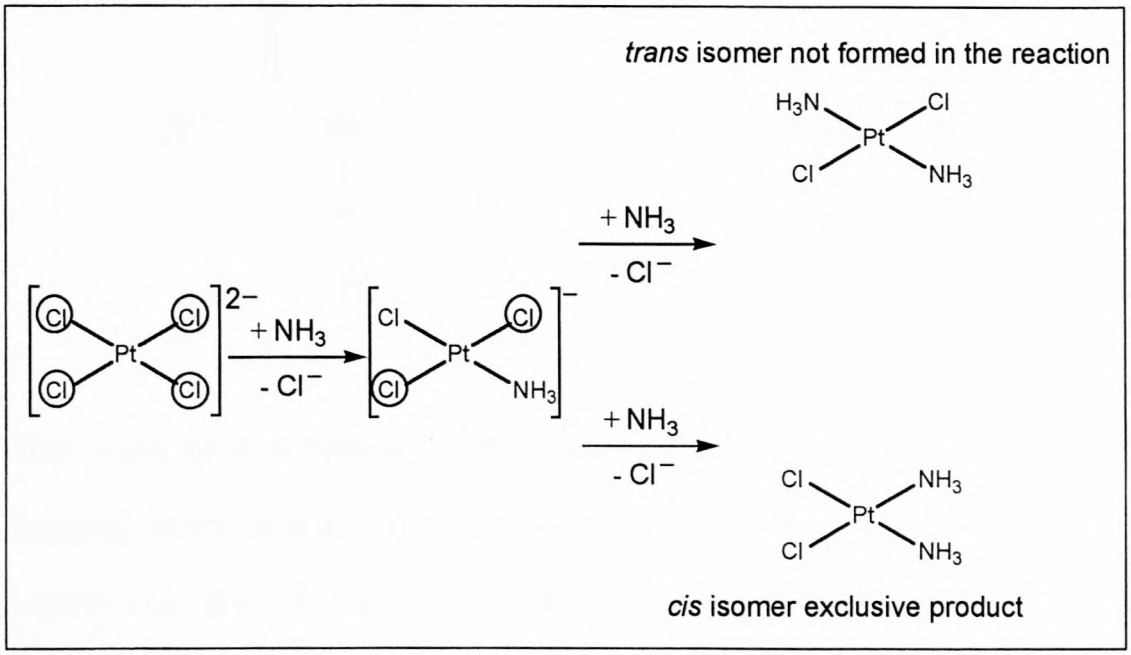

Figure 3: The *trans effect* phenomenon in synthesis: The formation of *cis*-diamminedichloroplatinum(II) exclusively in this reaction is due to the substitution of one of the cycled chloride ions, in step 2, (Cl^- is more *trans-directing* than NH_3).

1.2.2 *N,N*-Dialkyl-*N'*-acyl(aroyl)thiourea ligands and their coordination chemistry

N,N-dialkyl-*N'*-acyl(aroyl)thioureas (HL) and the corresponding *N*-alkyl-*N'*-acyl(aroyl)thioureas (H_2L) are synthesised in high yield from readily available, cheap starting materials following a synthetic route by Douglass and Dains.[12] These ligands show high selective coordination of the platinum group metals over other transition metal ions under appropriate conditions.[13] The fundamental coordination chemistry of such d^8 metal complexes has recently been investigated by Koch *et al* [14, 15] and shows that HL tends to form *S,O* bonded chelates while H_2L prefers to bind to the soft metal through its sulphur atom only.

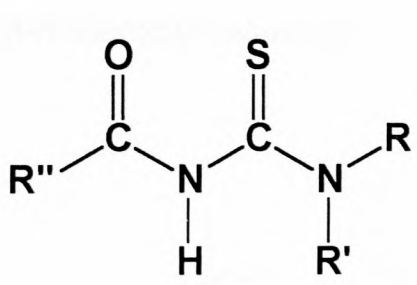

HL

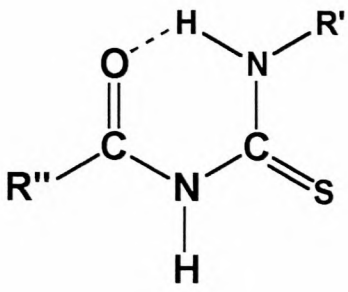

H_2L

The mode of coordination of H_2L mimics that of a simple unsubstituted thiourea, which was first reported more than a century ago by Kurnakov.[16] Ligand H_2L with **R** and **R"** groups being alkyl substituents, reveals an interesting coordination chemistry towards platinum(II) ion. Treatment of $[PtCl_4]^{2-}$ with two-mole equivalents of the ligand in the presence of a base (sodium acetate) results in a mixture of three complexes, one third of which is an unprecedented *trans*-[Pt(HL-*N,S*)$_2$] complex. The formation of this complex is contrary to the expectation of *S,O* donor and *cis* coordination displayed by most related ligands. The crystal structure of this complex has been reported by Koch.[17] This is an indication of the broader chemistry brought about by the intramolecular hydrogen bonding between the amidic oxygen atom and the **HRNC(S)-** moiety of this ligand. In the above reported case and other H_2L ligands, the oxygen donor is locked in the H-bonding described above, rendering it unavailable for coordination.

_N,N_-dialkyl-_N'_-benzoylthioureas, HL

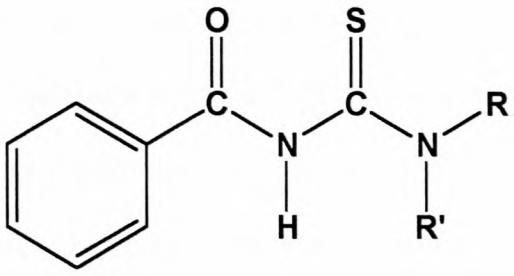

HL

The *N,N*-dialkyl-*N'*-benzoylthioureas have been shown to form neutral complexes in bidentate coordination (losing a proton in the process), with lipophilic properties and thus readily extractable into apolar organic solvents. This property has led to practical applications of these ligands, with regard to the enrichment and normal phase (NP)-TLC separation of transition metals from matrices containing interfering materials.[18, 19, 20, 21] Examples of such practical applications include the analysis of catalytic residues in process solutions and assessment of effluents in PGM plants, which are important industrial issues. The nature of the separated complexes does however present some disadvantages when *normal-phase* high performance liquid chromatography (NP-HPLC) is attempted to quantify them at ultra-trace levels. The complexes tend to decompose and be irreversibly retained on the column because of the effect of the acidity of the packing material.[22] In controlled experiments, the effect of mineral acid (HX, X = Cl, Br and I), on the platinum(II) chelates has been demonstrated by Koch *et al.*[14] The complex gets protonated, leading to partial opening of the six membered chelate ring. Over time, both chelate rings open, yielding a *cis*-[Pt(HL-*S*)$_2$X$_2$] complex,

which isomerises to the polar *trans* complex. In this complex, the oxygen donor is pendent because of its displacement by X while the sulphur donor remains coordinated. As mentioned earlier, refinement and separation of PGMs in PGM industries takes place in highly acidic aqueous media, with the initial complexes being chloro species, i.e. $[MCl_4]^{2-}$ and $[MCl_6]^{n-}$, (M = PGM metal ion).[6] This renders the use of benzoylthioureas as complexing agents in conjunction with (NP)-HPLC useless due to the anticipated on-column irreversible retention of the polar species generated.

_N,N_-dialkyl-_N'_-acylthioureas, HL

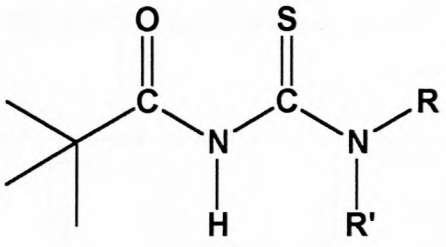

HL

As expected *N,N*-dialkyl-*N'*-acylthioureas also form stable bidentately coordinated chelates with PGMs. The resulting complexes are somewhat more water-soluble compared to the corresponding complexes derived from the benzoylthioureas. The complexes formed are well suited to be separated by means of *reverse-phase* (RP)-HPLC and this has been demonstrated by Mautjana,[22] where the $[M(L\text{-}S,O)_2]$, M = Pt and Pd and $[Rh(L\text{-}S,O)_3]$ complexes were separated. The ligand chosen by this author, *N*-Pyrrolidyl-*N'*-2,2-dimethylpropanoylthiourea, is relatively water-soluble. This preliminary

work may be extended to other transition metals and may be used as an on-line mode of analysis in large-scale operations.

1.2.3 *N*-Thiophosphorylated thioamide and *N,N*-thiophosphenylthiourea ligands and their coordination chemistry

The structural features of *N*-diisopropoxythiophosphoryl thiobenzamide (**I**) and *N*-diisopropoxythiophosphoryl-*N'*-phenylthiourea (**II**) (**figure 4**) closely resemble *N,N*-dialkyl-*N'*-benzoylthioureas discussed in the previous section **1.2.2**. Ligands of this type and the diphenylphosphine chalcogenides reported by Bhattacharyya *et al*[23] seem to display heavy metal extractant properties, hence the growing interest in their coordination chemistry.

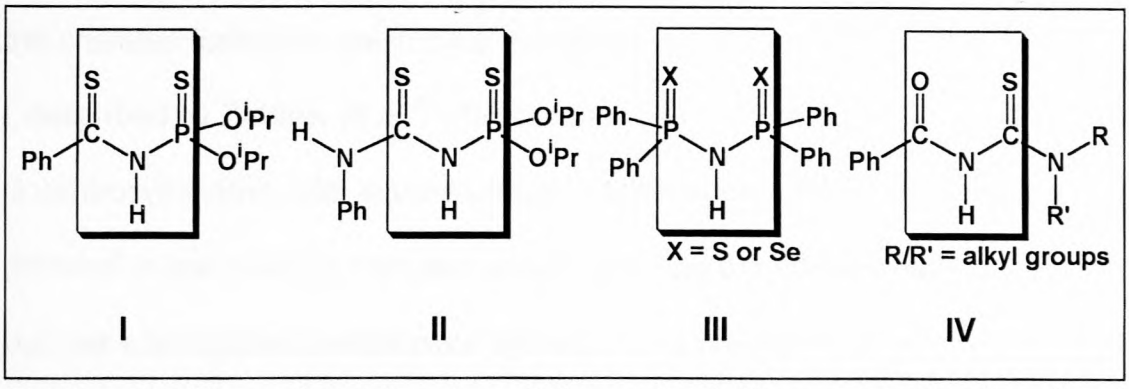

Figure 4: The pictorial presentation of *N*-diisopropoxythiophosphoryl thiobenzamide (**I**), *N*-diisopropoxythiophosphoryl-*N'*-phenylthiourea (**II**), diphenylphosphine chalcogenide (**III**) and *N,N*-dialkyl-*N'*-benzoylthiourea (**IV**).

The ligands **I** and **II** donated by Brusko V., were prepared according to the synthetic route described by Zimin *et al.*[24] These ligands also have a dissociable proton, which is relatively acidic (**I** has a pKa value of 8.07 for example[24]). This proton is lost on coordination with a metal centre, hence a viable means to follow their coordination by either IR or ^{1}H NMR

spectroscopy. Their structural unit **-(S)CNP(S)-** is similar to **-(X)PNP(X)-** and **-(O)CNC(S)-** structural units of diphenylphosphine chalcogenides and of *N,N*-dialkyl-*N'*-benzoylthioureas respectively, which leads to a favourable bidentate coordination with transition metals.

Unlike the *S,O* donors *N,N*-dialkyl-*N'*-benzoylthioureas, **I** and **II** are *S,S* donors making them suitable to coordinate strongly to a considerable range of soft metal ions like Cu^{+}, Ag^{+}, Au^{+}, Hg^{+}, Pd^{2+}, Cd^{2+}, Pt^{2+} and Hg^{2+}. According to the Hard and Soft Acids and Bases (HASB) principle,[4] sulphur is considered as a soft base hence it preferentially coordinates to such metals. Indeed, it has been demonstrated that **I** and **II** react to form stable chelates with many transition and heavy metals.[24-33] The complexes formed are *S,S* bound with a six membered, unstrained chelate ring. An ideal illustration of the chelates formed is given by a molecular structure of a complex of Pd with **I**, described by Zabirov *et al.*[25] The complex has a 1:2 metal to ligand ratio and is centrosymmetric, with square-planar coordination to Pd. This is significantly different to the mercury complex, which also has the same metal ligand ratio, but has a tetragonal coordination sphere.[32] The crystal structure described by Zabirov *et al*[25] reveals that the sulphur atoms of the ligand coordinate marginally but notably different. The thiophosphoryl sulphur is believed to form a weaker coordination bond with Pd-S(P) = 2.341(1) Å, compared to the thiocarbonyl sulphur with Pd-S(C) = 2.310(1) Å. Another significant revelation in this complex is the lengthening of C(S) = 1.635(4) Å and P(S) = 1.912(1) Å double bonds of the unbound ligand, to C(S) = 1.712(4) Å and P(S) = 1.991(1) Å in the complexed ligand. The bond lengths of C(S) = 1.712(4) Å and P(S) =

1.991(1) Å in the complex correspond more to partial single bonds rather than double bonds. These features are indeed indicative of coordination.

In the absence of a crystal structure, other structural changes in the ligand as it changes from an unbound state to a coordinated state can be monitored by means of either IR or NMR spectroscopy. The ν(PS) IR band is shifted to lower frequencies by about 30-50 cm^{-1} while a ν(POC) IR vibration is shifted by about 20-30 cm^{-1} in complexes of both Pd and Pt with **I** as a ligand.[25] $^{31}P\{^{1}H\}$ NMR spectroscopy is also a suitable tool to study the nature of coordination. In the same complexes that have been described above, a 4-9 ppm upfield shift is noted for the phosphorus peaks as the ligand coordinates to the metal centre. As the ligand coordinates, the delocalised electrons in the chelate ring shield the phosphorus atoms, hence, these ^{31}P resonances appear at higher field relative to the unbound ligand phosphorus atoms.

1.3 OBJECTIVES OF THE STUDY

This study consists of mainly two parts, the first being a study of the fundamental coordination chemistry and donor properties of *N,N*-dialkyl-*N'*-acyl(aroyl)thioureas as selective ligands for platinum(II) ions. The second part is a study of the coordination chemistry of *N*-diisopropoxythiophosphoryl thiobenzamide and *N'*-diisopropoxythiophosphoryl-*N*-phenylthiourea as they also form stable chelates with many transition metals including platinum(II).

As part of the continuing study of *N,N*-dialkyl-*N'*-acyl(aroyl)thioureas (HL), the relative donicity of *S* and *O* donor atoms of the ligands and the possible effect of the substituent groups **R**, **R'** and **R"** on the coordination properties of HL were investigated.

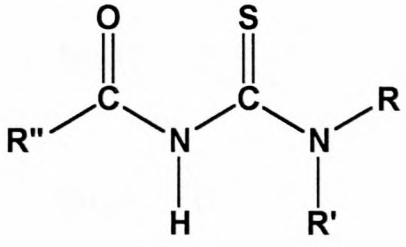

HL

Variations of the **R**, **R'** and **R"** groups may be expected to influence the donor properties of *S* and *O*, hence providing a wide scope for fine-tuning these ligands for specific metal complexation. This may find practical applications in transition metal pre-concentration, refinement and separation.

To this end, reactions of ligands with a *cis*-$[Pt(P^nBu_3)_2Cl_2]$ complex in solution have been chosen as an indirect means of probing the variations in the relative donicities of the *S* and *O* atoms in the ligands, as the **R**, **R'** and **R"** groups are varied. The complexation reactions takes place directly in the NMR tubes in the presence of triethylamine (see **figure 5**). These reactions are then monitored by means of high-resolution $^{31}P\{^1H\}$ and $^{195}Pt\{^1H\}$ NMR spectroscopy.

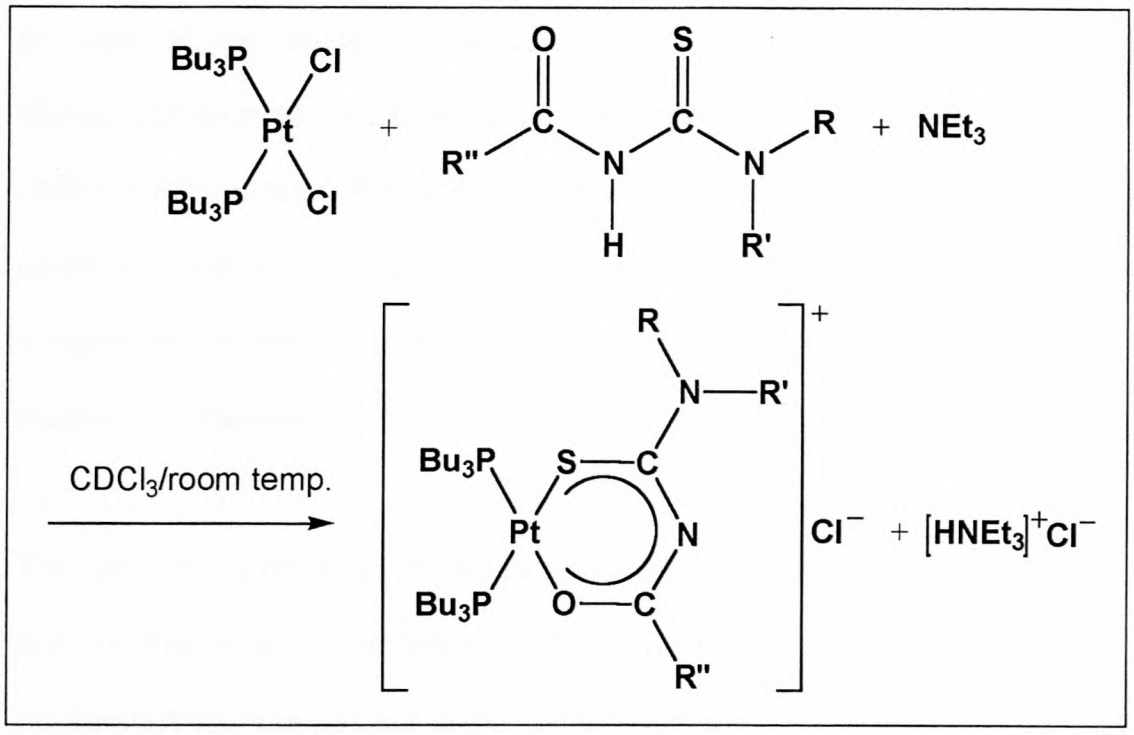

Figure 5: A general reaction scheme for the complexation of *N,N*-dialkyl-*N'*-acyl(aroyl)thiourea to the platinum(II) ion.

From the *trans influence* argument discussed in section **1.2.1.2**, it is hoped that the respective $^{1}J(^{195}Pt\text{-}^{31}P)$ spin coupling constants might reveal information about the relative donicities of the *S* and *O* donor atoms in the mixed ligand-platinum(II) complex, *cis*-$[Pt(P^{n}Bu_3)_2(L\text{-}S,O)]^{+}Cl^{-}$. A small $^{1}J(^{195}Pt\text{-}^{31}P)$ spin coupling constant would then imply weakening or lengthening of the Pt-P bond and it will be argued that this is a consequence of the strengthening of the *trans* bond, for example. The same argument holds for the reverse situation. It is also hoped that the $\delta(^{195}Pt)$ chemical shift values will reveal information about the relative donicity of *S* and *O* donor atoms of the ligands. For example, if the platinum(II) nucleus experiences a relative shielding or deshielding then the donor atoms must either be electron rich or electron deficient, which will be ascribed to the effects of **R**, **R'** or/and **R"** groups present.

As part of the study of the coordination chemistry of *N,N*-dialkyl-*N'*-acyl(aroyl)thioureas, asymmetrically disubstited *N,N*-dialkyl-*N'*-acylthioureas (with the alkyl groups **R** and **R'** not equivalent) will be synthesised and their respective platinum(II) complexes prepared from them. It was uncertain whether the asymmetry in the ligands will be carried through to the resultant platinum(II) chelates.

The structural similarities of *N*-diisopropoxythiophosphoryl thiobenzamide, **I** and *N'*-diisopropoxythiophosphoryl-*N*-phenylthiourea, **II** to *N,N*-dialkyl-*N'*-acyl(aroyl)thioureas has led to the second part of the project.

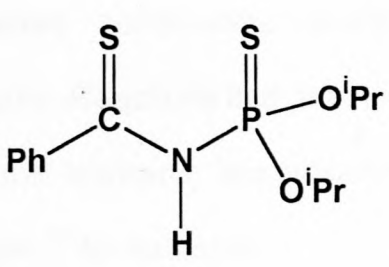

I

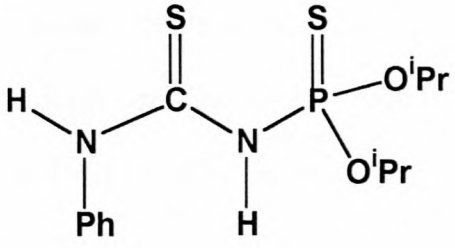

II

Here, the platinum chelates of these ligands are synthesised and compared to platinum chelates of related ligands. The *S,S* donor atoms of these ligands were also investigated in the same manner as the thioureas i.e. by reacting each ligand with *cis*-[Pt(P^nBu_3)$_2$Cl$_2$] in the presence of triethylamine. The crucial question to be answered with regard to the latter investigation, is whether the relative donicities of the two *S,S* donors will be sufficiently different to be observed from the NMR coupling and shielding parameters.

Having observed the $^{31}P\{^1H\}$ NMR sensitivity over $^{195}Pt\{^1H\}$ NMR, the investigation was only carried out using $^{31}P\{^1H\}$ NMR spectroscopy.

1.4 MULTINUCLEAR MAGNETIC RESONANCE SPECTROSCOPY AS A TOOL

Nuclear magnetic resonance (NMR) spectroscopy is widely used in virtually all fields of molecular sciences. Without this technique for structural elucidation, chemists would be seriously handicapped when facing the ever-increasing challenges in this field. Without crystal structures, chemists (organic and inorganic) often rely on this technique for the characterisation of synthesised compounds, whether those compounds are products or precursors. Reactions that are slow enough can also be followed by means of NMR, the *cis/trans* isomerisation of $[Pt(PR_3)_2Cl_2]$ studied by Chatt and Wilkinson,[34] for example.

Even though in NMR spectroscopy variations in the parameters of the active nuclei in the molecule are measured, structural information about the whole molecule can often be obtained from these data. A typical example of this is that some nuclei (^1H and ^{13}C for example) are located in the molecular framework, therefore, knowing their resonance frequencies is useful for structural elucidation. An interaction between a particular nucleus and the surrounding electrons, or interaction between this nucleus and neighbouring nuclei, identifies it distinctly from other nuclei that are not in the same chemical environment. This is the simplistic overview of NMR spectroscopy as

a tool for structural elucidation, more details of how an NMR experiment is carried out are contained in standard texts[35, 36, 37] and will not be discussed here.

The nuclei that are extensively used in this study are ^{1}H, ^{13}C, ^{31}P and ^{195}Pt; (all these nuclei have spin I = ½) hence, the suggestive subtitle: multinuclear magnetic resonance spectroscopy. The NMR phenomenon depends on the property of the nucleus called nuclear spin with symbol I, and I = ½ is most suitable for high resolution NMR spectroscopy. Other nuclei with spins, I > ½ do exist but are not as suitable for high resolution work since the short relaxation time of these nuclei lead to a broadening of the NMR signals. Often in NMR spectroscopy, chemical shifts of the nuclei, δ, coupling constants, J, and relaxation times, T_1 and T_2 are parameters of significant interest.

The first parameter depends on γ, which is an intrinsic property of the nucleus. For example, the resonance frequency, ν, in Hertz, can be expressed as follows:

$\nu = \gamma B_0(1-\sigma_t)/2\pi$, where γ = magnetogyric ratio constant for a given spin I = ½ nucleus

B_0 = static magnetic field

σ_t = total screening constant

From the above equation, it can be noted that a larger static magnetic field, B_0 results in higher resonance frequency, ν and a more dispersed chemical shift

range. Due to static magnetic field, B_0, dependence of the resonance frequency, ν, NMR signals are always expressed as chemical shifts, δ, in ppm, which is equivalent to the difference between the resonance frequency and resonance of a standard reference material divided by the operating frequency of the spectrometer employed.

Table 2: Magnetogyric ratios of common spin = ½ nuclei, their relative natural abundances and their receptivity, D^p relative to ^1H.[35]

Nucleus	Abundance (%)	Magnetogyric ratio, γ (10^7 rad.s^{-1}.T^{-1})	*Relative receptivity, D^p
^1H	99.985	26.7510	1
^{13}C	1.108	6.7263	$1.76x10^{-4}$
^{31}P	100	10.829	1.0663
^{195}Pt	33.8	5.7505	$3.36x10^{-3}$

* Receptivity = $\gamma^3NI(I + 1)$, where γ = magnetogyric ratio, N = natural abundance and I = nuclear spin = ½ in this case.

In **table 2**, the term relative receptivity, D^p, can be taken as a crude guide to the ease of obtaining an observable signal for a given concentration of the relevant atoms in the solution at a constant magnetic field, B_0. Receptivity is usually quoted relative to ^1H or ^{13}C and in **table 2** only the receptivity relative to ^1H are given. The signal-to-noise ratio depends on the receptivity of the nuclear active isotope, for example, in **table 2**, the ^1H is the most sensitive NMR nucleus (i.e. will give the largest signal-to-noise ratio), while ^{13}C NMR is the least sensitive of the four. To obtain a good spectrum for an insensitive nucleus, the NMR spectrum of the sample is then acquired for longer periods. Low natural abundance of the nucleus of interest is often viewed as a

disadvantage but this can sometimes be used to the experimenter's advantage. For example, isotopic enrichment at a specific location within a molecule can often provide pertinent information. This is very prominent in studying some biological systems, particularly proteins which can be ^{15}N enriched. Isotopic enrichment was also used in this project for a specific problem, which will be discussed later.

The second parameter, the spin-spin coupling constant, J is independent of the applied magnetic field but does depend on other molecular aspects such as hybridisation, electronegativity of substituents and dihedral bond angles. For example in the case of a one-bond coupling between a proton and a carbon, $^{1}J(^{13}C\text{-}^{1}H)$ = 125 Hz in ethane, 156.2 Hz for ethylene and 248.7 Hz for acetylene.[35] Therefore, the $^{1}J(^{13}C\text{-}^{1}H)$ increases and follows the sequence sp^3, sp^2 and sp hybridisation.

The Pople and Santry equation[38] for one bond coupling reveals a direct relation of the valence *s* electron densities of the coupling nuclei and the coupling constant. The equation is shown below:

$$J(A\text{-}B) = (\text{constant})\gamma_A\gamma_B \left|\Psi_A(0)\right|^2 \left|\Psi_B(0)\right|^2 \pi_{AB}$$

Where J(A-B) = coupling constant between the nuclei A and B

γ's = magnetogyric ratios

$\left|\Psi(0)\right|^2$'s = the valence *s* electron densities at nuclei A and B

π_{AB} = mutual polarisability

Generally, shortening of the A-B bond is associated with larger electron density in that particular bond, which in turn is associated with a larger ^{1}J(A-B) spin coupling constant.[39] The $^{1}J(^{195}Pt\text{-}^{31}P)$ spin coupling constants of platinum phosphine complexes have been shown to be different for the *cis* and *trans* isomers of complexes of the type *cis/trans*-$[Pt(PR_3)_2Cl_2]$.[40] Thus the $^{1}J(^{195}Pt\text{-}^{31}P)$ spin coupling constant in *cis*-dichlorobis(tributylphosphine)platinum(II) is generally significantly larger than the $^{1}J(^{195}Pt\text{-}^{31}P)$ spin coupling constant for the corresponding *trans* isomer. This difference in bonding can be attributed to the formation of d_π-d_π(Pt-P) bonding on the basis of Venanzi's[7] rationale which is as follows: In the *trans* complex, the same *d*-orbital would have to be used for the formation of both π-bonds while in the *cis* complex, each phosphorus atom can use different platinum *d*-orbital. As the phosphine ligands compete for the same platinum *d*-orbital (thereby weakening the π-contribution to the Pt-P bond) in the *trans* complex, the *s*-character of the Pt-P bond is reduced by synergic mechanism and subsequently the Pt-P bond lengthens and the $^{1}J(^{195}Pt\text{-}^{31}P)$ spin coupling constant is smaller. In the *cis* complex though, there is no such competition for the platinum *d*-orbital between the two phosphines hence these complexes have a larger $^{1}J(^{195}Pt\text{-}^{31}P)$ coupling constant. There are many more examples of *trans/cis* isomers of this kind in the literature[40] demonstrating these differences in the $^{1}J(M\text{-}^{31}P)$ values, where M represents an NMR active metal.

The other parameters, T_1 and T_2 are less significant for the purpose of this particular study and will not be discussed here but only one thing should be mentioned in this context: if T_1 is small, the acquisition of a spectrum can be

quick, which is valuable for practical purposes. This, however, is not without a drawback, because if T_1 is short then T_2 is also shortened and this translates into a broadening effect on the NMR signals. T_2 has an inverse relation to the peak width, $W_{1/2}$. Broad peaks are not desirable in NMR spectroscopy since relevant information may be lost within the broad peak.

NMR spectroscopy is mostly carried out in solutions, but can also be carried out solids as well. In NMR spectroscopy of solutions carried out in this project, the requirement is that a sample should be adequately soluble in a particular solvent. A $^{13}C\{^1H\}$ NMR spectrum of *N,N*-diethyl-*N'*-*4*-nitrobenzoylthiourea, HL^4, was measured in chloroform and dimethylsulphoxide. While this compound readily dissolves in the latter, it is sparingly soluble in the former solvent and this profound difference impacts on the spectra obtained within a reasonable time. **Figure 6** shows the $^{13}C\{^1H\}$ NMR spectra of HL^4 in the two solvents.

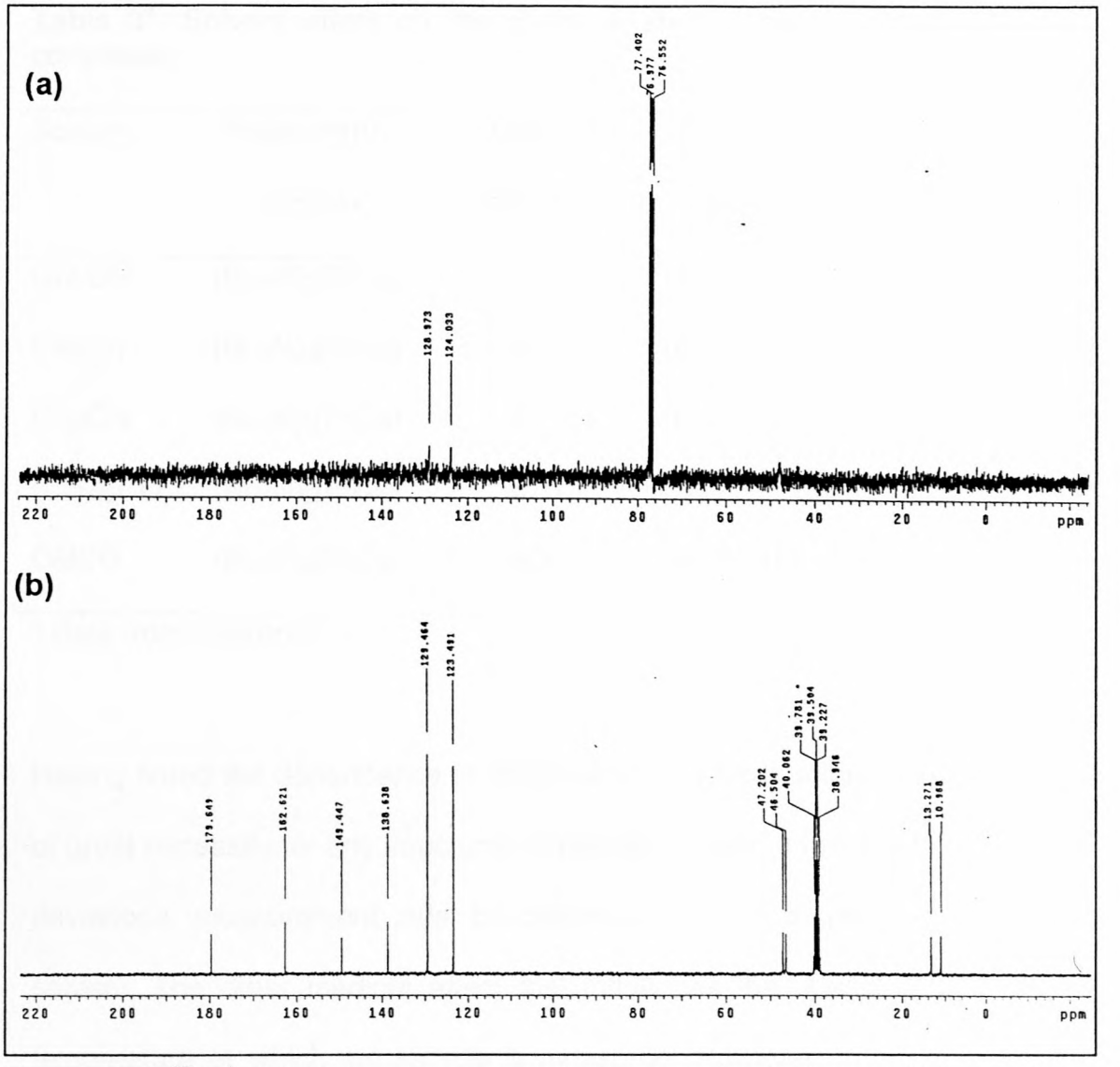

Figure 6: A $^{13}C\{^{1}H\}$ NMR spectrum of *N,N*-diethyl-*N'*-*4*-nitrobenzoylthiourea in **(a)** $CDCl_3$ ran for 1 hour, 12 minutes and **(b)** DMSO-d_6 ran for 36 minutes.

Most often, the solvent used is deuterated chloroform since it is relatively inexpensive compared to other deuterated solvents. Other solvents may sometimes be used depending on the question of interest. Nevertheless, it must be mentioned that solvents can also notably affect the chemical shifts. An example of the solvent effect was demonstrated by Pesek *et al*,[41] while studying platinum(II/IV) complexes.

Table 3*: Solvent effect on the chemical shift of selected platinum(II/IV) complexes.

Solvent	Platinum(IV) complex	Chemical shift/ppm	Platinum(II) complex	Chemical shift/ppm
CH_3OH	$(Bu_4N)_2[PtCl_6]$	-222	$(Bu_4N)_2[PtCl_4]$	-1477
CH_2Cl_2	$(Bu_4N)_2[PtCl_6]$	-260	$(Bu_4N)_2[PtCl_4]$	-1416
CH_3CN	$(Bu_4N)_2[PtCl_6]$	-327	$(Bu_4N)_2[PtCl_4]$	-1388
$(CH_3)_2CO$	$(Bu_4N)_2[PtCl_6]$	-370	$(Bu_4N)_2[PtCl_4]$	-1384
DMSO	$(Bu_4N)_2[PtCl_6]$	-400	$(Bu_4N)_2[PtCl_4]$	-1372

* Data from reference 41.

Having noted the dependence of chemical shifts on the solvent, it is therefore of great necessity for any structural comparison based on small chemical shift deviations, measurement must be derived from data obtained in the same solvent. The other medium effect that influences the chemical shift is the temperature at which the sample is measured. However, this is to a lesser extent in comparison to the solvent. Pregosin[40] reported that a temperature change of 100°C could result in platinum chemical shift change of about 40 to 50 ppm.

The use of different nuclei for obtaining certain structural information about complexes also features quite often. This is very important since observing different nuclei can often reveal information, which cannot be obtained from only one. For example, it would be futile to observe the ^1H NMR spectrum to identify the mixture of three "invertomers" of [PtIMe{MeSe$(CH_2)_2$SeMe}] as

studied by Abel *et al.*[42] Instead, a $^{195}Pt\{^{1}H\}$ NMR spectrum at room temperature clearly shows the three "invertomers" separated by more than 30 ppm from each other.

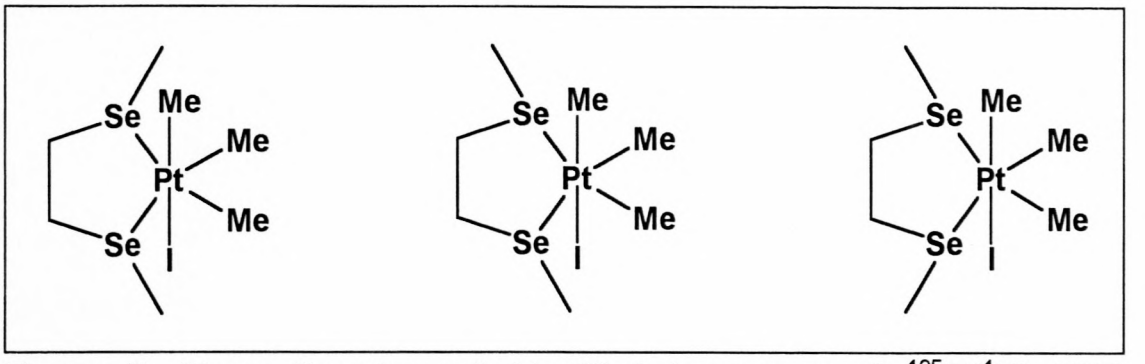

Figure 7: Three "invertomers" identified by means of $^{195}Pt\{^{1}H\}$ NMR spectroscopy at room temperature.

Though magnetic high fields increase the sensitivity of NMR, some specific problems need a low field instrument, as some information is lost at high field. Specific problems regarding this point are discussed later.

Chapter Two

Experimental approach

2 EXPERIMENTAL APPROACH

2.1 THE SYNTHESIS AND CHARACTERISATION OF LIGANDS

A series of ligands (shown in **tables 5**, **6** and **7**) of the type *N,N*-dialkyl-*N'*-acyl(aroyl)thiourea were prepared in high yield according to the method described by Douglass and Dains.[12] Both *N*-piperidyl-*N'*-*2,6*-dimethoxybenzolythiourea (HL^7) and *N,N*-diethyl-*N'*-*3,4,5*-trimethoxybenzoylthiourea (HL^8) were prepared and donated by Miller.[43] Their identity and purity were checked by means of ^1H and $^{13}C\{^1H\}$ NMR spectra, elemental (C, H, N and S) analysis and melting point determination. All other ligands were also fully characterised in the same manner. Additional to these modes of characterisation, the crystal structure of *N,N*-diethyl-*N'*-*4*-nitrobenzoylthiourea (HL^4) was determined by means of X-ray diffraction (see section **2.1.4**). With the exception of *N,N*-dimethyl-*N'*-acetylthiourea (HL^{12}), whose synthesis will be described later, the typical synthetic route of all the ligands is described below.

A specific amount of potassium thiocyanate dried in a vacuum-oven, (typically 0.03 mol) is dissolved in 75 ml anhydrous acetone in a two-necked round bottom flask, under a nitrogen atmosphere. An equimolar amount (0.03 mol) of either acyl chloride or benzoyl chloride, is dissolved in about the same volume of anhydrous acetone, then added drop-wise through a dropping funnel into the stirred potassium thiocyanate solution. Once the addition is

complete, the mixture is heated to reflux for 45 minutes. From experience,[12] it is known that the formation of either acyl isothiocyanate or benzoyl isothiocyanate is complete under these reaction conditions. If necessary, the reaction can be monitored by thin layer chromatography with 5% acetone in dichloromethane as an eluent. The mixture is cooled to room temperature and insoluble potassium chloride is observed settling at the bottom of the flask. With minimum exposure to atmosphere, dialkylamine is transferred to a dropping funnel. This is then dissolved in about the same volume of anhydrous acetone before being added drop-wise to the stirring reaction vessel. It is unnecessary to separate the potassium chloride at this stage, since it will not take part in any side reaction with the secondary amine. The mixture is heated to reflux for further 45 minutes after the addition is complete. The mixture is allowed to cool to room temperature, then poured into an open beaker containing 100 ml of water. The water has a dual purpose of dissolving the potassium chloride salt and precipitating the insoluble organic product. To recover more product, the contents of the beaker are left in the fume hood for almost all of the acetone to evaporate, typically 200 ml. The precipitate is filtered off and washed with water to remove any trapped inorganic salt. The crude product is recrystallised from a acetone/water mixture and collected by filtration. To remove all the solvent, the product is dried under vacuum at room temperature.

All the reactions are carried out under dry and inert atmosphere since the acyl chloride and benzoyl chloride are moisture sensitive and will be converted to

their respective carboxylic acids. The synthesis of these ligands follows **reaction scheme 1**.

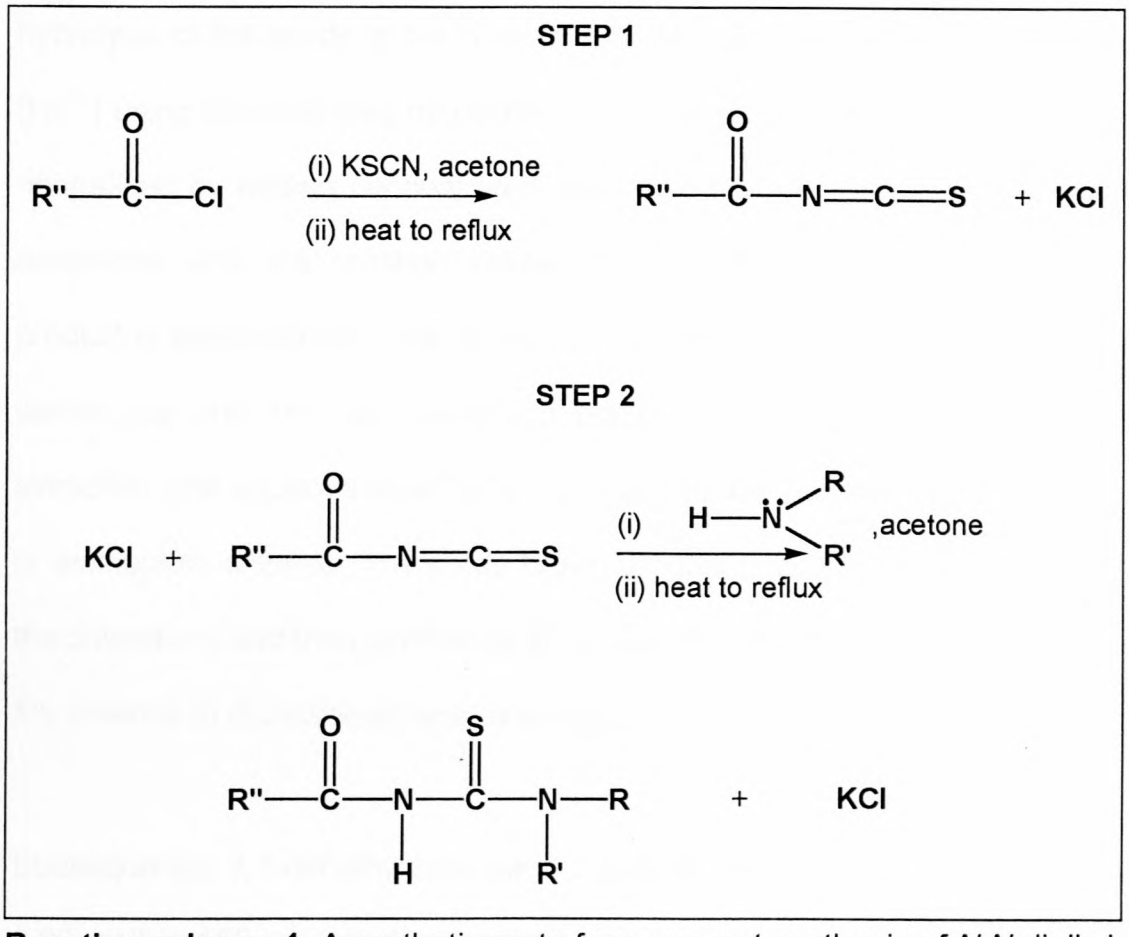

Reaction scheme 1: A synthetic route for a one-pot synthesis of *N,N*-dialkyl-*N'*-acyl(aroyl)thiourea with **R"** either a bulky alkyl group or a benzyl group (or derivative thereof). **R** and **R'** are similar alkyl groups unless stated otherwise.

It must be mentioned that some products, in particular the *N,N*-dialkyl-*N'*-acylthioureas, are relatively soluble in water and, hence, they may need to be extracted into an organic phase. The typical solvent used for this purpose is chloroform. Retrieving the product in this manner is also employed when the ligand forms an "oil", instead of being a solid, which is the case for *N*-(2-methylpyrrolidine)-*N'*-*2,2*-dimethylpropanoylthiourea (HL[13]).

As mentioned before, a deviation to this synthetic route is necessary when *N,N*-dimethyl-*N'*-acetylthiourea (HL^{12}) is being prepared. The *1,1*-dimethylthiourea, (HL^{12}-intermediate) moiety was first synthesised by acid hydrolysis of the amide of the *N,N*-dimethyl-*N'*-*2,2*-dimethylpropanoylthiourea (HL^{11}) using concentrated hydrochloric acid. Any residual hydrochloric acids neutralised by adding concentrated ammonia. The neutralisation reaction is exothermic and the reaction vessel is cooled to room temperature. The product is extracted with five 40 ml portions of chloroform. The extraction is carried out until the last chloroform portion adopts no colour. During the extraction, the aqueous layer turns milky due to the increasing concentration of ammonium chloride. The crude brown product is collected by evaporating the chloroform and then purified by Silica Gel 60 column chromatography with 5% acetone in dichloromethane as an eluent.

Subsequently, *1,1*-dimethylthiourea (2.1 g, 0.02 mol) and triethylamine (2.2 g, 0.02 mol) in 150 ml anhydrous acetone are added drop-wise to a solution of acetyl chloride (2.1 g, 0.03 mol) in 50 ml anhydrous acetone. The triethylamine acts as a "proton sponge". The reaction mixture is heated to reflux for 45 minutes and there after cooled to room temperature. The contents are then poured into an open beaker containing 100 ml of water. Acetone is allowed to evaporate to concentrate the product. The product is collected by filtration, but since the product is relatively soluble in water, a significant portion remains in solution. This is extracted by five 40 ml portions of chloroform. After evaporating the chloroform, the two crops are combined. The reaction procedure is summarised in **reaction scheme 2**.

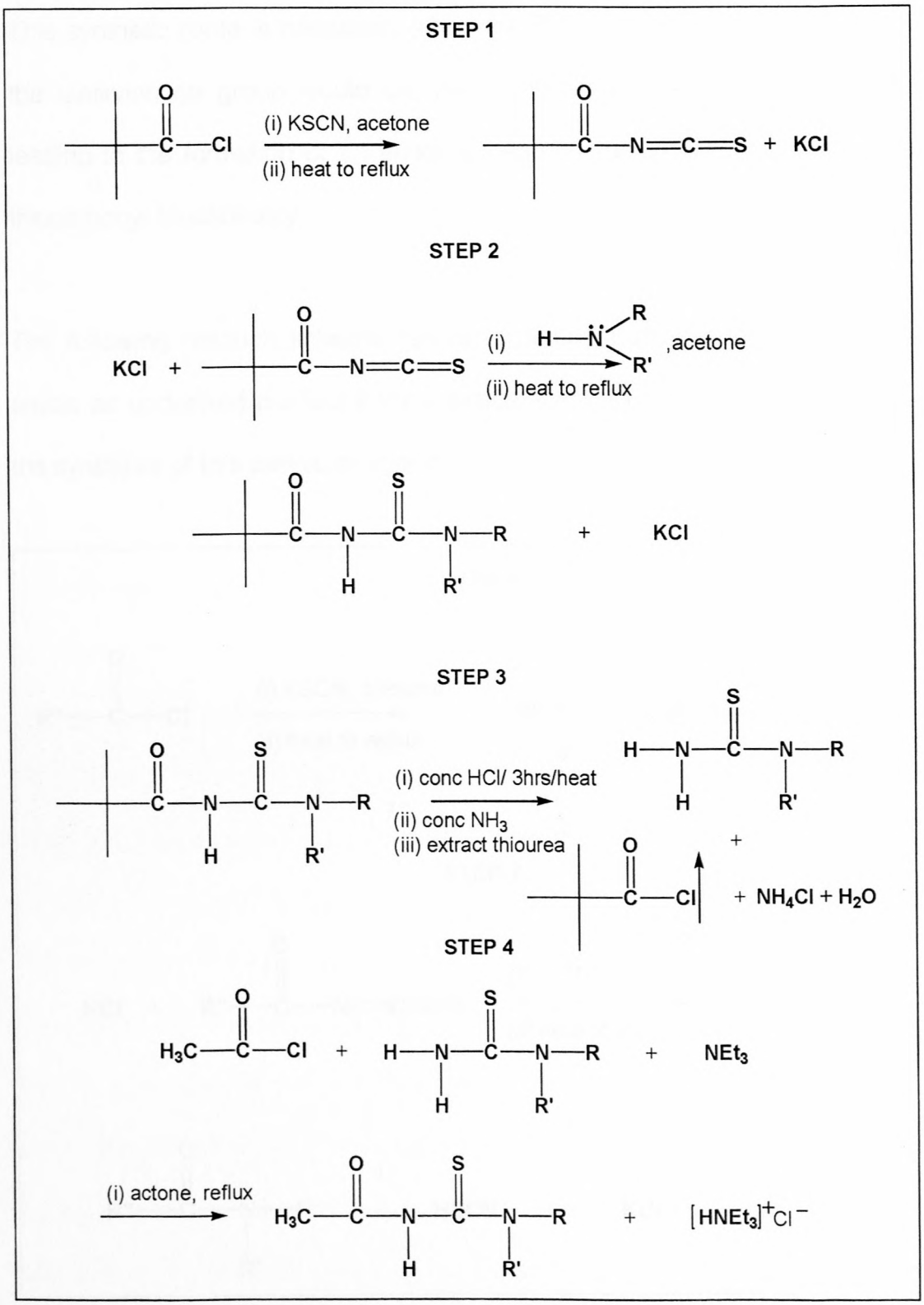

Reaction scheme 2: The synthesis of *N,N*-dimethyl-*N'*-acetylthiourea. In step 1, **R"** is a bulky alkyl group (typically a tertiary butyl) while in step 4 it is a methyl group.

This synthetic route is necessary when the **R"** group is not bulky otherwise the dialkylamine group would be introduced at the carbonyl functionality, leading to the formation of an amide instead of nucleophilic addition to the thiocarbonyl functionality.

The following reaction scheme serves to demonstrate the formation of the amide as undesired product if the classical synthetic scheme is adopted for the synthesis of this particular ligand.

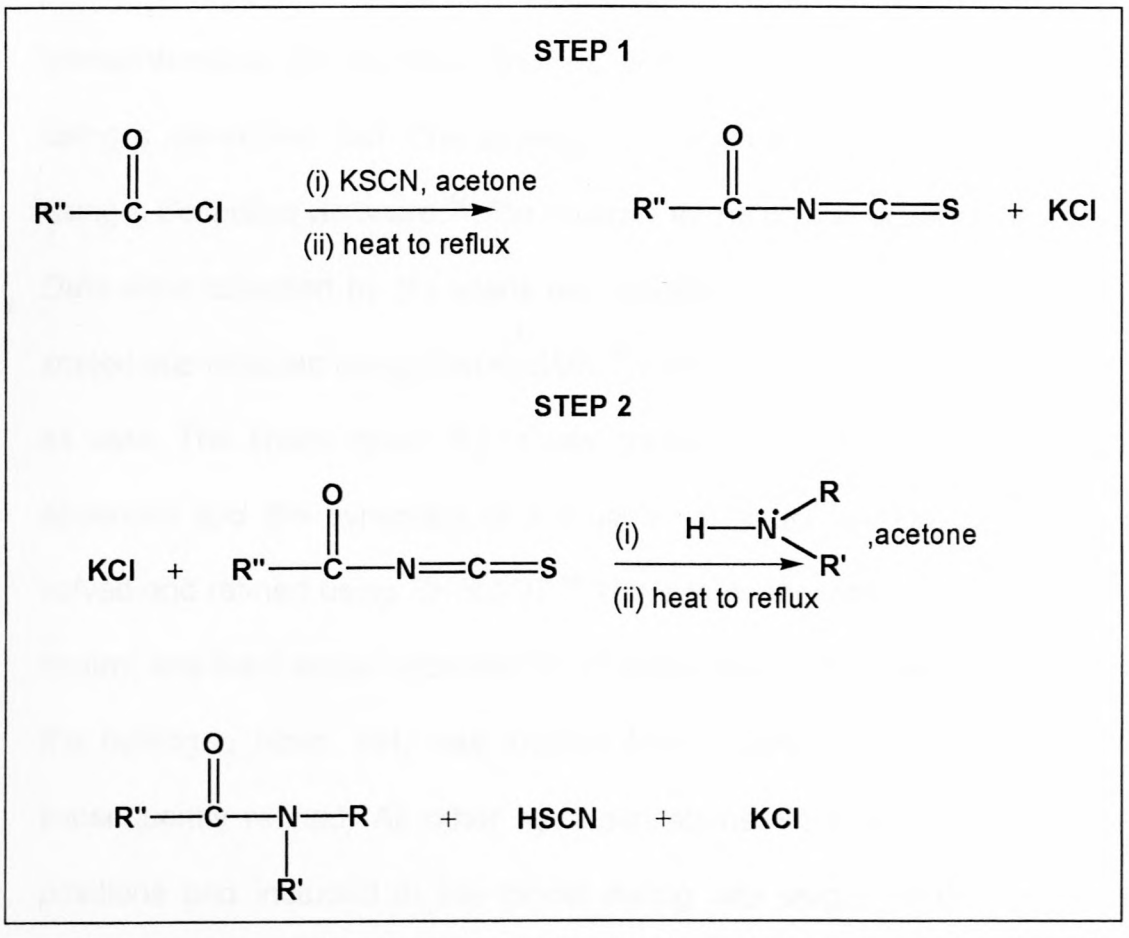

Reaction scheme 3: Synthetic route for the formation of an amide when the traditional synthetic route is adopted with no bulky **R"** alkyl group in place. **R** and **R'** are similar alkyl groups.

2.1.1 The molecular structure determination of *N,N*-diethyl-*N'-4*-nitrobenzoylthiourea (HL^4) by means of single crystal X-ray diffraction

The ligand HL^4 was synthesised as described in the experimental section **2.7**. The crude product was subsequently recrystallised in ac acetone-water solvent system. Single crystals of this ligand were grown in the refrigerator, isolated by suction and washed with water. Like most of these ligands, *N,N*-diethyl-*N'-4*-nitrobenzoylthiourea is air stable. X-ray intensity data were collected at 298 K using a Nonius Kappa CCD with 1.5 kW graphite monochromated Mo-Kα radiation. The diffraction patterns could be indexed using a monoclinic cell. The strategy for the data collection was evaluated using a *Collection* Software.[44] The detector to the crystal distance was 57mm. Data were collected by phi scans and several omega scans. The data were scaled and reduced using *Denzo-SMN*.[45] Unit cell dimensions were refined on all data. The space group $P2_1/c$ was chosen on inspecting the systematic absences and the symmetry of the diffraction patterns. The structure was solved and refined using *SHELX97*.[46] There is no disorder in terminal carbon chains, and the thermal ellipsoids for all atoms are reasonable. The position of the hydrogen atom, NH, was located from a difference Fourier map and subsequently refined. All other hydrogen atoms were placed in calculated positions and included in the model during late stages of the refinement. Refinement converges with a final R-factor of 0.046 and the maximum residual peak and hole was 0.2 and -0.2 electrons $Å^{-3}$ respectively. The goodness-of-fit was 1.0 indicating an excellent agreement between the calculated and the observed structure factors. Estimated deviations of bond

lengths and angles are generally within 0.002 Å and 0.2° respectively. Plots of the molecular structure were obtained with *ORTEP*[47] and *PLATON*.[48]

Table 4: Crystal data and structure refinement for *N,N*-diethyl-*N'*-*4*-nitrobenzoylthiourea, HL^4

Identification code	HL^4	
Empirical formular	$C_{12}H_{15}N_2O_3S$	
Molecular mass	281.33	
Temperature	293(2) K	
Wavelength	0.717073 Å	
Crystal system	Monoclinic	
Space group	$P2_1/c$	
Unit cell dimensions	a = 6.887(1) Å	α = 90°.
	b = 19.244(3) Å	β = 93.01(1)°.
	c = 10.147(1) Å	γ = 90°.
Volume	1342.0(5) Å	
Z	4	
Density (calculated)	1.391 Mg/m^3	
Absorption coefficient	0.249 mm^{-1}	
F(000)	592	
Crystal size	0.35 x 0.54 x 0.27 mm^3	
Theta range for data collection	3.15 to 27.47°.	
Index ranges	-8<=h<=6, -17<=k<=24, -13<=l<=5	
Reflections collected	3617	

Independent reflections	2464 [R(int) = 0.0276]
Completeness to theta = 27.47°	80.2%
Refinement method	Full-matrix least squares on F^2
Data / restraints / parameters	2464 / 0 / 179
Goodness-of-fit on F^2	1.027
Final R indices (I>2σ(I)]	R1 = 0.0459, wR2 = 0.1069
R indices (all data)	R1 = 0.0800, wR2 = 0.1216
Extinction coefficient	0.011(3)
Large diff. Peak and hole	0.215 and -0.244 e. $Å^{-3}$

The molecular structure of this ligand and selected bond lengths and angles are discussed in the results section, **chapter 3**.

2.1.2 Summary of synthesised ligands – the structures and numbering schemes

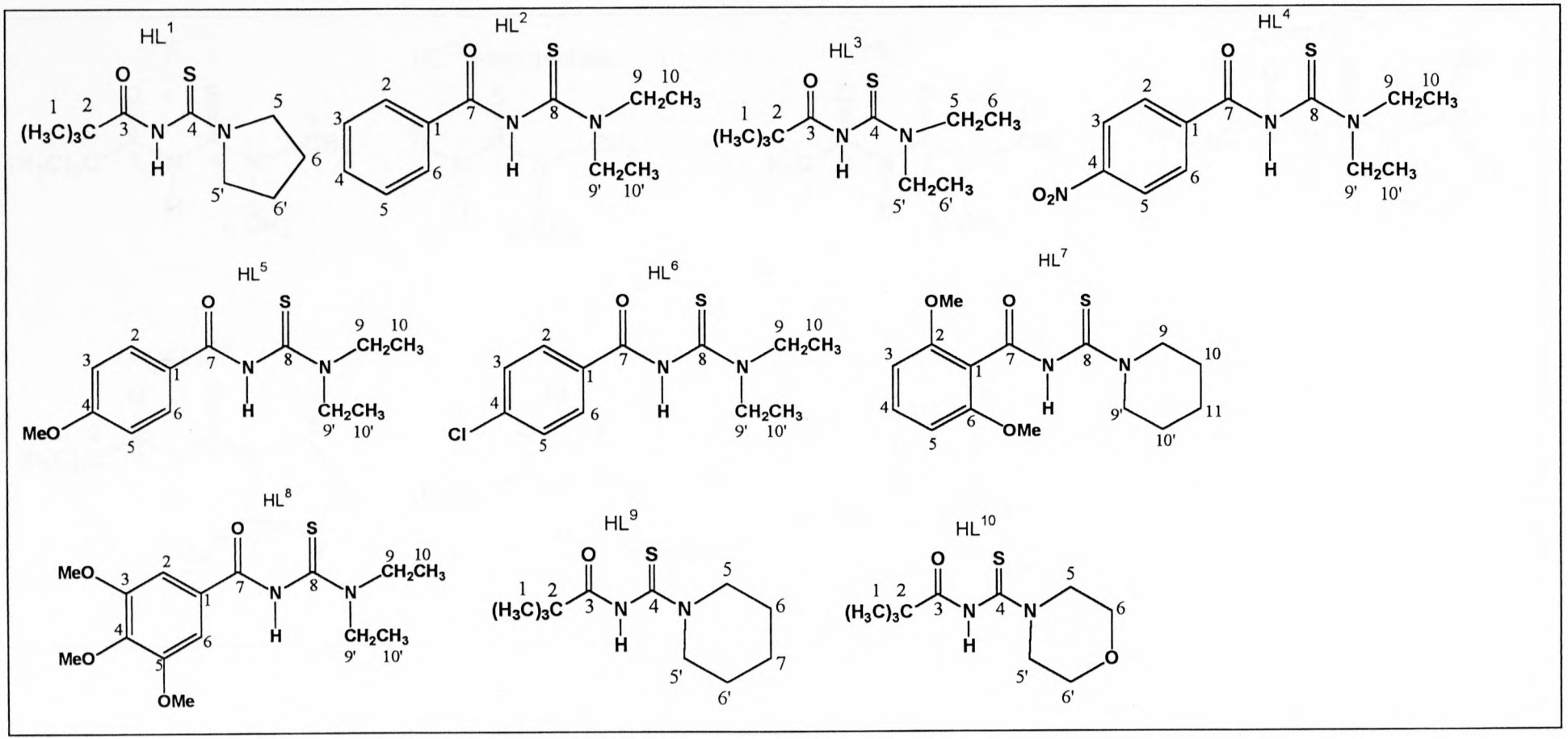

The structures of the synthesised compounds (continued)

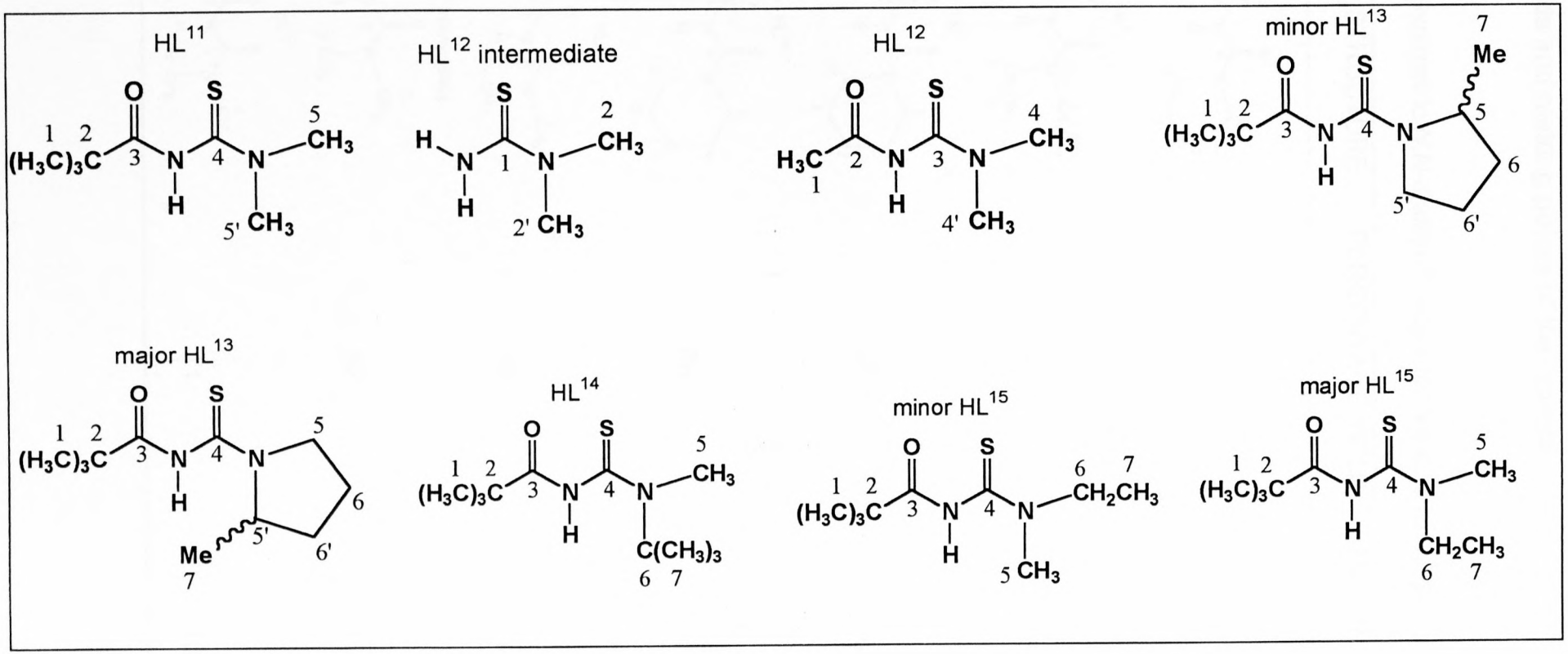

2.1.3 Yields and melting points of the ligands

Table 5: Symmetric *N,N*-dialkyl-*N'*-acylthiourea structures, yields and mp's

LIGAND STRUCTURE	PERCENTAGE YIELD	MELTING POINT/°C
HL^1 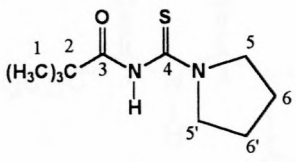	77	136-138
HL^3 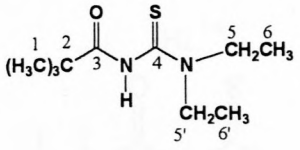	70	89-90
HL^9 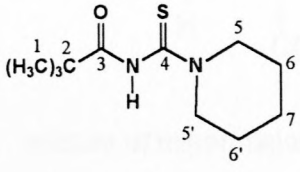	67	89-91
HL^{10} 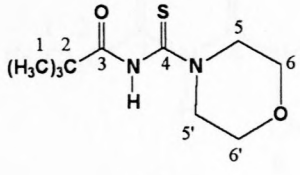	66	131-134
HL^{11} 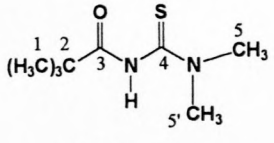	45	78-81
HL^{12} intermediate 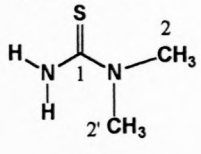	67	158-160
HL^{12} 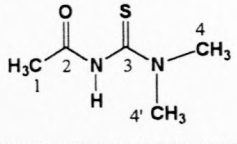	71	103-105

Table 6: Asymmetric *N,N*-dialkyl-*N'*-acylthiourea structures, yields and mp's

LIGAND STRUCTURE	PERCENTAGE YIELD	MELTING POINT/°C
mixture of minor/major HL[13] 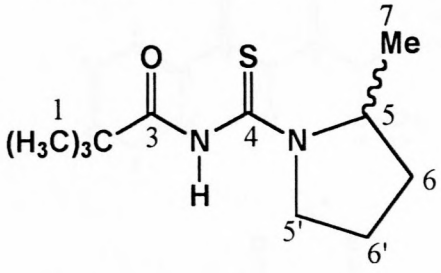	79	81-82
HL[14] 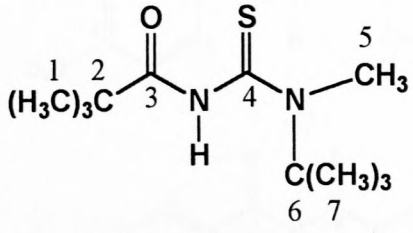	95	91-93
mixture of minor/major HL[15] 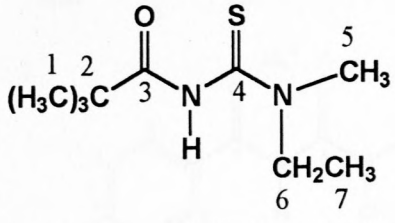	90	54-55

Table 7: Symmetric *N,N*-dialkyl-*N'*-aroylthiourea structures, yields and mp's

LIGAND STRUCTURE	PERCENTAGE YIELD	MELTING POINT/°C
HL^2 & (HL^2)* 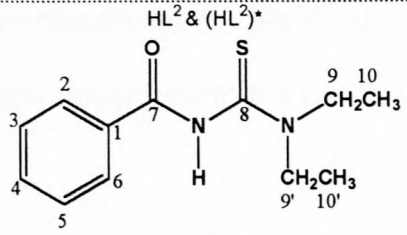	86, (73)*	98-100
HL^4 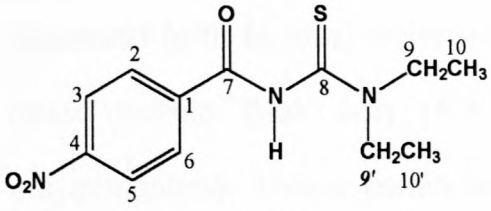	42	164-166
HL^5 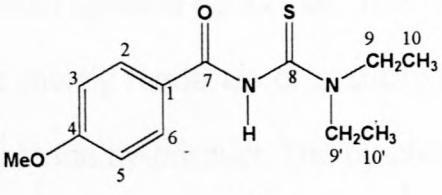	79	92-95
HL^6 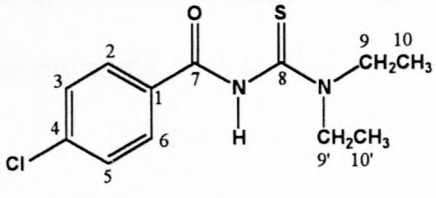	86	149-151
HL^7 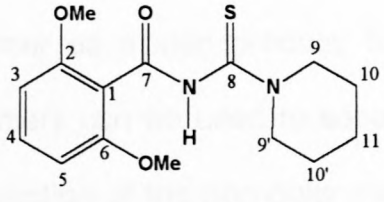	-	155-158
HL^8 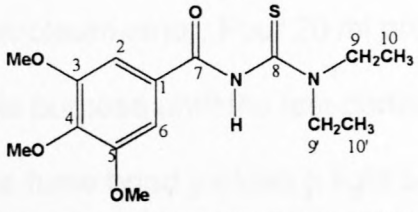	-	161-164

(HL^2)* is the same as HL^2 but 47% ^{13}C enriched at the thiocarbonyl carbon.
- synthesised and donated by Miller. Their purity was checked by means of mp measurement and ^1H and $^{13}C\{^1H\}$ NMR spectroscopy.

2.2 THE SYNTHESIS AND CHARACTERISATION OF *cis*-DICHLOROBIS(TRI-n-BUTYLPHOSPHINE)PLATINUM(II)

The compound *cis*-[Pt(P^nBu_3)$_2Cl_2$] was prepared according to Kaufman,[49] with some deviations in the purification steps.

A solution of (4.2 g, 0.010 mol) potassium tetrachloroplatinate(II), K_2PtCl_4 in degassed (with N_2 gas) water was shaken vigorously in a stoppered 250 ml round bottom flask with (4.3 g, 0.020 mol) of freshly distilled tri-n-butylphosphine. This is continued until the initially deep orange supernatant liquid lightens no further. This is attained after three hours. The crude product is mainly made up of a sticky brown material covered with white potassium chloride by-product. The by-product is easily removed by washing with several 10 ml portions of water. The washed product is dried under vacuum at room temperature.

The crude product is thought to be mainly the *cis*-isomer with some *trans*-isomer as a side product. Ideally, the differences in the polarity of these isomers can be used to separate them. This can be attained by continuous extraction of the non-polar *trans*-isomer by a non-polar low boiling (40-60°C) petroleum ether. Four 20 ml portions of ice-cold petroleum ether were used for this purpose until the last portion adopted no colour. Leaving the extractions in the fume hood yielded a light brown powder, which is mainly the *trans*-isomer, was collected and purified by recrystallisation. The purification of the *trans* product was effected as follows:

50 ml petroleum ether (40-60°C) is added to the crude product and heated to boiling, followed by addition of 96% ethanol drop-wise until the solid just dissolves. Cooling on an ice-salt bath a white powder crystallises, which can be collected by filtration. This procedure may be repeated several times for a highly pure white product. The portion that did not dissolve in cold petroleum ether, which is mainly the *cis*-isomer, underwent the same purification steps and produced a white powder. These two crops were individually characterised and were found to be identical. Collectively, a yield of 69% was obtained. The product was characterised by $^{31}P\{^{1}H\}$ NMR spectroscopy referenced to 85% H_3PO_4 external standard, elemental (C and H) analysis and melting point determination (see section **2.7**).

2.3 SYNTHESES AND CHARACTERISATION OF PLATINUM(II) CHELATES, *cis*-[Pt(L-*S,O*)$_2$], WITH ASYMMETRIC *N,N*-DIALKYL-*N'*-ACYLTHIOUREAS AS LIGANDS.

With the three asymmetric *N,N*-dialkyl-*N'*-acylthioureas (HL^{13}, HL^{14} and HL^{15}) synthesised (in **table 6**), their corresponding platinum(II) complexes were prepared. The synthetic route for the preparation of these platinum(II) complexes follows that described by Koch *et al.*[50]

To a specific amount of ligand dissolved in a mixture of an organic solvent (acetonitrile or dioxane) and water, a potassium tetrachloroplatinate solution is added drop-wise. (The platinum salt is insoluble in organic solvents while the ligands are insoluble in water, therefore, appropriate ratios of organic solvent

and water are used for the reactions). After the addition of the platinum(II) salt is complete, sodium acetate, dissolved in a minimum amount of water, is added. The reaction is usually carried out at elevated temperatures typically 50 to 60°C for three hours. To ensure that the reaction has proceeded to completion the reaction mixture is left stirring for further 15 hours at room temperature. A yellow solid precipitates in the reaction vessel. Water is added to the reaction vessel to precipitate more product (as it is insoluble in water). The slurry is then placed in a refrigerator, and the product is collected by centrifugation after a few hours. For characterisation, melting point determinations are carried out, elemental analysis and ^{1}H, $^{13}C\{^{1}H\}$ and $^{195}Pt\{^{1}H\}$ NMR spectra are measured. For complexes resulting for both HL^{13} and HL^{15}, mixtures of *EE*, *ZZ* and *EZ* isomers are anticipated to form. This is verified by low field (50 MHz) $^{13}C\{^{1}H\}$ as well as high field (129 MHz) $^{195}Pt\{^{1}H\}$ NMR spectra. The semi double bond character of the C-N bond of the **-(S)CN(R)(R')-** moiety results in *E* and *Z* isomers of the ligands. This isomerism is carried through to the resulting complexes and hence configurational isomers result. The configurational isomers *cis*-[Pt(*E,E*-$L^{13,15})_2$], *cis*-[Pt(*Z,Z*-$L^{13,15})_2$] and *cis*-[Pt(*E,Z*-$L^{13,15})_2$] isomers were observed to be chromatographically equivalent and hence alternative means of determining the ^{195}Pt peaks for each complex was devised. Full structural elucidation of the complexes resulting from HL^{13} is carried out using high field two-dimensional ^{1}H-(^{13}C)-^{195}Pt correlation NMR spectroscopy.

2.4 SYNTHESES AND CHARACTERISATION OF PLATINUM(II) CHELATES WITH *N*-THIOPHOSPHORYLATED BENZAMIDE AND *N,N'*-THIOPHOSPHENYLTHIOUREA AS LIGANDS

N-diisopropoxythiophosphoryl thiobenzamide (**I**) and *N'*-diisopropoxythiophosphoryl-*N*-phenylthiourea (**II**) were prepared and donated by Brusko V. following a procedure by Zimin *et al.*[24] Their identity and purity was checked from their ^{1}H and ^{13}C NMR spectra. K_2PtCl_4 and CH_3COONa are commercially available and were used without further purification.

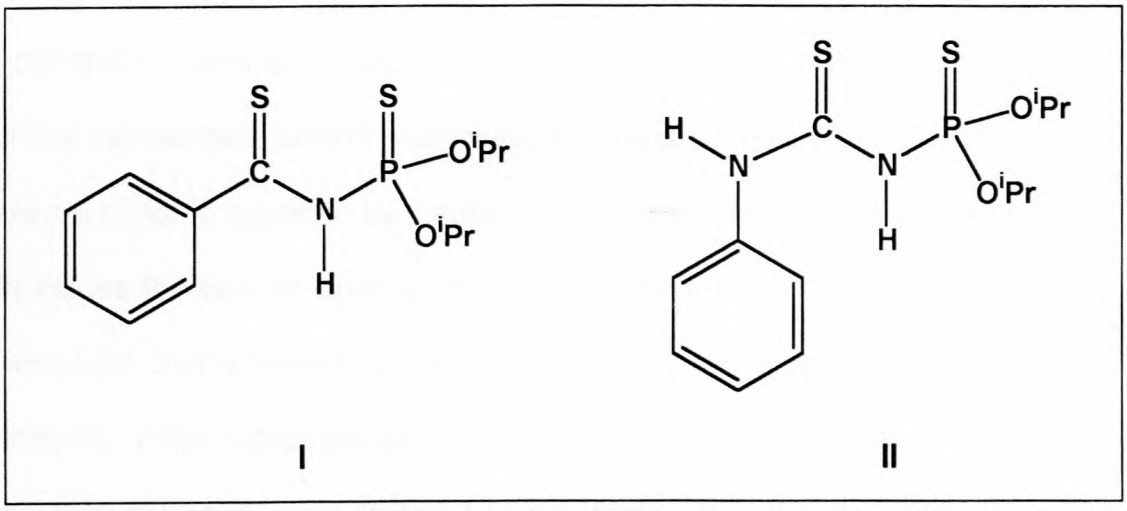

Figure 8: Sulphur-sulphur donor *N*-diisopropoxythiophosphoryl thiobenzamide (**I**) and *N'*-diisopropoxythiophosphoryl-*N*-phenylthiourea (**II**) ligands.

Improved and almost quantitative yields of the platinum(II) chelates of **I** and **II** were obtained using a different method of preparation to that of Mashkina *et al*,[51] which uses H_2PtCl_6 as a starting material. The synthetic route employed for the synthesis of these complexes is as follows: A 40 cm^3 solution of K_2PtCl_4 (0.20 g, 0.48 mmol) in water-acetonitrile (1:1 v/v) is added drop-wise to a warm (60°C) solution of the ligand (2 x 0.48 mmol) in 20 cm^3 acetonitrile - 10 cm^3 water mixed with CH_3COONa (4 x 0.48 mmol), which was dissolved in

a minimum quantity of water. The reaction mixture is stirred for three hours at 60°C and left stirring at room temperature for further 15 hours to ensure completion of the reaction. An excess amount of water (50 cm^3) is added and the reaction mixture is cooled to 4°C in a refrigerator for about two hours and a bright yellow solid is observed settling at the bottom of the reaction vessel. This is collected by centrifugation and recrystallised from acetonitrile/chloroform mixtures. When employing the same synthetic method (metal to ligand) with ligand **II**, a mixture of *cis* and *trans*-isomers of the complex is obtained in 44:56 ratios.

Adding the ligand and sodium acetate mixture to the K_2PtCl_4, in local excess drives the reaction to form exclusively the *trans*-isomer. The *trans/cis* isomers are not trivial to separate by means of TLC despite having different but similar R_f values for various organic eluents and solvent mixtures. The complexes were fully characterised by means of melting point measurement, elemental analysis, NMR spectroscopy as well as X-ray crystallography. The *trans* complex obtained using ligand **I** is air stable while the one obtained using ligand **II**, disintegrate within a few hours when taken out of the mother liquor. This necessitates the latter complex to be covered with paratone oil before X-ray data collection.

2.5 REACTIONS OF *cis*-[Pt(P^nBu_3)$_2Cl_2$] WITH THE LIGANDS

2.5.1 *N,N*-dialkyl-*N'*-acyl(aroyl)thioureas as ligands

The coordination chemistry of *N,N*-dialkyl-*N'*-acyl(aroyl)thioureas has been investigated and reviewed by Koch.[17] As part of our continuing study of these ligands, investigations of the relative donicity of the *S* and *O* donor atoms of HL^n and the possible effect of the substituent groups **R/R'** and **R"** on the co-ordination properties of HL^n have been undertaken. To this end, we have chosen to examine the reaction of HL^n with *cis*-[Pt(P^nBu_3)$_2Cl_2$] complexes in chloroform.

A 0.1 molar *cis*-[Pt(P^nBu_3)$_2Cl_2$] solution is prepared by dissolving an appropriate amount of *cis*-[Pt(P^nBu_3)$_2Cl_2$] in deuterated chloroform. The $^{31}P\{^1H\}$ NMR spectrum of this is measured before an equimolar amount of each ligand is added to separate samples of the *cis*-[Pt(P^nBu_3)$_2Cl_2$] solutions. Once again the $^{31}P\{^1H\}$ NMR spectrum of each sample mixture of *cis*-[Pt(P^nBu_3)$_2Cl_2$] + ligand is measured. No evident reaction is noted to take place visually and from the $^{31}P\{^1H\}$ NMR spectra taken.

Addition of a base (triethylamine) rapidly deprotonates and activates the ligand to react with *cis*-[Pt(P^nBu_3)$_2Cl_2$]. As the ligand coordinates to the platinum(II) centre, two chloride ions are expelled in the immediate coordination sphere of the platinum. One chloride ion becomes a counter ion of the resulting positively charged mixed ligand-platinum(II) complex, *cis*-[Pt(P^nBu_3)$_2$(L-S,O)]$^+Cl^-$, while the other is an anion of the formed

triethylammonium chloride salt. The mixed ligand-platinum(II) complex formed is such that it is coordinated as a six membered chelate with sulphur and oxygen being the donors of the ligand. The **reaction scheme 4** serves to illustrate the species formed as the reaction takes place.

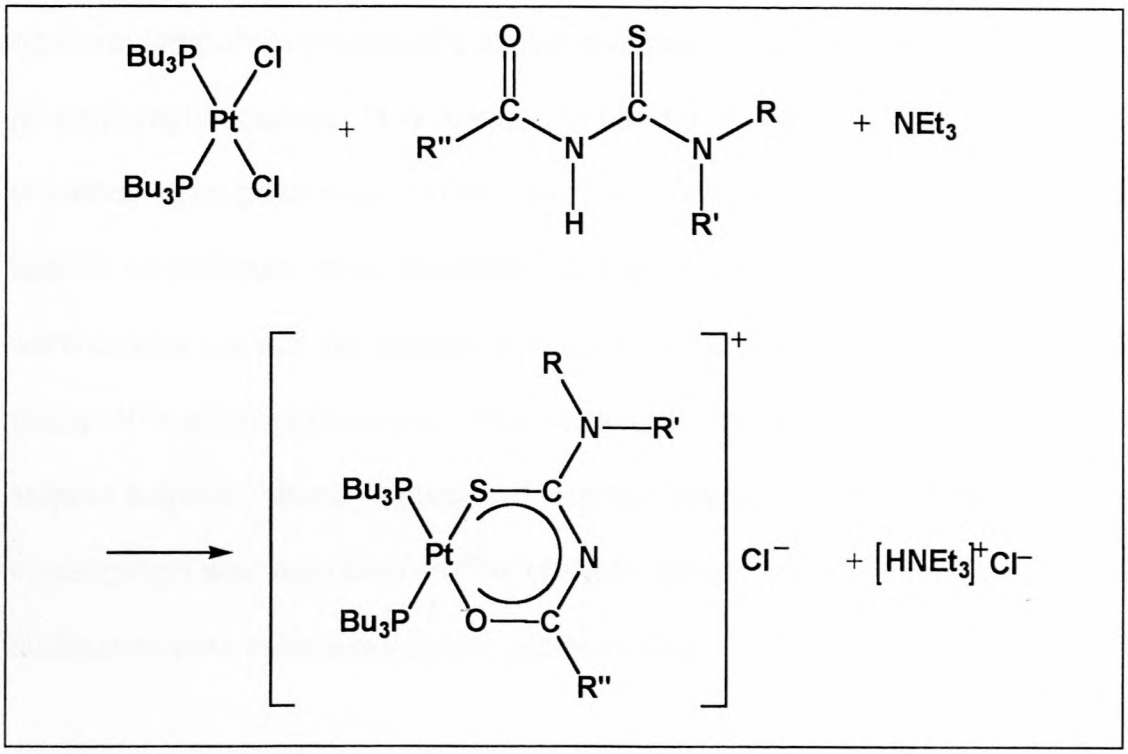

Reaction scheme 4: A general reaction of *N,N*-dialkyl-*N'*-acyl(aroyl)thiourea with *cis*-$[Pt(P^nBu_3)_2Cl_2]$ in the presence of a base.

These simple reactions were conveniently studied by means of $^{31}P\{^1H\}$ and $^{195}Pt\{^1H\}$ high-resolution nuclear magnetic resonance spectroscopy.

In special cases, other nuclei were used as probes to answer specific questions. For example, when the *N,N*-diethyl-*N'*-benzoylthiourea, ^{13}C enriched at the thiocarbonyl carbon, was reacted with *cis*-$\{Pt(P^nBu_3)_2Cl_2]$, the $^{13}C\{^1H\}$ NMR spectrum of this sample revealed important information as described in section **3.2.3**.

2.5.2 *N*-diisopropoxythiophosphoryl thiobenzamide, and *N'*-diisopropoxythiophosphoryl-*N*-phenylthiourea, as ligands

The similarity of *N*-diisopropoxythiophosphoryl thiobenzamide (**I**) and *N'*-diisopropoxythiophosphoryl-*N*-phenylthiourea (**II**) to *N,N*-dialkyl-*N'*-acyl(aroyl)thioureas prompted a similar investigation conducted to *N,N*-dialkyl-*N'*-acyl(aroyl)thioureas. Tthe reaction of **I** and **II** with *cis*-$[Pt(P^nBu_3)_2Cl_2]$ in the presence of a base was carried out. The coordination properties of these ligands to platinum were compared to that of other ligands. The reactions were carried out with no deviations to the previous method employed for *N,N*-dialkyl-*N'*-acyl(aroyl)thioureas. The expected chelates here, however, are sulphur-sulphur bound instead of sulphur-oxygen bound. The mode of investigation was restricted to $^{31}P\{^1H\}$ NMR spectroscopy as the phosphorus nucleus is more sensitive than the platinum one.

2.6 ISOMERISATION OF PLATINUM(II) CHELATES WITH *N,N*-THIOPHOSPHENYLTHIOUREA AS A CHELATING LIGAND

In solution, some of the complexes synthesised in section **2.4** were noted to undergo rare *trans*/*cis* and *cis*/*trans* chelate isomerism. Both the isolated *cis* and *trans* complexes formed from ligand **II** undergo this chelate isomerism resulting in a mixture of *cis* and *trans* complexes. Such a phenomenon has been reported in relatively few articles.[52, 53, 54] This prompted further investigations as to what triggers this to happen and its dependence on the

polarity of the solvent. The isomerism of the *trans*-isomer to the *cis*-isomer was studied in detail and the kinetics of this process were followed.

In about 0.7 ml of three different deuterated solvents of different polarity, viz: dimethylformamide, chloroform and benzene, about 10 mg of the pure *trans*-isomer were dissolved. $^{31}P\{^{1}H\}$ NMR spectra of each were then measured at regular intervals over a length of time to monitor the isomerism. When necessary, adequate amounts of solvent were added to the samples to maintain a constant volume over the period of the experiment.

After one week, catalytic amounts (a drop) of a dilute (0.5%) organic acid (trifluoroacetic acid) were added to the benzene sample to see if it would encourage this isomerism. Ideally, the $^{31}P\{^{1}H\}$ NMR spectra of this sample should be measured against a control where no acid is added. Limitations on the amount of sample of the available *trans*-isomer did not allow this. The $^{31}P\{^{1}H\}$ NMR spectra were adequate to serve as the only means to monitor this process

2.7 EXPERIMENTAL DETAILS

The melting points (mp's) were determined using a Reichet Thermova microscope. The elemental analysis for C, H, N and S were carried out using a Heraeus CHN rapid combustion analyzer. The ^{1}H, ^{13}C nuclear magnetic resonance spectra were recorded in 5mm tubes in $CDCl_3$ solution unless stated otherwise. The instruments used were either Varian Unity 300 or 400 or

600 spectrometer operating at 300, 400 and 600 MHz for ^{1}H spectra, or at 75, 100 and 150 MHz for ^{13}C spectra. All the ^{1}H and ^{13}C spectra were measured at 25°C and the chemical shifts (δ) are referenced to tetramethylsilane (TMS) as an internal standard. The ^{1}H-(^{13}C)-^{195}Pt NMR correlation experiments (which achieved remarkable results) for assigning the ^{195}Pt peaks of the platinum(II) chelates of asymmetrically disustituted acylthioureas were carried out by Hoffmann, E. and Agyropoulos, D., courtesy of Varian GmbH in Germany, as we did not have the equipment to do this. All reagents are commercially available and were used with no further purification except being dried appropriately as previously described.

N-Pyrrolidyl-*N'*-*2,2*-dimethylpropanoylthiourea, HL^1

A recrystallised yield of (5.0 g, 0.023 mol, 77%) was recovered. For characterisation mp 98-100°C, (Found C, 60.95; H, 6.95; N, 11.50, S, 13.36. $C_{10}H_{18}N_2SO$ required C, 60.99; H, 6.82; N, 11.85; S, 13.57%); δ_H(400 MHz, $CDCl_3$) 1.33 (6H, s, $C_{10/10'}$), 3.62 and 4.03 (4H, s, $C_{9/9'}$), 7.55 (2H, m, $C_{3/5}$), 7.57 (1H, m, C_4), 7.83 (2H, d, $C_{2/6}$), 8.35 (1H, s, NH); δ_C(100 MHz, $CDCl_3$) 11.5 and 13.2 ($C_{10/10'}$), 47.8 ($C_{9/9'}$), 179.4 (C_8), 163.8 (C_7), 132.8 (C_4), 127.8 ($C_{3/5}$), 128.9 ($C_{2/6}$), 132.9 (C_1).

N,N-Diethyl-*N'*-benzoylthiourea, HL^2

A recrystallised yield of (6.1 g, 0.026 mol, 86%) was recovered. For characterisation mp 98-100°C, (Found C, 60.91; H, 6.81; N, 11.79, S, 13.34.

$C_{12}H_{16}N_2SO$ required C, 60.99; H, 6.82; N, 11.85; S, 13.57%); δ_H(400 MHz, $CDCl_3$) 1.33 (6H, s, $C_{10/10'}$), 3.62 and 4.03 (4H, s, $C_{9/9'}$), 7.55 (2H, m, $C_{3/5}$), 7.57 (1H, m, C_4), 7.83 (2H, d, $C_{2/6}$), 8.35 (1H, s, NH); δ_C(100 MHz, $CDCl_3$) 11.5 and 13.2 ($C_{10/10'}$), 47.8 ($C_{9/9'}$), 179.4 (C_8), 163.8 (C_7), 132.8 (C_4), 127.8 ($C_{3/5}$), 128.9 ($C_{2/6}$), 132.9 (C_1).

_N,N_-Diethyl-_N'_-benzoylthiourea, (HL^2)* - 47% ^{13}C enriched at C(S)

A recrystallised yield of (0.7 g, 0.003 mol, 73%) was recovered. For characterisation mp 98-100°C, (Found C, 60.91; H, 6.81; N, 11.79, S, 13.34. $C_{12}H_{16}N_2SO$ required C, 60.99; H, 6.82; N, 11.85; S, 13.57%); δ_H(400 MHz, $CDCl_3$) 1.33 (6H, s, $C_{10/10'}$), 3.62 and 4.03 (4H, s, $C_{9/9'}$), 7.55 (2H, m, $C_{3/5}$), 7.57 (1H, m, C_4), 7.83 (2H, d, $C_{2/6}$), 8.35 (1H, s, NH); δ_C(100 MHz, $CDCl_3$) 11.5 and 13.2 ($C_{10/10'}$), 47.8 ($C_{9/9'}$), 179.4 (C_8), 163.8 (C_7), 132.8 (C_4), 127.8 ($C_{3/5}$), 128.9 ($C_{2/6}$), 132.9 (C_1).

_N,N_-Diethyl-_N'_-_2,2_-dimethylpropanoylthiourea, HL^3

A recrystallised yield of (4.7 g, 0.021 mol, 70%) was recovered. For characterisation mp 89-90°C, (Found C, 55.80; H, 10.19; N, 12.76, S, 14.66. $C_{10}H_{20}N_2SO$ required C, 55.52; H, 9.32; N, 12.95; S, 14.82%); δ_H(400 MHz, $CDCl_3$) 1.24 (15H, s, C_1 and $C_{6/6'}$), 3.50 and 3.95 (4H, s, $C_{5/5'}$), 7.64 (1H, s, NH); δ_C(100 MHz, $CDCl_3$) 11.5 and 13.1 ($C_{6/6'}$), 27.1 (C_1), 39.6 (C_2), 47.5 and 48.0 ($C_{5/5'}$), 174.7 (C_3), 179.7 (C_4).

N,N-Diethyl-*N'*-*4*-nitrobenzoylthiourea, HL^4

A recrystallised yield of (3.5 g, 0.013 mol, 42%) was recovered. For characterisation mp 164-166°C, (Found C, 51.15; H, 5.67; N, 15.09, S, 11.35. $C_{12}H_{15}N_3SO_3$ required C, 51.12; H, 5.37; N, 14.94; S, 11.40%); δ_H(300 MHz, DMSO) 1.21 (6H, m, $C_{10/10'}$), 3.53 and 3.93 (4H, q, $C_{9/9'}$), 8.10 (2H, d, $C_{2/6}$), 8.32 (2H, d, $C_{3/5}$), 10.90 (1H, s, NH); δ_C(75 MHz, DMSO) 11.0 and 13.3 ($C_{10/10'}$), 46.5 and 47.2 ($C_{9/9'}$), 179.6 (C_8), 162.6 (C_7), 138.6 (C_4), 129.5 ($C_{3/5}$), 123.5 ($C_{2/6}$), 149.4 (C_1).

N,N-Diethyl-*N'*-*4*-methoxybenzoylthiourea, HL^5

A recrystallised yield of (6.4 g, 0.024 mol, 79%) was recovered. For characterisation mp 92-95°C, (Found C, 58.59; H, 6.89; N, 10.34, S, 11.34. $C_{13}H_{18}N_2SO_2$ required C, 58.62; H, 6.81; N, 10.52; S, 12.04%); δ_H(400 MHz, $CDCl_3$) 1.34 (6H, s, $C_{10/10'}$), 3.60 and 4.02 (4H, s, $C_{9/9'}$), 7.27 (2H, m, $C_{2/6}$), 7.37 (2H, m, $C_{3/5}$), 8.25 (1H, s, NH); δ_C(100 MHz, $CDCl_3$) 11.5 and 13.2 ($C_{10/10'}$), 47.9 ($C_{9/9'}$), 179.3 (C_8), 163.6 (C_7), 129.3 (C_4), 112.8 ($C_{3/5}$), 134.1 ($C_{2/6}$), 160.0 (C_1) 55.5 (methoxy substituent).

N,N-Diethyl-*N'*-*4*-chlorobenzoylthiourea, HL^6

A recrystallised yield of (7.0 g, 0.026 mol, 86%) was recovered. For characterisation mp 149-151°C, (Found C, 52.95; H, 5.65; N, 10.08, S, 11.78. $C_{12}H_{15}N_2SOCl$ required C, 53.23; H, 5.58; N, 10.35; S, 11.84%); δ_H(400 MHz,

$CDCl_3$) 1.32 (6H, s, $C_{10/10'}$), 3.60 and 4.02 (4H, s, $C_{9/9'}$), 7.44 (2H, m, $C_{2/6}$), 7.77 (2H, d, $C_{3/5}$), 8.33 (1H, s, NH); δ_C(100 MHz, $CDCl_3$) 11.5 and 13.2 ($C_{10/10'}$), 47.9 ($C_{9/9'}$), 179.1 (C_8), 162.8 (C_7), 139.3 (C_4), 129.2 ($C_{3/5}$), 129.1 ($C_{2/6}$), 157.9 (C_1).

N-Piperidyl-*N'*-*2,6*-dimethoxybenzolythiourea, HL[7]

For characterisation mp 155-158°C, (Found C, 54.99; H, 7.24; N, 8.61, S, 9.65. $C_{15}H_{20}N_2SO_3$ required C, 55.20; H, 6.79; N, 8.58; S, 9.82%); δ_H(300 MHz, $CDCl_3$) 1.32 (6H, s, 2 methoxy substituents), 3.59 and 4.02 (4H, s, $C_{9/9'}$), 3.89 (6H, s, $C_{10/10}$ and C_{11}) 7.06 (3H, s, $C_{3/5}$and C_4), 8.55 (1H, s, NH); δ_C(75 MHz, $CDCl_3$) 11.4 and 13.2 ($C_{10/10'}$), 47.7 ($C_{9/9'}$), 179.5 (C_8), 163.3 (C_7), 105.3 (C_4), 127.5 ($C_{3/5}$), 153.2 ($C_{2/6}$), 142.2 (C_1) 55.5 and 60.9 (methoxy substituents).

N,N-Diethyl-*N'*-*3,4,5*-trimethoxybenzoylthiourea, HL[8]

For characterisation mp 161-164°C, (Found C, 58.38; H, 6.69; N, 9.05, S, 10.01. $C_{15}H_{22}N_2SO_3$ required C, 58.42; H, 6.54; N, 9.08; S, 10.40%); δ_H(300 MHz, $CDCl_3$) 1.74 (9H, s, 3 methoxy substituents) 3.83 (6H, s, $C_{10/10'}$), 3.7 and 4.1 (4H, s, $C_{9/9'}$), 7.27 and 6.55 (2H, m, $C_{2/6}$) 8.19 (1H, s, NH); δ_C(75 MHz, $CDCl_3$) 24.0 and 25.4 ($C_{10/10'}$), 52.8 ($C_{9/9'}$), 177.8 (C_8), 161.4 (C_7), 104.0 (C_4), 114.1 ($C_{3/5}$), 157.7 ($C_{2/6}$), 131.7 (C_1) 56.11, and 56.15 (methoxy substituents).

N-Piperidyl-*N'*-*2,2*-dimethylpropanoylthiourea, HL[9]

A recrystallised yield of (2.2 g, 0.010 mol, 67%) was recovered. For characterisation mp 89-91°C, (Found C, 59.53; H, 8.81; N, 11.95, S, 13.94. $C_{11}H_{20}N_2SO$ required C, 57.86; H, 8.83; N, 12.27; S, 14.04%); δ_H(300 MHz, $CDCl_3$) 1.24 (9H, s, C_1), 1.67 (6H, m, $C_{6/6'}$ and C_7), 3.45 and 4.08 (4H, s, $C_{5/5'}$), 7.80 (1H, s, NH); δ_C(75 MHz, $CDCl_3$) 23.9 (C_7), 27.1 (C_1), 39.6 (C_2), 52.8 and 52.9 ($C_{5/5'}$), 174.1 (C_3), 178.4 (C_4).

N-Mopholine-*N'*-*2,2*-dimethylpropanoylthiourea, HL[10]

A recrystallised yield of (2.2 g, 0.010 mol, 66%) was recovered. For characterisation mp 131-134°C, (Found C, 52.02; H, 7.82; N, 11.92, S, 13.60. $C_{10}H_{18}N_2SO$ required C, 52.15; H, 7.88; N, 12.16; S, 13.92%); δ_H(300 MHz, $CDCl_3$) 1.25 (9H, s, C_1), 3.50 and 4.15 (4H, s, $C_{5/5'}$), 3.79 (4H, s, $C_{6/6'}$), 7.89 (1H, s, NH); δ_C(75 MHz, $CDCl_3$) 27.0 (C_1), 39.7 (C_2), 51.6 and 52.4 ($C_{5/5'}$), 174.2 (C_3), 179.5 (C_4).

N,N-Dimethyl-*N'*-*2,2*-dimethylpropanoylthiourea, HL[11]

A recrystallised yield of (2.6 g, 0.014 mol, 45%) was recovered. For characterisation mp 78-81°C, (Found C, 51.14; H, 8.90; N, 14.89, S, 16.49. $C_8H_{16}N_2SO$ required C, 51.03; H, 8.57; N, 14.88; S, 16.94%); δ_H(300 MHz, $CDCl_3$) 1.25 (9H, s, C_1), 3.13 and 3.43 (6H, s, $C_{5/5'}$), 7.82 (1H, s, NH); δ_C(75 MHz, $CDCl_3$) 27.1 (C_1), 39.7 (C_2), 42.9 and 44.2 ($C_{5/5'}$), 174.4 (C_3), 180.4 (C_4).

1,1-Dimethylthiourea, intermediate for HL[12]

A yield of (2.1 g, 0.020 mol, 68%) is recovered. For characterisation mp 158-160°C, (Found C, 34.54; H, 7.98; N, 26.34; S, 29.91 $C_3H_8N_2S$ required C, 34.59; H, 7.74; N, 26.89; S, 30.78%); δ_H(300 MHz, DMSO) 3.11 (6H, s, $C_{2/2'}$), 7.13 (2H, s, NH_2); δ_C(75 MHz, DMSO) 39.50 ($C_{2/2'}$), 181.58 (C_1).

N,N-Dimethyl-*N'*-acetylthiourea, HL[12]

A yellow solid is recovered by extraction and collected by evaporating the solvent. A yield of (2.0 g, 0.014 mol, 71%) is recovered. For characterisation mp 103-105°C, (Found C, 41.49; H, 6.64; N, 19.11; S, 21.56. $C_5H_{10}N_2SO$ required C, 41.07; H, 6.89; N, 19.16; S, 21.93%) δ_H(400 MHz, $CDCl_3$) 2.10 (3H, s, C_1), 3.17 and 3.41 (6H, s, $C_{4/4'}$), 8.66 (1H, s, NH); δ_C(100 MHz, $CDCl_3$) 23.78 (C_1 and $C_{4/4'}$), 166.50 (C_2), 180.00 (C_3).

N-(2-Methylpyrrolidine)-*N'*-*2,2*-dimethylpropanoylthiourea, HL[13]

A brown solid is recovered by extraction and collected by evaporating the solvent. A yield of (2.1 g, 0.009 mol, 95%) was recovered. For characterisation mp 81-82°C, (Found C, 58.45; H, 9.14; N, 12.30, S, 13.85. $C_{11}H_{20}N_2SO$ required C, 58.11; H, 8.42; N, 12.32; S, 14.10%); δ_H(300 MHz, $CDCl_3$) 1.23 (9H, s, C_1 major and minor), 1.37 (3H, s, C_7 major) 1.39 (3H, s, C_7 minor) 1.95 (4H, m, $C_{6/6'}$ major and minor) 7.81 (1H, s, NH); δ_C(75 MHz, $CDCl_3$) 19.3 and 22.2 ($C_{6/6'}$)minor, 18.2 and 24.3 ($C_{6/6'}$)major, 27.1 (C_1)major

and minor, 32.4 (C_7)major, 33.8 (C_7)minor 39.6 (C_2)major and minor, 52.6 and 60.2 ($C_{5/5'}$)major, 54.9 and 58.8 ($C_{5/5'}$)minor, 174.3 (C_3)major, 174.4 (C_3)minor, 176.4 (C_4)major 176.5 (C_4)minor.

_N_-tert-butyl-_N_-methyl- _N'_-2,2-dimethylpropanoylthiourea, HL[14]

A recrystallised yield of (1.8 g, 0.008 mol, 95%) was recovered. For characterisation mp 91-93°C, (Found C, 57.49; H, 9.54; N, 12.38, S, 13.40. $C_{11}H_{22}N_2SO$ required C, 57.35; H, 9.63; N, 12.16; S, 13.92%); δ_H(400 MHz, $CDCl_3$) 1.22 (9H, s, C_1), 1.63 (9H, s, C_7), 3.04 (3H, s, C_5), 7.85 (1H, s, NH); δ_C(100 MHz, $CDCl_3$) 27.0 (C_1), 27.5 (C_7) 39.1 (C_5), 39.7 (C_2), 61.6 (C_6), 173.2 (C_3), 179.8 (C_4).

_N_-Methyl-_N_-ethyl- _N'_-2,2-dimethylpropanoylthiourea, HL[15]

A recrystallised yield of (1.8 g, 0.009 mol, 90%) was recovered. For characterisation mp 54-55°C, (Found C, 53.93; H, 8.71; N, 13.69, S, 15.05. $C_9H_{18}N_2SO$ required C, 53.43; H, 8.97; N, 13.85; S, 15.85%); δ_H(600 MHz, $CDCl_3$) 1.24 (12H, s, C_1 minor/major and C_7major), 1.30 (3H, t, C_7)minor, 3.08 (3H, s, C_5), 3.93 (2H, q, C_6), 7.26 (1H, s, NH); δ_C(100 MHz, $CDCl_3$) 27.0 (C_1), 10.8 (C_7)major, 12.8 (C_7)minor 39.6 (C_5)major, 40.1 (C_5)minor, 51.1 (C_6)major, 50.1 (C_6)minor 39.7 (C_2), 174.3 (C_3), 179.7 (C_4).

cis-dichlorobis(tri-n-butylphosphine)platinum(II)

A recrystallised yield of (4.6 g, 0.007 mol, 69%) was recovered. For characterisation, mp 142-144°C, (Found C, 43.44; H, 7.58 $PtP_2C_{24}H_{54}Cl_2$ required C, 42.98; H, 8.12%), $\delta(^{31}P)$: 1.27 ppm and $^1J(^{195}Pt\text{-}^{31}P)$: 3515 Hz.[40]

cis-bis(2-methylpirrolidyl-_N'_-2,2-dimethylpropanoylthioureato)platinum(II), _cis_-[Pt(L^{13}-_S,O_)$_2$]

The yellow precipitate obtained was collected by centrifugation and vacuum dried. A crude yield of (307 mg, 0.474 mmol, 79%) was obtained. For characterisation mp 175-177°C (Found: C, 40.06; H, 5.99; N, 8.48; S, 9.30 $PtC_{22}H_{38}N_4S_2O_2$ required C, 40.79; H, 5.66; N, 8.65; S, 9.90%); δ_C(50 MHz, $CDCl_3$) 19.1 and 22.8 ($C_{6/6'}$)_EE_ and _EZ_, 18.4 and 22.0 ($C_{6/6'}$)_ZZ_ and _EZ_, 28.2 (C_1)_EE_, _ZZ_ and _EZ_, 31.7 (C_7)_EE_ and _EZ_, 42.0 and 42.1(C_2)_EE_, _ZZ_ and _EZ_, 50.2 and 57.0 ($C_{5/5'}$)_EE_ and _EZ_, 49.8 and 56.5 ($C_{5/5'}$)_ZZ_ and _EZ_, 164.2 (C_4)_EE_ and _EZ_ 163.8 (C_4)_ZZ_ and _EZ_, 182.5 (C_3)_EE_ and _EZ_, 182.9 (C_3)_ZZ_ and _EZ_.

cis-bis(_N_-tert-butyl-_N_-methyl-_N'_-2,2-dimethylpropanoylthioureato)platinum(II), _cis_-[Pt(L^{14}-_S,O_)$_2$]

A crude yield of (221 mg, 0.338 mmol, 84%) was obtained. For characterisation (Found: C, 39.36; H, 6.69; N, 8.41; S, 7.69 $PtC_{22}H_{42}N_4S_2O_2$ required C, 40.41; H, 6.47; N, 8.57; S, 9.81%); δ_H (600 MHz, $CDCl_3$) 1.22 (9H, s, C_1); 1.54 (9H, s, C_7); 3.31 (3H, s, C_5) δ_C(151 MHz, $CDCl_3$) 28.3 (C_1), 28.9

(C_7), 37.7 (C_5), 42.4 (C_6), 61.9 (C_2), 169.3 (C_4), 181.8 (C_3) δ_{Pt}(129 MHz, $CDCl_3$) -2733.

***cis-bis*(*N*-ethyl-*N*-methyl-*N'*-2,2-dimethylpropanoylthioureato)platinum(II), *cis*-[Pt(L^{15}-*S,O*)$_2$]**

A crude yield of (232 mg, 0.388 mmol, 81%) was obtained. For characterisation mp 110-111°C (Found: C, 36.45; H, 6.08; N, 9.42; S, 8.84 $PtC_{18}H_{34}N_4S_2O_2$ required C, 36.17; H, 5.73; N, 9.37; S, 10.73%); δ_C(50 MHz, $CDCl_3$) 12.3 (C_7)*EE* and *EZ*, 11.8 (C_7)*ZZ* and *EZ*, 28.2 (C_1)*EE*, *ZZ* and *EZ*, 37.9 (s, C_5)*ZZ* and *EZ*, 39.5 (s with Pt satellites, C_5)*EE* and *EZ*, 42.2 (C_2)*EE*, *ZZ* and *EZ*, 47.9 (s, C_6)*EE* and *EZ* 48.6 (couples to Pt, C_6)*ZZ* and *EZ*, 166.9 (C_4)*ZZ* and *EZ*, 167.3 (C_4)*EE* and *EZ*, 183.0 (C_3) *EE* and *EZ*, 183.3 (C_3)*ZZ* and *EZ* δ_{Pt}(129 MHz, $CDCl_3$) -2731, -2735 and -2739 (s, sharp, *ZZ*, *ZE* and *EE* respectively).

***trans*-[Pt{$C_6H_5C(S)NP(S)(O^iPr)_2$}$_2$], Ia**

The crude product (0.37 g, 0.427 mmol, 92%) was recrystallised from chloroform and acetonitrile. Bright yellow *crystals* of *trans* [Pt{$C_6H_5C(S)NP(S)(O^iPr)_2$}$_2$] were collected with mp 160-162°C (Found: C, 37.97; H, 4.96; N, 3.37; S, 15.24; $PtP_2C_{26}H_{38}N_2S_4O_4$ required C, 37.72; H, 4.63; N, 3.38; S, 15.49%); $\delta_P(CDCl_3)$ 42.6 [2P, s, ^2J(PtP) 119 Hz], $\delta_{Pt}(CDCl_3)$ -3923.

trans, IIa and _cis_, IIb isomers of $[Pt\{C_6H_5NHC(S)NP(S)(O^iPr)_2\}_2]$

A mixture of orange and yellow powder of $Pt\{C_6H_5NHC(S)NP(S)(O^iPr)_2)\}_2]$ (0.37 g, 0.431 mmol 90%), which turned out to be a mixture of *trans* and *cis* isomers was obtained (Found: C, 36.34; H, 4.73; N, 6.48; S, 14.65; $PtP_2C_{26}H_{40}N_4S_4O_4$ required C, 36.48; H, 4.70; N, 6.53; S, 14.95%); $\delta_P(CDCl_3)$ 43.6 [2P, s, ^2J(PtP) 106 Hz] and 44.4 [2P, s, ^2J(PtP) 101 Hz]; $\delta_{Pt}(CDCl_3)$ -3964 and -3956 respectively.

trans-isomer of $[Pt\{C_6H_5NHC(S)NP(S)(O^iPr)_2\}_2]$, IIa

The crude product was recrystallised from chloroform and acetonitrile. Bright orange *crystals* of *trans* $[Pt\{C_6H_5NHC(S)NP(S)(O^iPr)_2)\}_2]\cdot 2CH_3CN$ were collected (0.186 g,0.198 mmol 41%). For characterisation mp 180-183°C (Found: C, 37.94; H, 4.75; N, 8.36; S, 13.63; $PtP_2C_{26}H_{40}N_4S_4O_4\cdot 2CH_3CN$ required C, 38.33; H, 4.93; N, 8.94; S, 13.64%); $\delta_P(CDCl_3)$ 43.6 [2P, s, ^2J(PtP) 105 Hz], $\delta_{Pt}(CDCl_3)$ -3964.

Chapter Three

Results and Discussion

3 RESULTS AND DISCUSSION

3.1 *N,N*-DIALKYL-*N'*-ACYL(AROYL)THIOUREA LIGANDS

3.1.1 General properties

In the previous chapter the synthesis of *N,N*-dialkyl-*N'*-acyl(aroyl)thioureas was described in detail. Here, a study of the relative donicity of the *S* and *O* donor centres of the ligands is described as their alkyl groups **R** and **R'** are varied while the group **R"** is fixed. The second case that is presented is where the **R** and **R'** alkyl groups are fixed and variations on the benzoyl or benzoyl derivatives are studied. Prior to this, the nature of the ligands is first discussed.

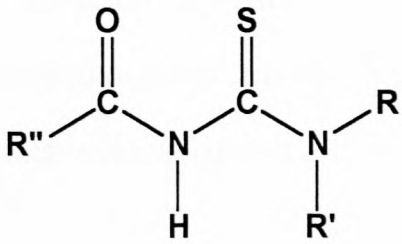

Most of the ligands were found to be stable in air and remain as solids for long periods without decomposing. The exception to this is *N*-tert-butyl-*N*-methyl-*N'*-2,2-dimethylpropanoylthiourea (HL^{14}), which turns into a liquid at room temperature after standing for several weeks. The ^{1}H NMR spectrum of this liquid is similar to that of the solid material whereas the $^{13}C\{^{1}H\}$ NMR spectrum has the carbonyl peak missing. It is not easy to decide with absolute

certainty whether the compound has undergone structural changes, but no further investigation was undertaken, and only the pure solid was used for further studies.

In general, all the ligands are soluble in chloroform except *N,N*-diethyl-*N'-4*-nitrobenzoylthiourea (HL^4), which is only slightly soluble in this solvent. The solubility of acylthioureas in water is observed to increase as the alkyl substituents **R**, **R'** and **R"** get less bulky. For example, HL^{12} with **R**, **R'** and **R"** all being methyl groups is more soluble in water than HL^{11} with **R**, **R'** methyl groups but **R"** a tertiary butyl group. Fixing **R"** as a tertiary butyl and changing the ethyl groups **R**, **R'** in HL^3 to methyl groups as in HL^{11} also increases the solubility of these ligands in water. The solubility of the ligand in water has important implications regarding their retrieval after being synthesised and left to crystallise from water. Both the soluble and the sparingly water-soluble ligands then need to be extracted by means of a water immiscible organic solvent. In some analytical and process chemistry applications of *N,N*-dialkyl-*N'*-acyl(aroyl)thioureas, water soluble ligands are however ideal, as illustrated by Mautjana.[22]

3.1.2 X-ray crystal structure of *N,N*-diethyl-*N'-4*-nitrobenzoylthiourea, HL^4

The molecular structure of *N,N*-diethyl-*N'-4*-nitrobenzoylthiourea (HL^4), was determined by means of X-ray diffraction method as described in chapter two, section **2.1.1**. This ligand is monoclinic and crystallised in the space group $P2_1/c$ with a = 6.887(1) Å, b = 19.244(3) Å, c = 10.147(1) Å, β = 93.01(1)° and

Z = 4. The molecular structure of HL^4 is shown in **figure 9**, with selected bond lengths and torsion angles. The rest of the crystallographic data of this molecule is in appendix **1**, **tables 1 and 2**.

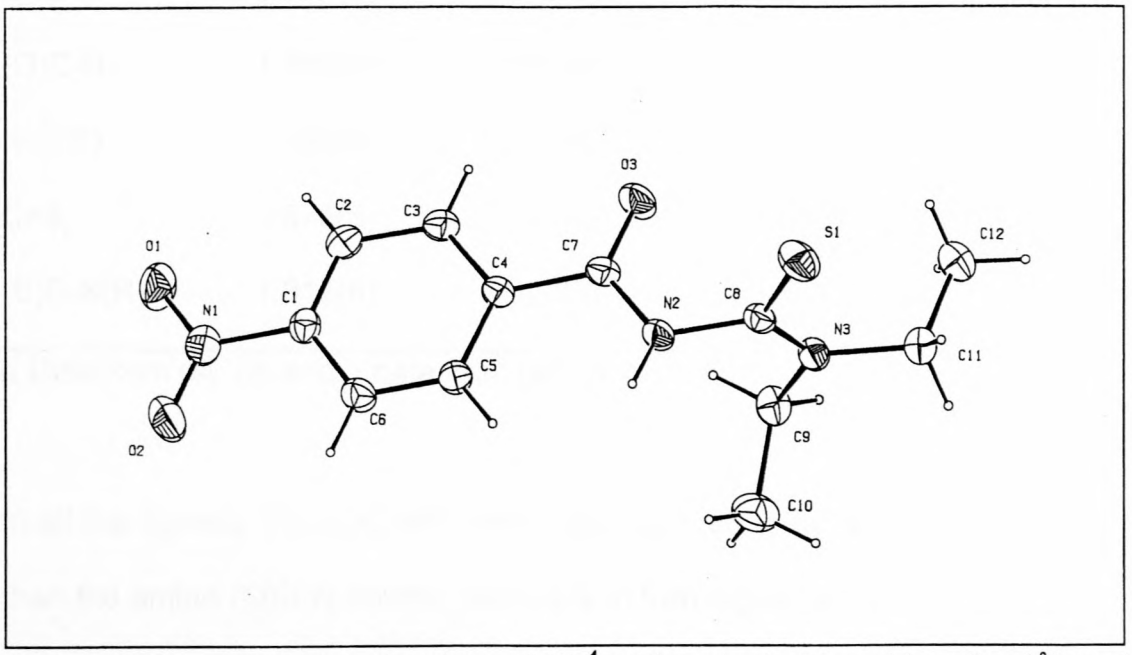

Figure 9 The molecular structure of HL^4, with selected bond lengths (Å) and torsion angles (°). S(1)-C(8) 1.663(2), O(3)-C(7) 1.230(2), N(3)-C(8) 1.324(3), N(2)-C(7) 1.344(2), N(2)-C(8) 1.430(3), O(3)-C(7)-N(2)-C(8) 4.2(3), S(1)-C(8)-N(2)-C(7) 90.7(2).

The molecular structure of HL^4 is very similar to other published structures with no significant difference between its bond lengths and those in previously characterised benzoylthiourea type ligands, (see **table 8**).

Table 8: Comparison of relevant bond lengths (Å) for ligands 1 (*N*-(n-butyl)-*N'*-benzoylthiourea), 2 (*N,N*-di(n-butyl)-*N'*-naphthoylthiourea), 3 (*N*-(n-propyl)-*N'*-benzoylthiourea) and HL^4 (*N,N*-diethyl-*N'*-*4*-nitrobenzoylthiourea).

Bond	Ligand 1[b]	Ligand 2[b]	Ligand 3[a]	HL^4
C=O	1.226(6)	1.215(3)	1.226(5)	1.230(2)
(O)C-N	1.368(6)	1.376(4)	1.383(4)	1.344(2)
N-C(S)	1.386(6)	1.420(6)	1.393(5)	1.430(3)
C=S	1.676(5)	1.662(2)	1.678(4)	1.663(2)
(S)C-N(R)	1.317(6)	1.320(3)	1.332(7)	1.324(3)

a Data from ref. 55 and b data from ref. 56

In all the ligands, the (S)C-NR bonds are observed to be significantly shorter than the amide (O)C-N bonds, which are in turn significantly shorter than the N-C(S) bonds. This trend indicates a decreasing general degree of partial bond character in these bonds. It is evident that all the N-C bonds are, on average, significantly shorter than the average C-N single bond of 1.472(5) Å,[57] more so for the (S)C-NR bonds. The implications of the double bond character of the alkyl-substituted thiourea (S)C-NR bond are discussed in the section **3.1.3**.

In solid state, the *S* and *O* donor atoms of these ligands are observed to be pointing in opposite directions. For example, in HL^4, the torsion angles O(3)-C(7)-N(2)-C(8) and S(1)-C(8)-N(2)-C(7) are 4.2(3)° and 90.7(2)° respectively. By contrast, for the monoalkyl-substituted ligands 1 and 3, this phenomenon may be enhanced by the hydrogen bonding of the carbonyl oxygen atom with the -(S)CNHR moiety. This hydrogen bonding essentially locks the *O* donor in

a planar six-membered ring, with deviations less than 0.1 Å from the plane for ligand 1[55] (see the illustration, below).

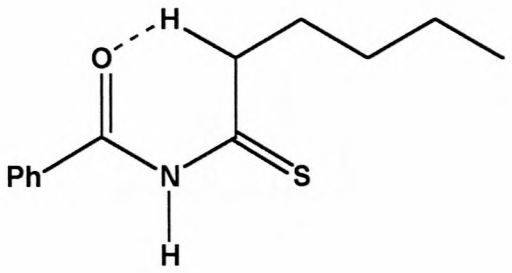

3.1.3 Implications of the partial double bond character of alkyl-substituted thiourea (S)C-NRR' bond: asymmetrically disubstituted acylthioureas.

As has been discussed in the previous section, the C-N bonds are observed to be significantly shorter than the average C-N single bond, even more so for the alkyl-substituted thiourea (S)C-NR bonds. Now, comparing the possible resonance structures of the ligand in **figure 10**, and various molecular structures studied by Koch *et al*,[58, 59] suggest that structure **i** is more favoured than **ii** and **iii**.

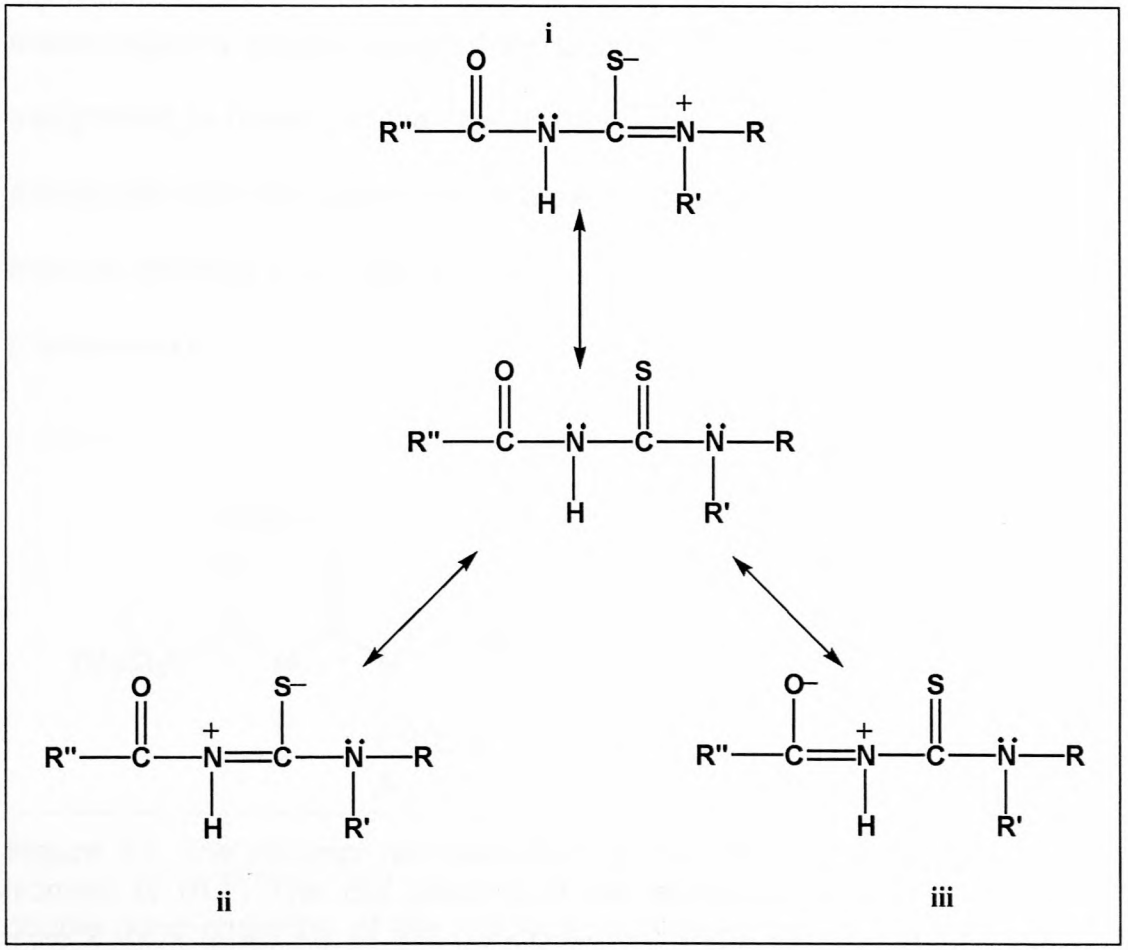

Figure 10: The possible resonance structures of *N,N*-dialkyl-*N'*-acyl(aroyl)thioureas, with **i** being the most favoured.

This partial double bond character of the alkyl-substituted thiourea N-C bond has profound implications when it comes to the synthesis of *N,N*-dialkyl-*N'*-acylthioureas with different alkyl groups. Configurational *E*/*Z* isomers, which are produced in unequal amounts result, for example, the *E*/*Z* isomers of *N*-(2-methylpyrrolidine)-*N'*-*2,2*-dimethylpropanoylthiourea (HL^{13}) and *N*-ethyl-*N*-methyl-*N'*-*2,2*-dimethylpropanoylthiourea (HL^{15}). From a semi-quantitative $^{13}C\{^1H\}$ NMR spectrum, the *E*/*Z* isomer distribution is 3:1 in favour of the *E* isomer in the latter case, for example. Assigning the asymmetrically disubstituted dialkyl thiourea ligands as to which is the major and which is the minor component was achieved by means of $^{13}C\{^1H\}$ NMR spectroscopy. The assignment is based on the knowledge of the shielding effect of

electronegative groups reported by Günther.[36] In this particular case, the assignment is based on the reasonable assumption that the sulphur atom shields the carbons closest to it, whereas such an effect is not experienced by carbons pointing away from it. The ligand HL^{15} is a good illustration of this phenomenon:

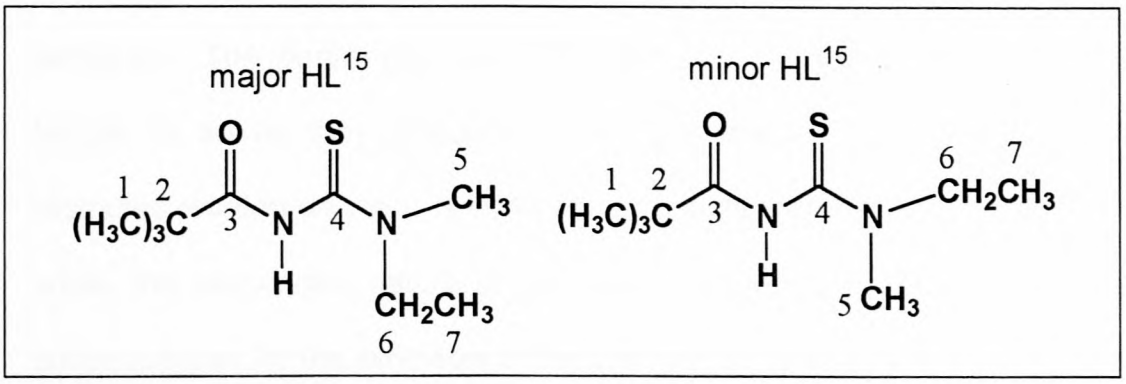

Figure 11: The pictorial representation of the major (*E*) and the minor (*Z*) isomers of HL^{15}. The *E*/*Z* labeling of the isomers is based on the partial double bond character of the (S)C-N(Et)(Me) bond that forces the ligand to orientate itself in the two configurational isomers shown. The distribution of these major(*E*) and minor(*Z*) isomers was determined by means of semi-quantitative $^{13}C\{^1H\}$ NMR spectroscopy.

In the $^{13}C\{^1H\}$ NMR spectrum of *N*-ethyl-*N*-methyl-*N'*-2,2-dimethylpropanoylthiourea (HL^{15}), C_5 of the *E* isomer is expected to appear at higher field relative to C_5 of the minor isomer due to the shielding effect of the sulphur atom, with C_6 of the *E* isomer appearing at lower field relative to C_6 of the *Z* isomer. C_7 of the *Z* isomer is thought to be bent towards the sulphur atom hence its resonance peak appears at higher field than C_7 of the *E* isomer. This information is sufficient for an unambiguous assignment of the *E* and the *Z* isomers of these ligands.

3.1.4 The behaviour of asymmetrically disubstituted acylthioureas at elevated temperature as monitored by means of $^{13}C\{^1H\}$ NMR spectroscopy.

The $^{13}C\{^1H\}$ NMR spectra of the asymmetrically disubstituted acylthiourea ligands (HL^{13} and HL^{15}) at elevated temperatures reveal an interesting behaviour. The peaks distinguishing the major (*E*) from the minor (*Z*) no longer do so as they coalesce into single peaks. The ligands lose the restricted rotation on the C-N bond at higher temperatures. On the NMR time scale, the asymmetric nature of the ligands is then lost. This has important consequences for the synthesis of the platinum complexes with these ligands. Since the synthesis is carried out at elevated temperatures, it is not easy to predict the isomer distribution of the resulting complexes before hand, even if the initial distribution of major (*E*) and minor (*Z*) isomers of the ligands had been determined. The $^{13}C\{^1H\}$ NMR spectrum of HL^{15} was run at 25°C and at 50°C (**figure 12**) to illustrate the phenomenon described. When the spectrum is rerun at 25°C, the isomers reemerge with the same distribution as in with a fresh solution.

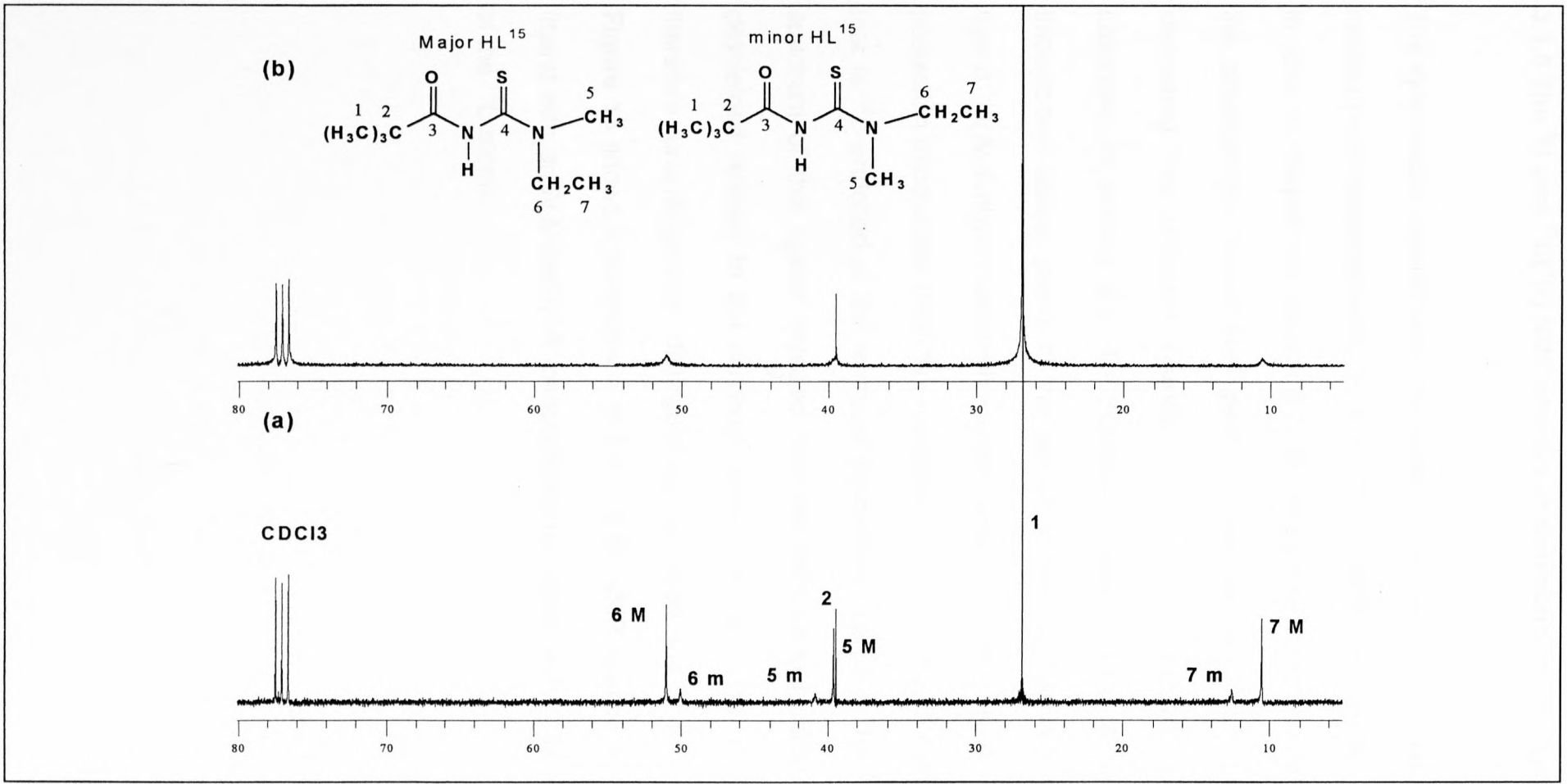

Figure 12: A section of a $^{13}C\{^{1}H\}$ NMR spectrum of *N*-ethyl-*N*-methyl-*N'*-2,2-dimethylpropanoyl, HL^{15}, that distinguishes the major (*E*) and minor (*Z*) isomers measured at **(a)** 25°C and at **(b)** 50°C. M in the spectrum run at 25°C corresponds to the major isomer while m corresponds to the minor isomer.

3.1.5 The ^{1}H and $^{13}C\{^{1}H\}$ NMR spectra assignments of the ligands

The synthesised ligands were characterised by means of elemental analysis, melting point measurements, ^{1}H and $^{13}C\{^{1}H\}$ NMR spectroscopy as reported in detail in chapter two section **2.7**. Of importance in the ^{1}H NMR spectra, is the characteristic broad N-H peak of the ligands. This is important in comparing the unbound ligands and the resultant *bis*-Pt(II)complexes described in section **3.3**. To distinguish between the carbonyl and the thiocarbonyl carbon peaks of the ligands in the $^{13}C\{^{1}H\}$ NMR spectra, one ligand (*N,N*-diethyl-*N'*-benzoylthiourea) was prepared using ^{13}C-enriched potassium thiocyanate (KSC*N), resulting in a *N,N*-diethyl-*N'*-benzoylthiourea that is ^{13}C-enriched at the eventual thiocarbonyl carbon. The $^{13}C\{^{1}H\}$ NMR spectrum of this ligand revealed that the thiocarbonyl carbon, -^{13}C(S) is deshielded relative to the carbonyl carbon, -C(O) in the unbound ligand, therefore unambiguously distinguishing between these two resonances. **Figure 13** shows a comparison of the $^{13}C\{^{1}H\}$ NMR spectra of ^{13}C-enriched ligand with an *N,N*-diethyl-*N'*-benzoylthiourea ligand with natural abundance of the ^{13}C atoms.

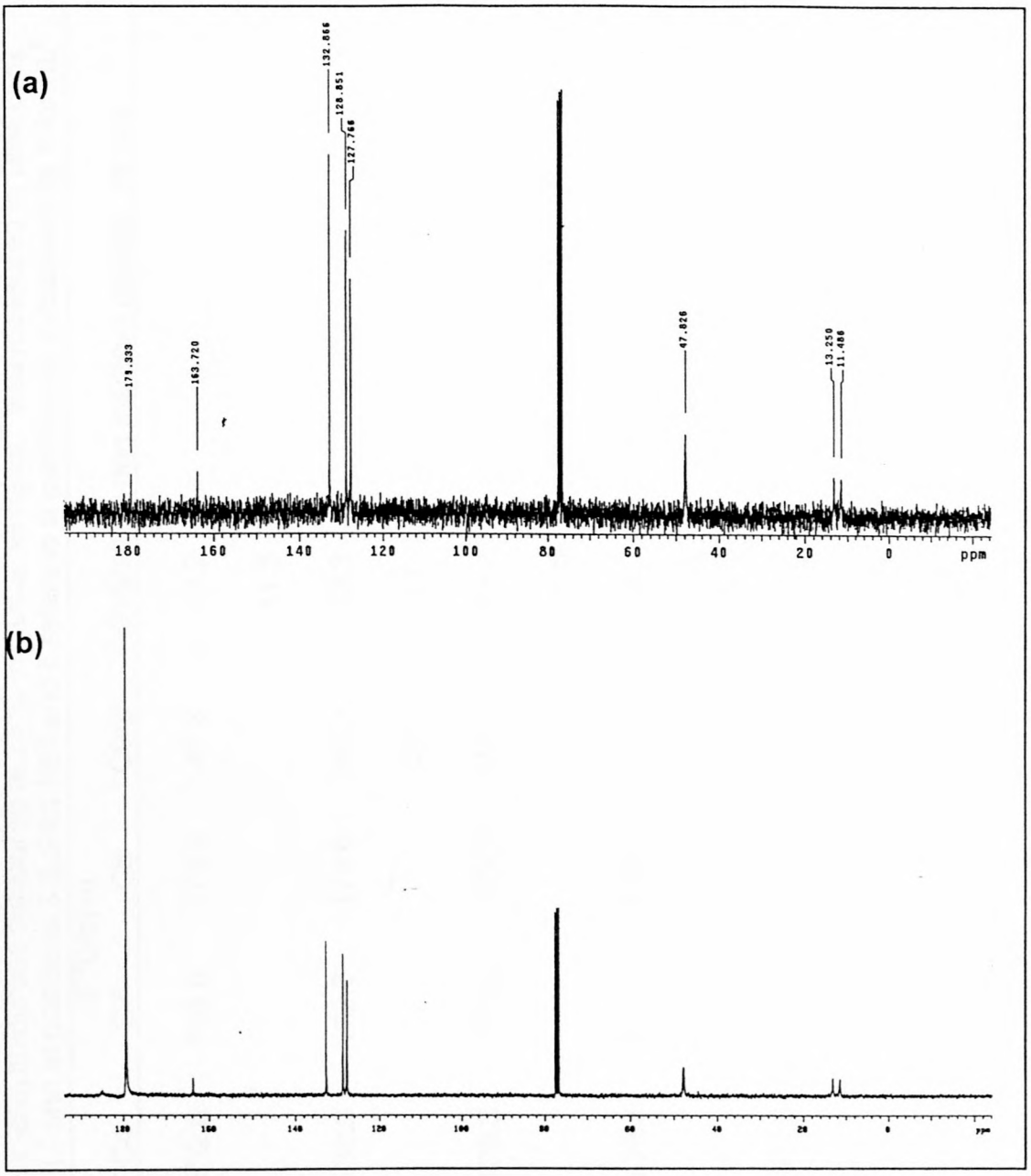

Figure 13: $^{13}C\{^{1}H\}$ NMR spectra of **(a)** *N,N*-diethyl-*N'*-benzoylthiourea **(b)** thiocarbonyl ^{13}C-enriched *N,N*-diethyl-*N'*-benzoylthiourea . The thiocarbonyl carbon stands out unambiguously at 179.3 ppm in the ^{13}C-enriched ligand, while it is of equal intensity with the carbonyl carbon at 163.7 ppm in the unenriched ligand.

A summary of the $^{13}C\{^{1}H\}$ NMR assignments of all the synthesised ligands is shown in **tables 9, 10 and 11**.(see numbering scheme in section **2.1.2** or **tables 5, 6** and **7** in chapter two, pages 36-40)

Table 9: $^{13}C\{^{1}H\}$ NMR data for *N,N*-dialkyl-*N'*-aroylthioureas measured at 25°C in $CDCl_3$, while HL^4 was measured in DMSO-d_6. a: refers to methoxy substituents for HL^5, HL^7 and at positions 3 & 5 for HL^8 and b refers to a methoxy at substituent at 4 for HL^8

	$\delta^{13}C$/ppm									
LIGAND	C1	C2/6	C3/5	C4	C7	C8	C9/9'	C10/10'	ring methoxy groups	others
HL^2	132.9	128.9	127.8	132.8	163.8	179.4	47.8	13.2		
								11.5		
HL^4	149.4	123.5	129.5	138.6	162.6	179.6	47.2	13.3		
							46.5	11		
HL^5	160.1	134.1	112.8	129.3	163.6	179.3	47.9	13.2	55.5[a]	
								11.5		
HL^6	157.9	129.1	129.2	139.3	162.8	179.1	47.9	13.2		
								11.5		
HL^7	142.2	153.2	127.5	105.3	163.3	179.5	47.7	13.2	56.4[a]	
								11.4		
HL^8	131.7	157.7	114.1	104	161.4	177.8	52.8	25.4	56.2[a]	60.9[b]
								24	56.1[a]	

Table 10: $^{13}C\{^{1}H\}$ NMR data for the symmetric disubstituted *N,N*-dialkyl-*N'*-acylthioureas measured at 25°C in $CDCl_3$.

LIGAND	C1	C2	$\delta^{13}C$/ppm C3(O)	C4(S)	C5/5'	C6/6'	C7/7'
HL^1	27.2	39.7	174.4	176.8	54.5/52.6	26.2/24.6	
HL^3	27.1	39.6	174.7	179.7	48.0/47.5	13.1/11.5	
HL^9	27.1	39.6	174.1	178.4	52.9/52.8	26.0/25.1	23.8
HL^{10}	27.0	39.7	174.2	179.5	52.4/51.6	66.2	
HL^{11}	27.1	39.7	174.4	180.4	44.2/42.9		
HL^{12}	23.8(C1)			166.5(C2)	180.0(C3)	23.8(C4/4')	

Table 11: $^{13}C\{^{1}H\}$ NMR data for the asymmetric disubstituted *N,N*-dialkyl-*N'*-acylthioureas measured at 25°C in $CDCl_3$.

	$\delta^{13}C$/ppm						
LIGAND	C1	C2	(O)C3	(S)C4	C5/5'	C6/6'	C7/7'
major $HL^{13}(E)$	27.1	39.6	174.3	176.4	52.6	18.2	32.4
					60.2	24.3	
minor $HL^{13}(Z)$	27.1	39.6	174.4	176.5	54.9	19.3	33.9
					58.8	22.2	
major $HL^{14}(E)$	27.0	39.5	173.2	179.8	31.9	61.6	27.5
major $HL^{15}(E)$	27.0	39.7	174.3	179.7	39.6	51.1	10.8
minor $HL^{15}(Z)$	27.0	39.7	174.3	179.7	41.0	50.1	12.8

3.2 REACTION OF *cis*-[Pt(P^nBu_3)$_2Cl_2$] WITH LIGANDS, HL^n

3.2.1 Synthesis and characterisation of *cis*-[Pt(P^nBu_3)$_2Cl_2$]

The preparation of *cis*-[Pt(P^nBu_3)$_2Cl_2$] followed a synthetic route by Kaufman[49] and was described in detail in chapter two, section **2.2**. Though elemental analysis is an essential as part of structural elucidation, the molecular formula of *cis*-[Pt(P^nBu_3)$_2Cl_2$] is the same as of the *trans*-isomer, $PtP_2C_{24}H_{54}Cl_2$, making differentiation impossible between the two isomers. One method of distinguishing the two isomers in a simple but very effective way, is the melting point determination of the products. The melting points of these isomers differ significantly, the *trans*-isomer having a lower melting point of 65°C-66°C whereas the *cis*-isomer has a melting point of 142°C-144°C.[49] Apart from the melting point determination, the $^{31}P\{^1H\}$ NMR spectra of the two indicate that the *cis*-isomer has a $^1J(^{195}Pt\text{-}^{31}P)$ coupling constant of 3515 Hz while the *trans*-isomer has a $^1J(^{195}Pt\text{-}^{31}P)$ coupling constant of 2397 Hz.[40] The strong *trans influence* of the two phosphine groups is such that they compete for the same platinum *d*-orbital resulting in a smaller coupling constant for *trans*-[Pt(P^nBu_3)$_2Cl_2$].[7] The two methods are therefore adequate to characterise and assess the relative purity of whichever product has been synthesised.

3.2.2 Reactions of *cis*-[Pt(P^nBu_3)$_2Cl_2$] with HL^n = *N,N*-dialkyl-*N'*-aroylthioureas

The relative donicity of *S* and *O* in the ligands of the type *N,N*-dialkyl-*N'*-aroylthioureas (HL^n) was investigated by reacting each ligand with an equimolar quantity of *cis*-[Pt(P^nBu_3)$_2Cl_2$] in the presence of a base. The base of choice here is triethylamine, whose role is to deprotonate the ligand at the weakly acidic **N-H** proton of the **-(O)CNHC(S)-** moiety, thereby significantly increasing the nucleophilicity of the ligands towards the platinum in *cis*-[Pt(P^nBu_3)$_2Cl_2$]. The monoionic ligand then rapidly displaces two chloride ions of *cis*-[Pt(P^nBu_3)$_2Cl_2$] via its *S* and *O* donors in the chloroform solution. All the reactions take place in the NMR tube.

The starting material, *cis*-[Pt(P^nBu_3)$_2Cl_2$] as well as some of the ligands are colourless in solution while others are yellow. Upon addition of the base, the solution in the NMR tube becomes brightly coloured (yellow) due to the spontaneous coordination of the ligand to the platinum(II) centre of *cis*-[Pt(P^nBu_3)$_2Cl_2$], expelling the two chloride ions. The result of the reaction is a mixed ligand-platinum(II) complex, *cis*-[Pt(P^nBu_3)$_2$(L-*S,O*)]$^+Cl^-$. The reaction progress was followed mainly by means of $^{31}P\{^1H\}$ and $^{195}Pt\{^1H\}$ NMR spectroscopy. Where necessary, other nuclei (^1H and $^{13}C\{1H\}$ NMR) were also employed to follow these reactions. The ^{31}P atoms in *cis*-[Pt(P^nBu_3)$_2Cl_2$] are equivalent and resonate as a singlet δ = 1.2, symmetrically flanked by $^1J(^{195}Pt\text{-}^{31}P)$ coupling satellites (see **figure 14(a)**). This magnetic equivalence is lifted once the ligand coordinates to the platinum(II) ion. This is

demonstrated with a $^{31}P\{^{1}H\}$ NMR spectrum of the mixed ligand-platinum(II) complex that shows two doublet signals, one resonating downfield and another upfield with respect to the chemical shift of the *cis*-$[Pt(P^{n}Bu_3)_2Cl_2]$ complex. Both doublets are symmetrically flanked by $^{1}J(^{195}Pt\text{-}^{31}P)$ coupling satellites (see **figure 14(b)**). As a result of the magnetic inequivalence of the phosphorus atoms in the mixed ligand-platinum(II) complex, *cis*-$[Pt(P^{n}Bu_3)_2(L\text{-}S,O)]^{+}Cl^{-}$, the phosphorus atoms couple to each other with a $^{2}J(^{31}P\text{-}^{31}P)$ spin coupling constant of 24 Hz. Examples of the spectra obtained for such reactions are shown in **figure 14** where the *cis*-$[Pt(P^{n}Bu_3)_2Cl_2]$ reacts with the *N,N*-dialkyl-*N'*-benzoylthiourea (47% ^{13}C-enriched at thiocarbonyl carbon).

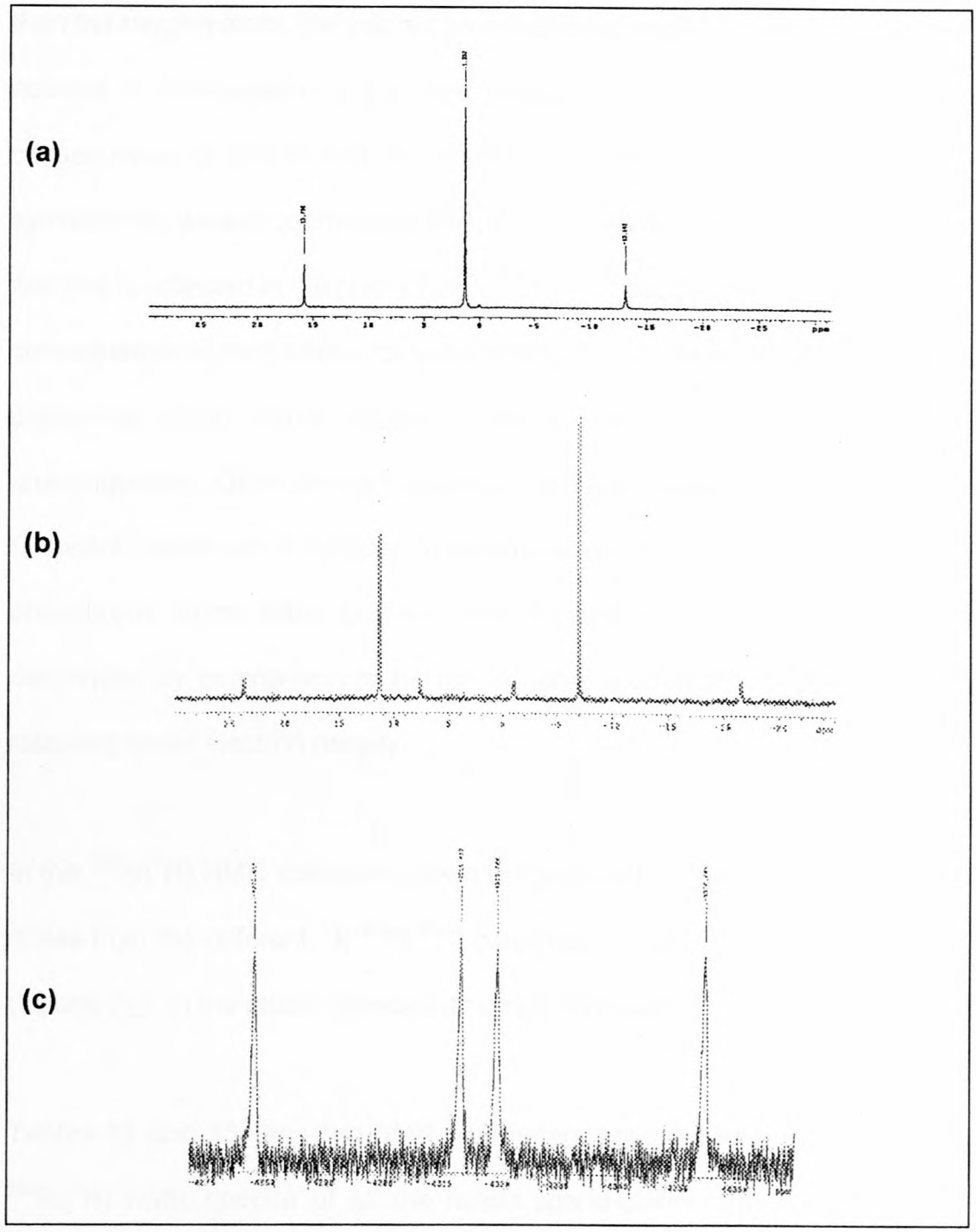

Figure 14: Reaction of *N,N*-dialkyl-*N'*-benzoylthiourea with *cis*-[Pt(P^nBu_3)$_2Cl_2$] followed by means of $^{31}P\{^1H\}$ NMR spectroscopy **(a)** before the addition of triethylamine, **(b)** after addition of triethylamine; and by means of $^{195}Pt\{^1H\}$ NMR spectroscopy **(c)** after the addition of triethylamine.

In **figure 14(b)**, the $^{31}P\{^1H\}$ NMR spectrum shows the relatively shielded peak with a larger coupling constant $^1J(^{195}Pt\text{-}^{31}P)$ value of 3547 Hz, and the other with a coupling constant of 3003 Hz. Since the sulphur atom is relatively softer

than the oxygen atom, the sulphur atom bonds strongly to the soft platinum(II) nucleus in comparison to the hard oxygen donor (HASB principle[4]). The consequence of this is that the phosphorus atom *trans* to *S,* (P_S) is anti-symbiotically weakly coordinated compared to the phosphorus *trans* to *O,* (P_O) and this is reflected in the respective $^1J(^{195}Pt\text{-}^{31}P)$ coupling constants. This is a consequence of competition for π-*d*-orbital between the sulphur and the *trans* phosphine group (*trans influence*), which helps to assign these peaks, unambiguously. Other strong evidence for different degrees with which *S* and *O* donors coordinate is reflected in the respective chemical shifts, $\delta(^{31}P)$ of the phosphorus atoms *trans* to them. The phosphorus atom *trans* to *S*, P_S is deshielded by comparison to P_O (phosphorus atom *trans* to *O*) reflecting a relatively lower electron density.

In the $^{195}Pt\{^1H\}$ NMR spectrum shown in **figure 14(c)**, the doublet of doublets arises from the different $^1J(^{195}Pt\text{-}^{31}P)$ couplings of the two phosphorus atoms, (P_S and P_O), in the mixed ligand-platinum(II) complex.

Tables 12 and 13 show the NMR parameters obtained from the $^{31}P\{^1H\}$ and $^{195}Pt\{^1H\}$ NMR spectra of all the mixed ligand-platinum(II) complexes with *N,N*-dialkyl-*N'*-aroylthioureas as ligands.

Table 12: Data from the $^{31}P\{^{1}H\}$ NMR spectra measured in $CDCl_3$ with the exception of the complex where the ligand is HL^4. Since this ligand was not soluble in $CDCl_3$, the experiment was conducted in DMSO-d_6. The $\delta(^{31}P)$ chemical shifts were referenced to the external standard 85% H_3PO_4 at 25°C.

$[Pt(P^nBu_3)_2L^n]^+Cl^-$	$\delta(^{31}P_O)$ /ppm	$^1J(^{195}Pt\text{-}^{31}P_O)$ /Hz	$\delta(^{31}P_S)$ /ppm	$^1J(^{195}Pt\text{-}^{31}P_S)$ /Hz
HL^2 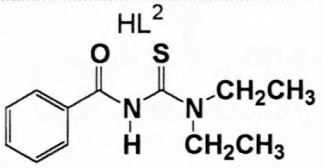	-6.99	3547	11.34	3003
HL^4 * 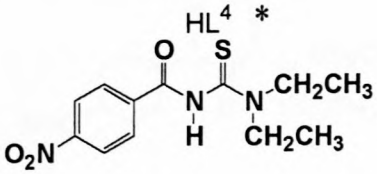	-0.35	3550	15.83	3043
HL^5 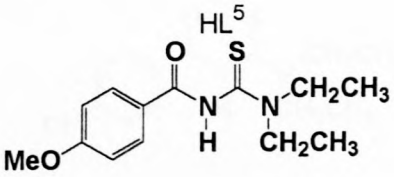	-7.02	3547	11.40	3003
HL^6 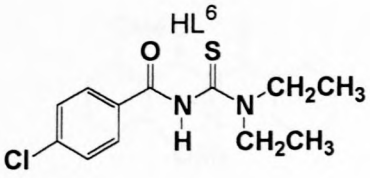	-6.83	3547	11.10	3005
HL^7 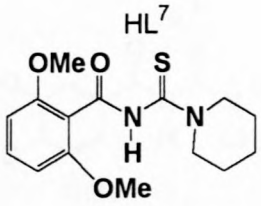	-7.73	3537	11.31	3019
HL^8 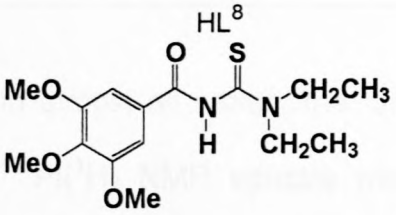	-6.90	3548	11.57	3000

*The chemical shifts $\delta(^{31}P_O)$ and $\delta(^{31}P_S)$ in the resultant complex $[Pt(P^nBu_3)_2(L^n\text{-}S,O)]^+Cl^-$ with n = 4 are significantly different from the rest of the complexes and this is thought to be due to solvent effects.

Table 13: Data from the $^{195}Pt\{^{1}H\}$ NMR spectra measured in deuterated chloroform. The $\delta(^{195}Pt)$ chemical shifts were referenced to H_2PtCl_6 {500mg in 1 cm^3 30% (v/v) D_2O-1M HCl} as an external standard at 30°C.

$[Pt(P^nBu_3)_2L^n]^+Cl^-$	$\delta(^{195}Pt)$ /ppm	$^1J(^{195}Pt-^{31}P_O)$ /Hz	$^1J(^{195}Pt-^{31}P_S)$ /Hz
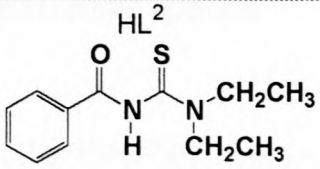	-4317	3548	3005
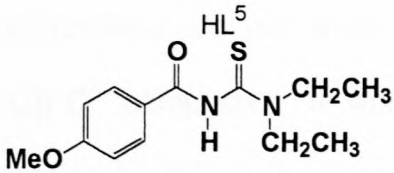	-4332	3534	2984
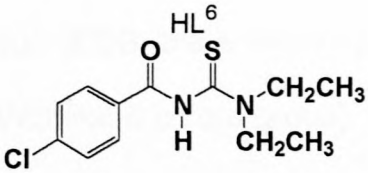	-4314	3534	2993
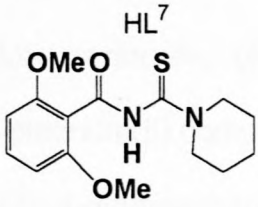	-4485	3264	3057
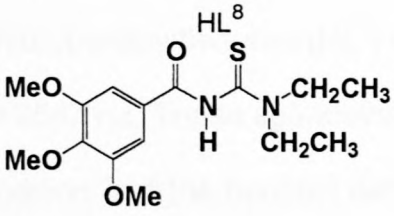	-4323	3525	3008

In almost all cases, the $^1J(^{195}Pt-^{31}P)$ values from the respective $^{31}P\{^1H\}$ and $^{195}Pt\{^1H\}$ NMR spectra were not exactly the same. The exception to this observation is the complex where the ligand is HL^2, which had comparable $^1J(^{195}Pt-^{31}P)$ values. This discrepancy in the $^1J(^{195}Pt-^{31}P)$ values was rather surprising as these values are expected to be the same. The larger line widths (average $W_{1/2}$ = 121 Hz) in the platinum peaks are thought to contribute a

larger uncertainty in the $^{1}J(^{195}Pt\text{-}^{31}P)$ values than the $^{31}P\{^{1}H\}$ NMR spectral line widths (average $W_{1/2}$ = 3.5 Hz). The $^{31}P\{^{1}H\}$ NMR spectra, therefore, give $^{1}J(^{195}Pt\text{-}^{31}P)$ coupling constant values which are more reliable than the $^{195}Pt\{^{1}H\}$ NMR spectra.

The $^{1}J(^{195}Pt\text{-}^{31}P)$ values obtained from the $^{31}P\{^{1}H\}$ NMR spectra, unfortunately, do not show any significant trends in the *cis*-$[Pt(P^{n}Bu_3)_2(L^{n}\text{-}S,O)]^{+}Cl^{-}$ complexes. It was expected that the $^{1}J(^{195}Pt\text{-}^{31}P)$ values could increase as **R"** on the ligand is changed from having an electron donating group (EDG like a methoxy group) to having an electron withdrawing group (EWG like a chloro group). This is expected to be so since the donor (*S* and *O*) strength would have decreased and this might have been transmitted to the NMR parameter of the phosphines in *trans* orientation. Three mixed ligand-platinum(II) complexes, with *N,N*-diethyl-*N'*-benzoylthiourea (HL^2); *N,N*-diethyl-*N'-4*-methoxybenzoylthiourea (HL^5) and *N,N*-diethyl-*N'-4*-chlorobenzoylthiourea (HL^6) as the ligands have the same $^{1}J(^{195}Pt\text{-}^{31}P_O)$ value of 3547 Hz. These ligands have hydrogen, methoxy and chloro substituents at position 4 of the benzoyl derivative, respectively. Evidently, the $^{1}J(^{195}Pt\text{-}^{31}P_O)$ value is not significantly sensitive to the subtle electronic variations in passing from the methoxy group (EDG) to the chloro group (EWG).

The ligand modified with two electron donating methoxy substituents at positions 2 and 6, HL^7 makes the oxygen donor relatively soft as reflected by the relatively small $^{1}J(^{195}Pt\text{-}^{31}P_O)$ values of 3537 Hz and 3264 Hz from the respective $^{31}P\{^{1}H\}$ NMR and $^{195}Pt\{^{1}H\}$ NMR spectra. While the oxygen donor

strength in this ligand is enhanced the $^{1}J(^{195}Pt\text{-}^{31}P_S)$ values of 3019 Hz and 3057 Hz from $^{31}P\{^{1}H\}$ NMR and $^{195}Pt\{^{1}H\}$ NMR spectra, respectively reveal that the sulphur donor strength is reduced. The apparent decrease in the *S* donor strength as reflected by the $^{1}J(^{195}Pt\text{-}^{31}P_S)$ values is rather surprising and it remains unclear why it is so. As the number of the electron releasing methoxy substituents were increased to three (at positions 3, 4 and 5) in HL^{8}, the donicity of *S* and *O* were affected in a similar way as in HL^{7} but only to a small extent. This is revealed by the $^{1}J(^{195}Pt\text{-}^{31}P_O)$ value of 3525 Hz and the $^{1}J(^{195}Pt\text{-}^{31}P_S)$ value of 3008 Hz from the $^{195}Pt\{^{1}H\}$ NMR spectrum. Comparing this mixed ligand-platinum(II) complex (with HL^{8} as the ligand) with the rest of other complexes, no significant changes on the *S* and *O* donor atoms are observed when the $^{1}J(^{195}Pt\text{-}^{31}P)$ values of the $^{31}P\{^{1}H\}$ NMR spectrum are used as probes (see **table 12**).

The $\delta(^{31}P)$ chemical shifts (**table 12**) of these mixed ligand-platinum(II) complexes vary, but only to a small extent, making it difficult to draw any conclusions from them. Even though chemical shifts usually reveal some information about electron density of the nuclei in question, the variations in the $\delta(^{31}P)$ chemical shifts seem to be random, suggesting that any slight variations in relative donicities in these ligands are not reflected in $\delta(^{31}P)$ shifts.

More informative are the $\delta(^{195}Pt)$ values, in **table 13**, which follow the expected trend: the ligand with a para substituted chloride (EWG) makes the ^{195}Pt nucleus of the mixed ligand-platinum(II) complex to be most deshielded

in comparison with other ligand-platinum(II) complexes with ligands that have EDG, which have a shielding effect on the respective ^{195}Pt nuclei. The $\delta(^{195}Pt)$ chemical shift variations can therefore be roughly correlated to these systematic changes of the substituents on the ligands (and hence variations on the complexes). Increasing the number of EDG on the ligand display the expected deshielding effect on the ^{195}Pt nuclei of the mixed ligand-platinum(II) complexes. An exception to this is observed when comparing the $\delta(^{195}Pt)$ chemical shifts of the mixed ligand-platinum(II) complexes, *cis*-$[Pt(P^nBu_3)_2(L^n\text{-}S,O)]^+Cl^-$, with ligands *N*-piperidyl-*N'*-*2,6*-dimethoxybenzolythiourea (HL^7) and *N,N*-diethyl-*N'*-*3,4,5*-trimethoxybenzoylthiourea (HL^8), with 2 and 3 methoxy substituents respectively. The differences in the position of substitution of these methoxy substituents in the ligands is believed to influence the extent of the ^{195}Pt shielding in the respective mixed ligand-platinum(II) complexes. In HL^7, the two methoxy substituents are at the *ortho* positions (2 and 6), while in HL^8, the three methoxy substituents are remotely positioned at the *para* position (4) and at *meta* positions (3 and 5). The $\delta(^{195}Pt)$ shift are respectively -4485 ppm and -4323 ppm as the ligand is changed from HL^7 to HL^8, with decreasing shielding effect on the platinum(II) centre. This is in accordance with a general rule that substituent effects at *para* and *ortho* positions are more pronounced than that at *meta* positions.

3.2.3 A $^{13}C\{^1H\}$ NMR spectrum of a $^{13}C(S)$ mixed ligand-platinum(II) complex

In an attempt to investigate further the coordination chemistry of these mixed ligand-platinum(II) complexes, a $^{13}C\{^1H\}$ NMR spectrum of $[Pt(P^nBu_3)_2(L^2\text{-}S,O)]^+Cl^-$, with a $^{13}C(S)$-enriched *N,N*-diethyl-*N'*-benzoylthiourea as ligand, was measured (see **figures 15 and 16**). From this spectrum, it was observed that the thiocarbonyl carbon atom couples to the platinum with a $^2J(^{195}Pt\text{-}^{13}C)$ value of 27 Hz. This carbon atom also couples to one of the phosphorus atoms with a $^3J(^{31}P\text{-}^{13}C(S))$ value of 2.3 Hz. The most favourable electronic pathway for which the thiocarbonyl carbon to couple, is to the phosphorus atom in a *trans* orientation.

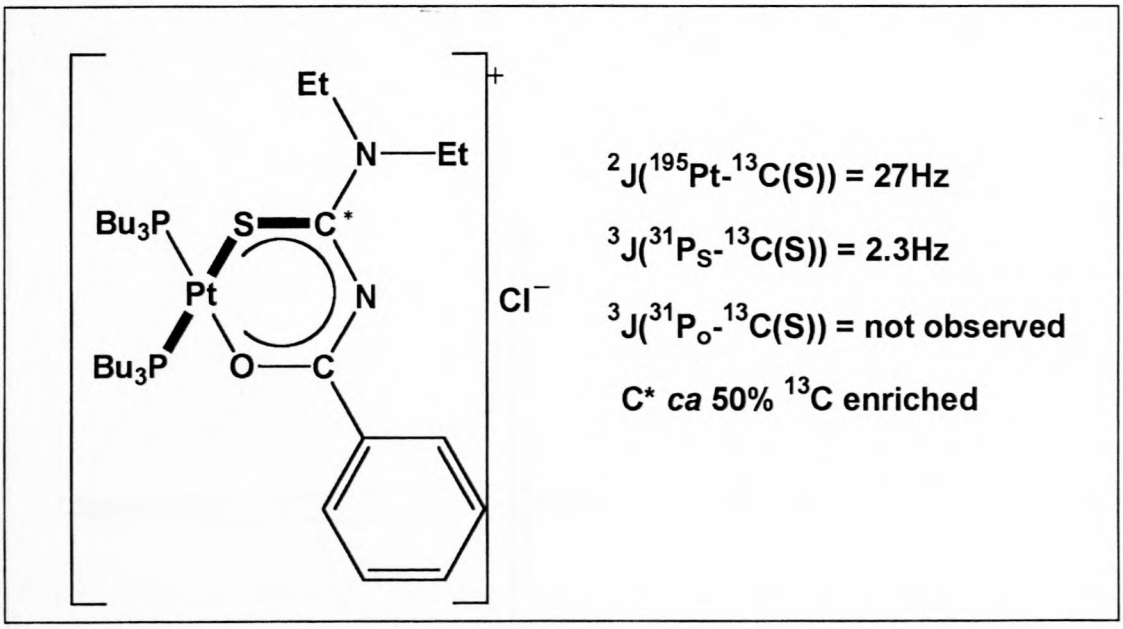

Figure 15: A pictorial representation of a mixed ligand-platinum(II) complex with a ^{13}C enriched thiocarbonyl carbon, $^{13}C(S)$ of the *N,N*-diethyl-*N'*-benzoylthiourea. Only $P_{S,}$ the phosphorus in the favoured electronic path, shown in bold, couples to $^{13}C(S)$.

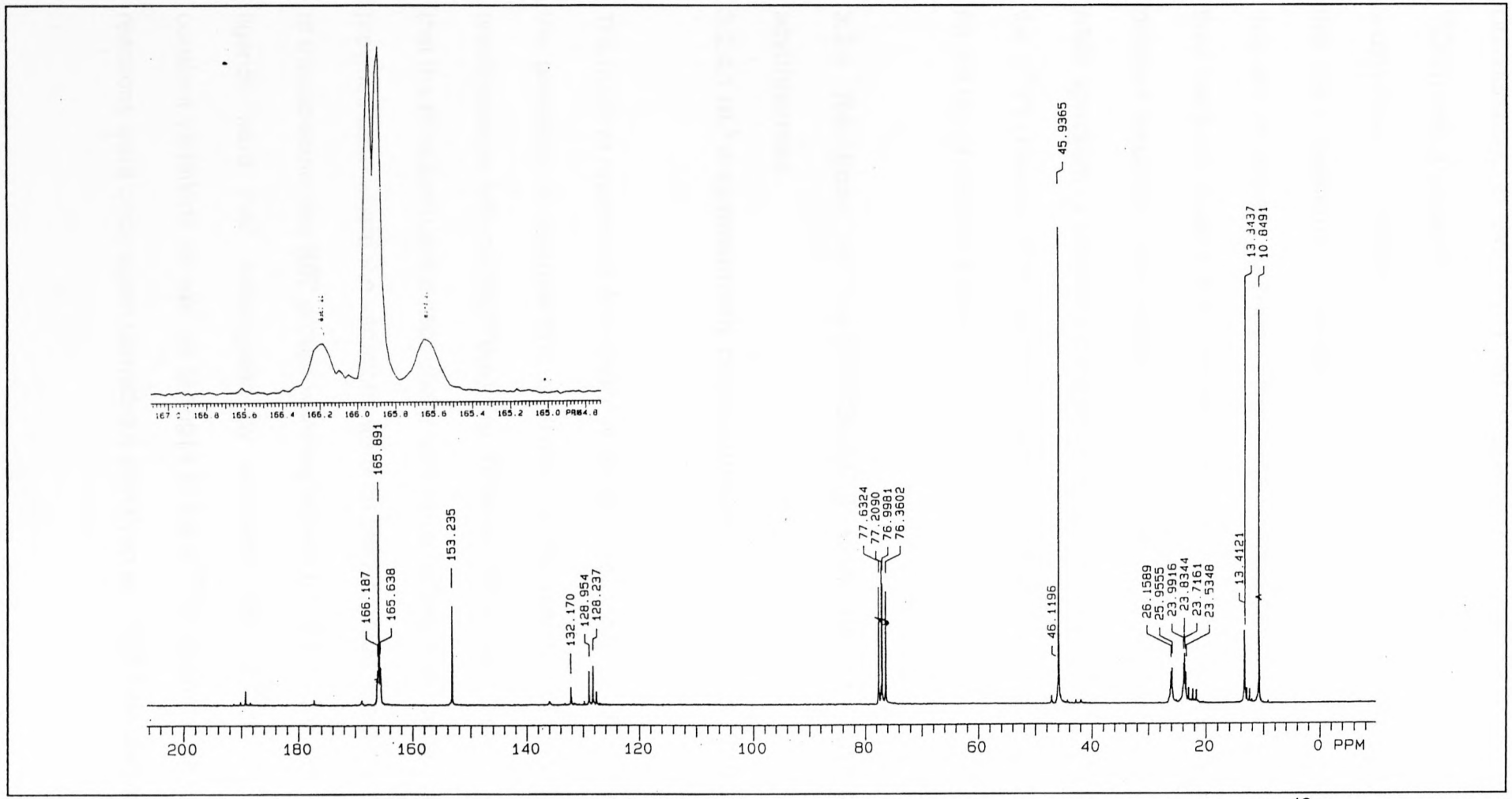

Figure 16: A $^{13}C\{^{1}H\}$ NMR spectrum of $[Pt(P^{n}Bu_3)_2(L^{2*}\text{-}S,O)]^{+}Cl^{-}$ the *N,N*-dialkyl-*N'*-benzoylthiourea is *ca* 47% ^{13}C enriched at the thiocarbonyl carbon. A coupling constant $^{3}J(^{31}P_S\text{-}^{13}C(S))$ of 2.3 Hz is only observed for the phosphorus in a favourable electronic pathway to C(S) resonating at 165.9 ppm but not both! $^{2}J(^{195}Pt\text{-}^{13}C(S))$ is about 27 Hz.

Unfortunately, in the $^{31}P\{^{1}H\}$ NMR spectrum of this complex, the $^{3}J(^{31}P_{s}$-$^{13}C(S))$ with a value of *ca* 2.3 Hz could not be observed due to the bigger line widths ($W_{1/2}$ > 3.5 Hz) of the ^{31}P resonances. This experiment only revealed that the phosphorus atoms are in different electronic environments, hence they are not equally coupling to the thiocarbonyl carbon, $^{13}C(S)$, even though they are both located three bonds away from it. This information about the different electronic environments of the ^{31}P nuclei obtained from the $^{13}C\{^{1}H\}$ NMR spectrum is therefore complimentary to the information obtained form the $\delta(^{31}P)$ chemical shifts as well as the different $^{1}J(^{195}Pt$-$^{31}P)$ values obtained for the two phosphorus atoms, P_S and P_O.

3.2.4 Reactions of *cis*-$[Pt(P^nBu_3)_2Cl_2]$ with HL^n = *N,N*-dialkyl-*N'*-acylthioureas

3.2.4.1 HL^n = symmetrically disubstituted *N,N*-dialkyl-*N'*-acylthioureas

The mode of reaction of *N,N*-dialkyl-*N'*-acylthioureas with *cis*-$[Pt(P^nBu_3)_2Cl_2]$ in the presence of triethylamine is similar to the reaction of *N,N*-dialkyl-*N'*-aroylthioureas with *cis*-$[Pt(P^nBu_3)_2Cl_2]$. What is different about these ligands is that the **R"** substituent is kept unchanged (as a tertiary butyl group) unlike the previous case where the variations were on the **R"** group. On the amide side of the molecule, the **R/R'** groups were varied and the *S* and *O* donicities of the ligands were then investigated by observing the $^{1}J(^{195}Pt$-$^{31}P)$ coupling constant variations as well as changes in the $\delta(^{195}Pt)$ chemical shifts. These reactions were once again carried out directly in an NMR tube and monitored

by means of $^{31}P\{^{1}H\}$ and $^{195}Pt\{^{1}H\}$ NMR spectra: the results are given in **tables 14 and 15.**

Table 14: Data from the $^{31}P\{^{1}H\}$ NMR spectra of mixed ligand-platinum(II) complexes with asymmetrically disubstituted *N,N*-dialkyl-*N'*-acythioureas as ligands, measured in $CDCl_3$. The $\delta(^{31}P)$ chemical shifts were referenced to the external standard 85% H_3PO_4 at 25°C

$[Pt(P^nBu_3)_2L^n]^+Cl^-$	$\delta(^{31}P_O)$ /ppm	$^1J(^{195}Pt\text{-}^{31}P_O)$ /Hz	$\delta(^{31}P_S)$ /ppm	$^1J(^{195}Pt\text{-}^{31}P_S)$ /Hz
HL^1 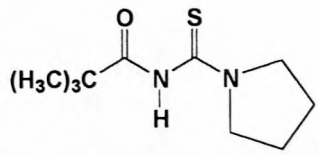	-7.93	3515	10.76	2990
HL^3 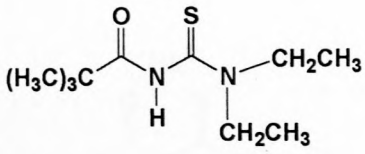	-7.65	3527	10.90	3010
HL^9 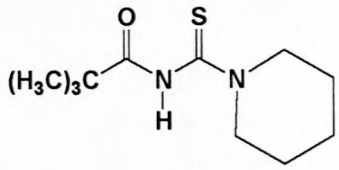	-7.11	3533	10.52	3022
HL^{10} 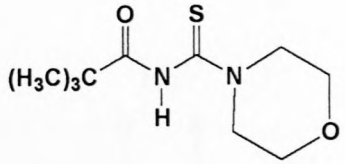	-7.69	3522	10.67	3011
HL^{11} 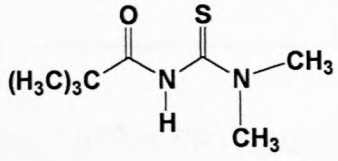	-7.02	3527	10.81	3030

Table 15: Data from the $^{195}Pt\{^{1}H\}$ NMR spectra of mixed ligand-platinum(II) complexes with symmetrically disubstituted *N,N*-dialkyl-*N'*-acythioureas as ligands, measured in deuterated chloroform. The $\delta(^{195}Pt)$ chemical shifts were referenced to H_2PtCl_6 {500mg in 1 cm^3 30% (v/v) D_2O-1M HCl} as an external standard at 30°C.

$[Pt(P^nBu_3)_2L^n]^+Cl^-$	$\delta(^{195}Pt)$ /ppm	$^1J(^{195}Pt-^{31}P_O)$ /Hz	$^1J(^{195}Pt-^{31}P_S)$ /Hz
HL^1 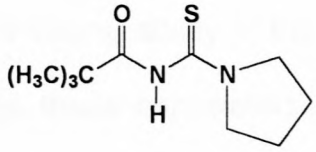	-4311	3498	2975
HL^3 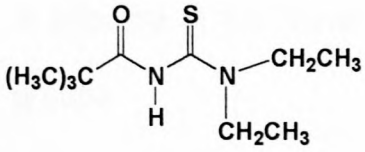	-4334	3512	2996
HL^9 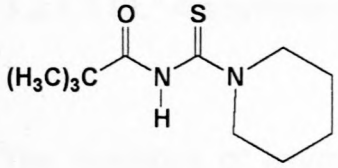	-4346	3519	3008
HL^{10} 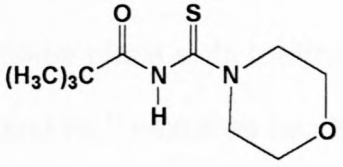	-4334	3510	2999
HL^{11} 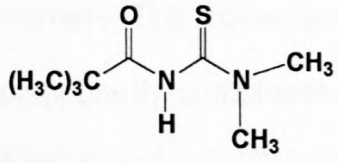	-4332	3534	3021

The $^1J(^{195}Pt-^{31}P)$ coupling constants from the $^{195}Pt\{^{1}H\}$ NMR spectra are always underestimates of what is predicted by the $^{31}P\{^{1}H\}$ NMR spectra, with a few exceptions. It can be argued once again that the $^{31}P\{^{1}H\}$ NMR spectra

give values that are more reliable than the $^{195}Pt\{^{1}H\}$ NMR spectra for the reasons discussed before. Even though there are significant changes in the $^{1}J(^{195}Pt\text{-}^{31}P)$ coupling constants, it is difficult to correlate these changes to parameters like the relative basicity of the amine groups. Unlike the previous case where the $\delta(^{195}Pt)$ chemical shifts could be correlated to the electron releasing ability of the benzoyl group, it is not easy to argue in a similar way as these parameters are numerically very close. For example, the $\delta(^{195}Pt)$ chemical shift = -4334 ppm for the mixed ligand-platinum(II) complex with HL^{3} is affected in the same way as HL^{10}, despite the structurally different **R/R'** groups.

3.2.4.2 HL^{n} = asymmetrically disubstituted *N,N*-dialkyl-*N'*-acylthioureas

The reactions of asymmetric disubstituted *N,N*-dialkyl-*N'*-acylthioureas with *cis*-$[Pt(P^{n}Bu_3)_2Cl_2]$ follow the same route as other ligands, and no reaction takes place until triethylamine is added. Having shown that the ligands (HL^{13} and HL^{15}) exist as two isomers, the *E* and the *Z* isomers, the reaction of these isomers with *cis*-$[Pt(P^{n}Bu_3)_2Cl_2]$ confirms clearly the existence of these isomers. The isomerism in the ligands is carried through to their mixed ligand-platinum(II) complexes. An example to demonstrate this is taken from the $^{31}P\{^{1}H\}$ and the $^{195}Pt\{^{1}H\}$ NMR spectra of the mixed ligand-platinum complex $[Pt(P^{n}Bu_3)_2(L^{n}\text{-}S,O)]^{+}Cl^{-}$ with the complexed ligand being the *N*-(2-methylpyrrolidine)-*N'*-2,2-dimethylpropanoylthiourea (HL^{13}). This ligand is known to exist in two isomeric forms from the ^{1}H and $^{13}C\{^{1}H\}$ NMR spectra.

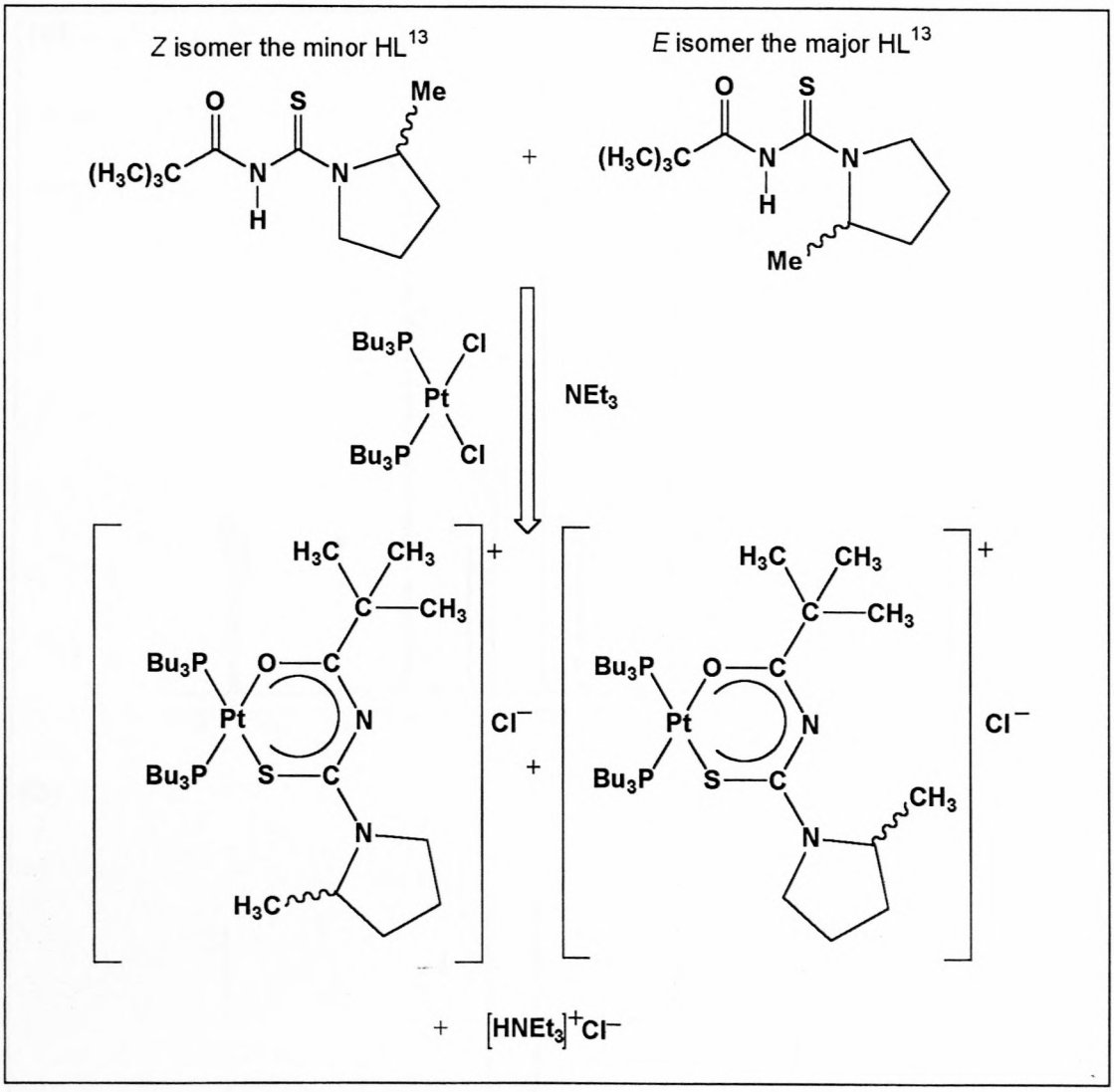

Figure 17: A demonstration of how isomerism in the ligand is carried through to the mixed ligand-platinum(II) complex formed from the reaction of *cis*-$[Pt(P^nBu_3)_2Cl_2]$ with HL^{13} in the presence of triethylamine.

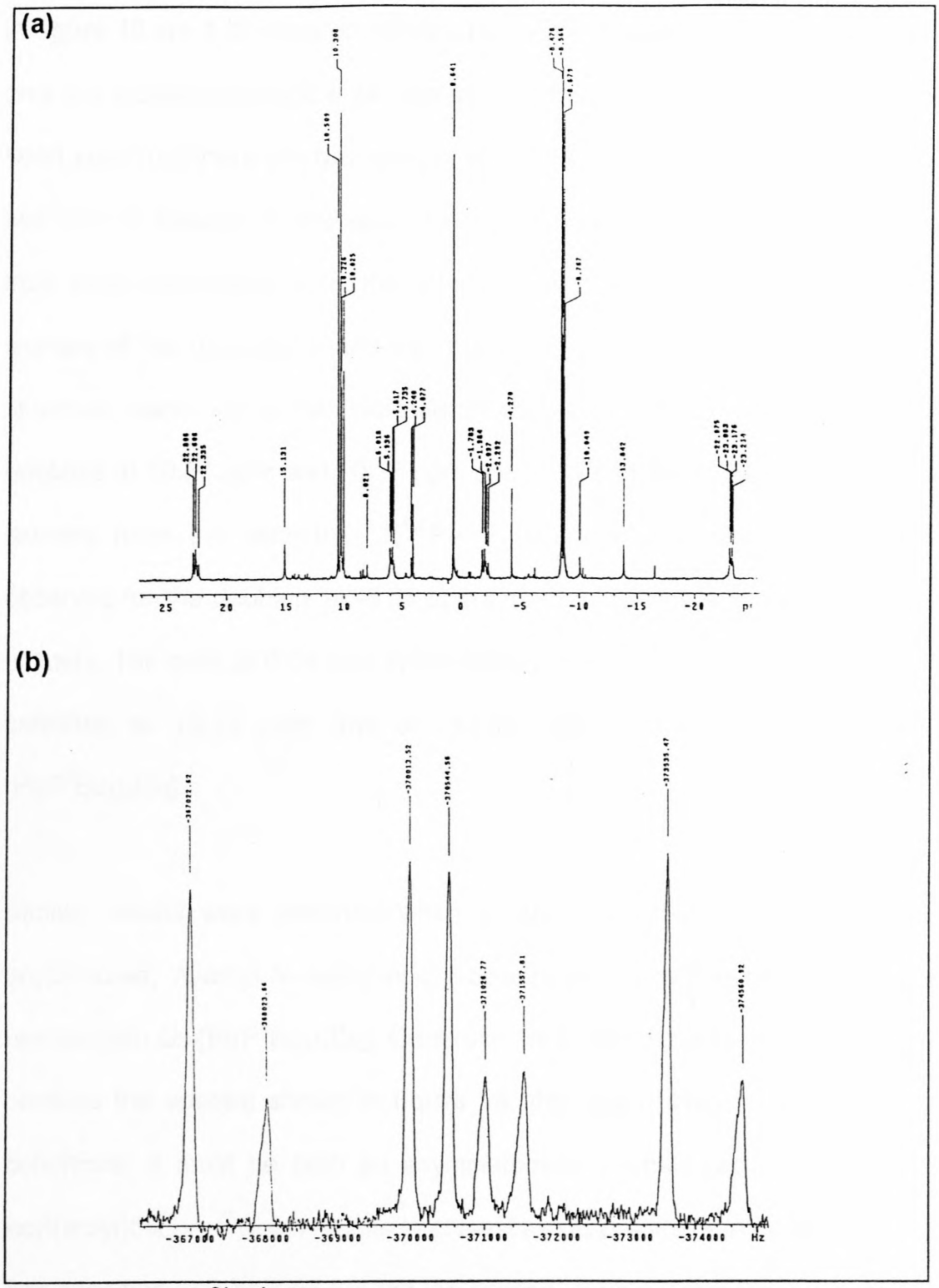

Figure 18: **(a)** A $^{31}P\{^{1}H\}$ NMR spectrum of a mixture of isomers of complexes resulting form *E* and *Z* isomers of *N*-(2-Methylpyrrolidine)-*N'*-*2,2*-dimethylpropanoylthiourea when reacted with *cis*-$[Pt(P^{n}Bu_3)_2Cl_2]$. **(b)** A complimentary $^{195}Pt\{^{1}H\}$ NMR spectrum of the mixture.

The spectroscopic evidence displayed here clearly demonstrate the presence of two isomers. Both the $^{31}P\{^{1}H\}$ NMR and the $^{195}Pt\{^{1}H\}$ NMR spectra shown

in **figure 18** are a lot more complicated than in the case where the ligand has only one isomer as in **figure 14**. Starting with the simpler case, in the $^{195}Pt\{^{1}H\}$ NMR spectrum there are two species of complexes hence these resonate as two sets of doublet of doublets. One complex is in larger quantity (judging from peak intensities) than the other, since the initial distribution of *E/Z* isomers of the unbound ligand was not equal. Similarly, in the $^{31}P\{^{1}H\}$ NMR spectrum, each isomer has two sets of doublets due to $^{31}P_S$ and $^{31}P_O$. The doublets at 10.61 ppm and 10.33 ppm due to P_S's of the major and the minor isomers have the expected $^{1}J(^{195}Pt\text{-}^{31}P)$ coupling satellites. The same is observed for the doublets at -8.58 ppm and -8.67 ppm due to the P_O's of the isomers. The peak at 0.64 ppm symmetrically flanked by $^{1}J(^{195}Pt\text{-}^{31}P)$ coupling satellites at 15.13 ppm and at -13.84 ppm is due to unreacted *cis*-$[Pt(P^{n}Bu_3)_2Cl_2]$.

Similar results were obtained when another asymmetrically disubstituted acylthiourea, *N*-ethyl-*N*-methyl-*N'*-*2,2*-dimethylpropanoylthiourea (HL^{13}) was reacted with *cis*-$[Pt(P^{n}Bu_3)_2Cl_2]$. Generally, for a ligand-platinum(II) complex to produce the spectra shown in **figure 18**, the ligand itself must satisfy two conditions: it must be both an asymmetrically disubstituted *N,N*-dialkyl-*N'*-acyl(aroyl)thiourea which results in at least two *E/Z* isomers. A case where the first condition was obeyed but not the second, such spectra (as in **figure 18**) were not produced and the reactions went on as normal. An example of such a ligand is *N*-tert-butyl-*N*-methyl-*N'*-*2,2*-dimethylpropanoylthiourea (HL^{14}). This ligand is produced exclusively as an *E* isomer. The $^{31}P\{^{1}H\}$ and the $^{195}Pt\{^{1}H\}$

NMR spectroscopic data of these mixed ligand-platinum(II) complexes are contained in **Tables 16 and 17** respectively.

Table 16: Data from the $^{31}P\{^{1}H\}$ NMR spectra of mixed ligand-platinum(II) complexes with asymmetrically disubstituted *N,N*-dialkyl-*N'*-acythioureas as ligands, measured in $CDCl_3$. The $\delta(^{31}P)$ chemical shifts were referenced to the external standard 85% H_3PO_4 at 25°C

$[Pt(P^nBu_3)_2L^n]^+Cl^-$	$\delta(^{31}P_O)$ /ppm	$^1J(^{195}Pt\text{-}^{31}P_O)$ /Hz	$\delta(^{31}P_S)$ /ppm	$^1J(^{195}Pt\text{-}^{31}P_S)$ /Hz
major HL[13] 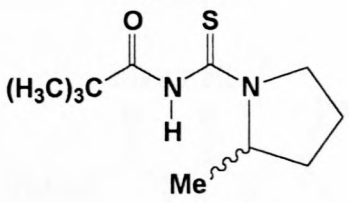	-8.58	3522	10.61	2987
minor HL[13] 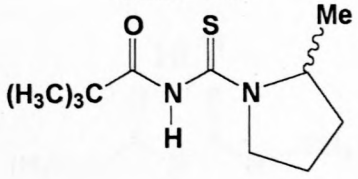	-8.67	3536	10.33	2992
HL[14] 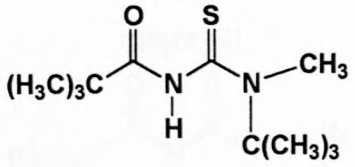	-6.01	3579	11.26	3053
major HL[15] 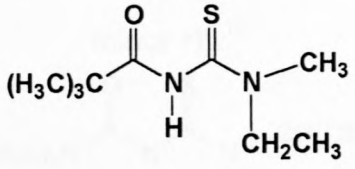	-7.61	3525	11.04	3004
minor HL[15] 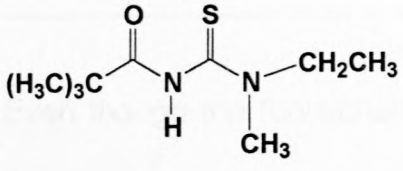	-7.61	3525	10.77	3012

Table 17: Data from the $^{195}Pt\{^{1}H\}$ NMR spectra of mixed ligand-platinum(II) complexes with asymmetrically disubstituted *N,N*-dialkyl-*N'*-acythioureas as ligands, measured in deuterated chloroform. The $\delta(^{195}Pt)$ chemical shifts were referenced to H_2PtCl_6 {500mg in 1 cm^3 30% (v/v) D_2O-1M HCl} as an external standard at 30°C.

$[Pt(P^nBu_3)_2L^n]^+Cl^-$	$\delta(^{195}Pt)$ /ppm	$^1J(^{195}Pt\text{-}^{31}P_O)$ /Hz	$^1J(^{195}Pt\text{-}^{31}P_S)$ /Hz
major HL[13] 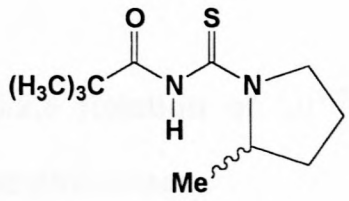	-4307	3522	2991
minor HL[13] 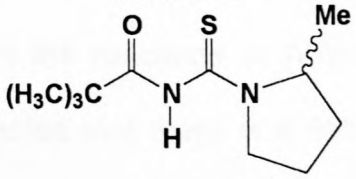	-4319	3534	3003
HL[14] 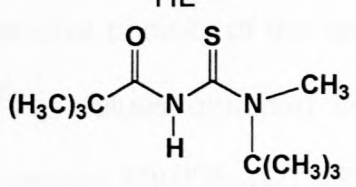	-4406	3567	3039
major HL[15] 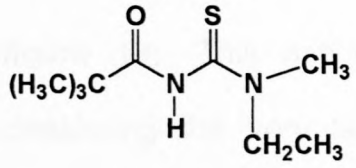	-4327	3512	2990
minor HL[15] 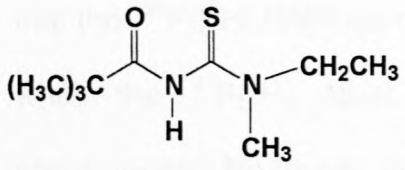	-4339	3519	3002

Even though the functionality is the same in the *E*/*Z* isomers, it is observed that the geometric orientation of the substituents notably influences the

relative donicities of the sulphur and the oxygen donors, judging from the $^{1}J(^{195}Pt\text{-}^{31}P)$ values. What is also remarkable is that the $\delta(^{195}Pt)$ shifts are different even though the *E* and *Z* isomers of the same ligand have the same functionalities. However, it is difficult to interpret these small but observable differences.

3.2.5 Relation of $^{1}J(^{195}Pt\text{-}^{31}P_S)$ values to the nature of *N,N*-dialkyl-*N'*-acylthioureas

In the reactions of *N,N*-dialkyl-*N'*-acylthioureas with *cis*-$[Pt(P^{n}Bu_3)_2Cl_2]$ it is noted that there is a definite dependence of the $^{1}J(^{195}Pt\text{-}^{31}P_S)$ values on the nature of the **R/R'** substituents, but this could not be reliably correlated to the relative basicity of the amines. Arranged in an increasing order, the $^{1}J(^{195}Pt\text{-}^{31}P_S)$ values obtained from the $^{195}Pt\{^{1}H\}$ and $^{31}P\{^{1}H\}$ NMR spectra in the complex $[Pt(P^{n}Bu_3)_2(L^{n}\text{-}S,O)]^{+}Cl^{-}$ with n = 1, 15 major, 3, 10, 15 minor, 9, 11 and 14, a systematic difference of 13 +/- 3 Hz between each other is observed (**figure 19**). This might be ascribed to instrumental frequency errors, considering the very large differences in the resonance frequencies of $^{195}Pt\{^{1}H\}$ and $^{31}P\{^{1}H\}$ NMR spectra. What could also explain the differences is that the $^{195}Pt\{^{1}H\}$ NMR spectra were measured using a 400 MHz spectrometer while the $^{31}P\{^{1}H\}$ NMR spectra were measured using a 300 MHz spectrometer. No trends similar to the one shown here were observed for the $^{1}J(^{195}Pt\text{-}^{31}P_S)$ values in *N,N*-dialkyl-*N'*-benzoylthioureas and $^{1}J(^{195}Pt\text{-}^{31}P_O)$ values.

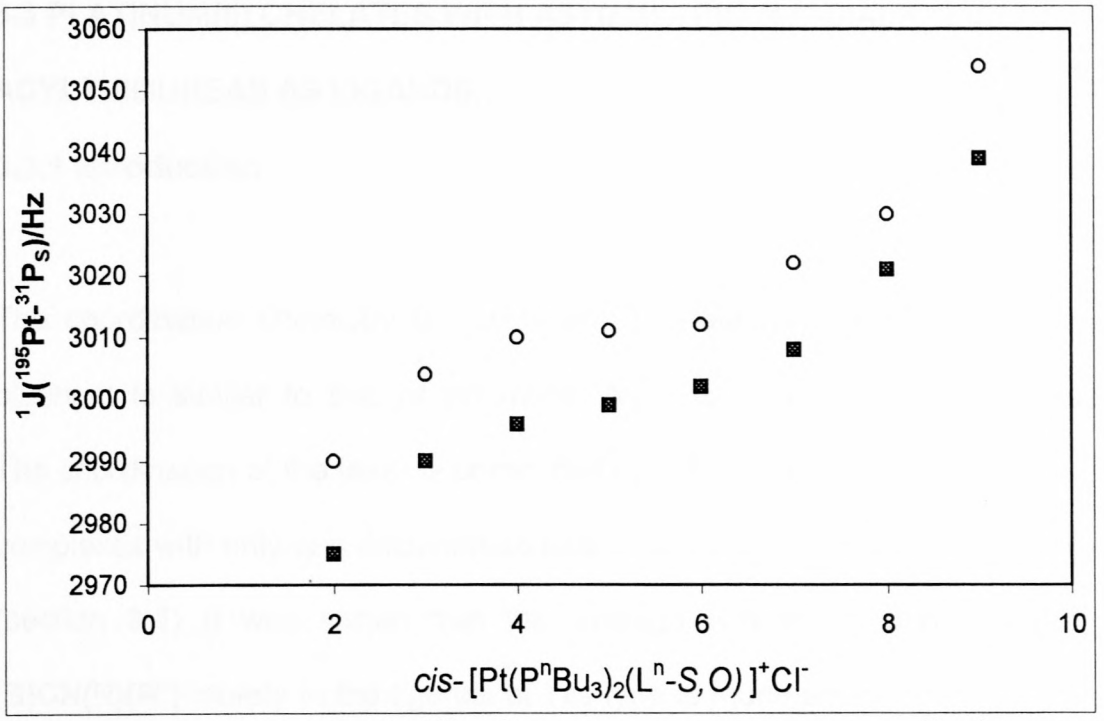

Figure 19: A plot of the $^1J(^{195}Pt\text{-}^{31}P_S)$ values from both the $^{31}P\{^1H\}$ NMR spectra (○) and the $^{195}Pt\{^1H\}$ NMR spectra (■) against the mixed ligand-platinum complexes. A systematic dependence of the $^1J(^{195}Pt\text{-}^{31}P_S)$ values on the nature of **R/R'** substituent is observed but could not be reliably correlated to the relative basicity of the amines.

3.3 PLATINUM(II) CHELATES WITH ASYMMETRIC *N,N*-DIALKYL-*N'*-ACYLTHIOUREAS AS LIGANDS.

3.3.1 Introduction

The coordination chemistry of asymmetric *N,N*-dialkyl-*N'*-acylthioureas with platinum is similar to that of symmetric *N,N*-dialkyl-*N'*-acyl(aroyl)thioureas. The coordination of the latter is dominated by the formation of *cis*-[Pt(L-*S,O*)$_2$] complexes with only one documented example of a *trans bis*-chelate.[59] Earlier (section **3.1**) it was shown that the average C-N bond length of the **-(S)CN(R)(R')** moiety in the ligands of this type is much shorter than that of a C-N single bond of 1.472(5) Å,[57] indicating a higher degree of partial double bond character.

Koch *et al*[56] have shown that the partial double bond character of C-N of the **-(S)CN(R)(R')** moiety in the ligand is retained in the resulting complexes. The ligand used in that particular case was the *N*-butyl-*N*-methyl-*N'*-benzoylthiourea. Koch *et al*[56] demonstrated that the *Z* (73%): *E* (27%) isomer ratios of the ligand (determined by semi-quantitative $^{13}C\{^1H\}$ NMR spectroscopy), converted to configurational isomers *Z,Z* (37.6%): *E,Z* (48.5%): *E,E* (13.9%) in the complexes.

Here, the coordination chemistry of the asymmetric ligands, HL[13], HL[14] and HL[15] to platinum(II) is discussed. Though these ligands are similar, they have some differences in their coordination chemistry in relation to one another, with only ligand HL[15] displaying similarities to the ligand described by Koch *et*

al.[56] One particular difference amongst them is observed from their $^{13}C\{^1H\}$ NMR spectra. Both HL^{13} and HL^{15} have the *E* and *Z* isomers whereas HL^{14} forms only as one isomer, viz. *E* isomer, under comparable conditions. In both cases where there are two isomers, the *E* isomer is the major isomer. This may be because the larger functional group is pointing away from sulphur, thereby reducing steric hindrance. The synthesis of platinum complexes with these ligands was described in detail in **chapter 2**.

3.3.2 Platinum(II) chelates with *N*-tert-butyl-*N*-methyl-*N'*-2,2-dimethylpropanoylthiourea, HL^{14}

As mentioned before, HL^{14} occurs as only the *E* isomer, therefore, will react as an ordinary acylthiourea and a neutral complex *cis-bis*(*N*-tert-butyl-*N*-methyl-*N'*-2,2-dimethylpropanoylthioureato)platinum(II), *cis*-$[Pt(L^{14}\text{-}S,O)_2]$ is formed. The reaction of the ligand only takes place in the presence of a base which deprotonates at the acidic amido proton of the **-OCNHCS-** moiety. The reaction scheme is as follows:

$$K_2PtCl_4 + \mathbf{2}HL^{14} + \mathbf{4}CH_3COONa \longrightarrow cis\text{-}[Pt(L^{14}\text{-}S,O)_2] + \mathbf{2}NaCl + \mathbf{2}KCl + \mathbf{2}CH_3COOH + \mathbf{2}CH_3COONa$$

Reaction scheme 5: Formation of platinum(II) chelate with HL^{14} as the asymmetric ligand.

An excess of base (CH_3COONa) was used to ensure complete reaction. The ^1H NMR spectrum of the complex is comparable with the one of the ligand, with the disappearance of the N-H peak at 7.85 ppm being the major

difference. Significant differences in the $^{13}C\{^1H\}$ NMR spectrum of the complex compared to the unbound ligand are observed for the carbonyl carbon, C(O) and the thiocarbonyl carbon, C(S). While in the unbound ligand, the C(O) resonates at 173.2 ppm in the complex the C(O) resonates at a lower field at 181.8 ppm. The C(S) in the complex resonates at a higher field (169,3 ppm) compared to that of the unbound ligand, which resonates at 179.8 ppm. The reasons for these phenomenon could be that the sulphur donor gets involved in π-back donation while the oxygen donor does not. The detailed ^1H, $^{13}C\{^1H\}$ NMR assignments are trivial are mentioned in **chapter 2**. A singlet at -2733 ppm in the $^{195}Pt\{^1H\}$ NMR spectrum confirms the existence of one isomer, *cis*-[Pt(L^{14}-*S,O*)$_2$].

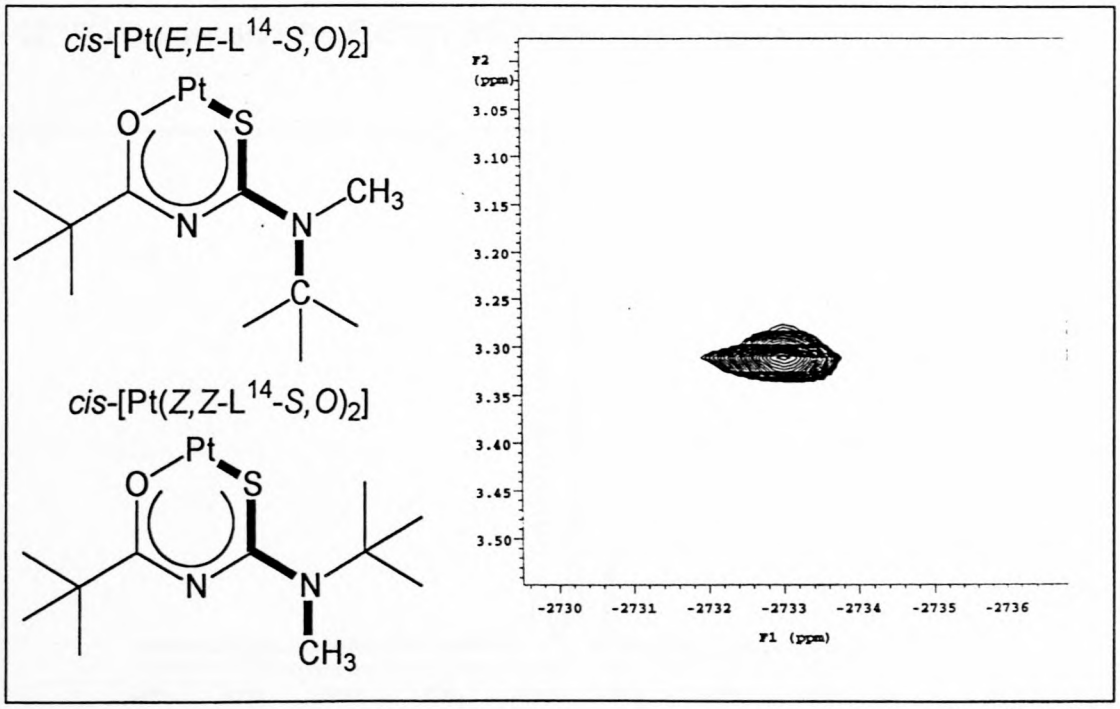

Figure 20: The **W** electronic pathway in which the four-bond $^4J(^{195}Pt\text{-}^{13}C)$ coupling is transmitted for the two possible configurational isomers and a correlation $^1H\text{-}(^{13}C)\text{-}^{195}Pt$ NMR spectrum which unambiguously assigns the ^{195}Pt peak at -2733 ppm to correlate only to the methyl group of the *cis*-[Pt(*Z,Z*-L^{14}-*S,O*)$_2$].

3.3.3 Platinum(II) chelates with *N*-ethyl-*N*-methyl-*N'*-2,2-dimethylpropanoylthiourea, HL^{15}

In the case of HL^{15}, the *E/Z* isomerism of the ligand is carried over to the complexes, resulting in three configurational isomers. Starting with the *E* (75%) and *Z* (25%) isomers of the ligand (as determined by means of semi quantitative $^{13}C\{^1H\}$ NMR spectroscopy), one might expect the statistical distribution for the complexes to be *ca E,E* (62.5%):*E,Z* (25%):*Z,Z* (12.5%) (see **appendix 2** for calculation of ratio). This is not the case since the reaction is carried out at elevated temperature (50°C) where the ligand does not retain one configuration. The experimentally determined peak integrals indicate that the *E,Z* isomer is most favoured (46.1%) followed by the *Z,Z* (42.1%) isomer and the *E,E* (11.8%) isomer (see **figure 21**).

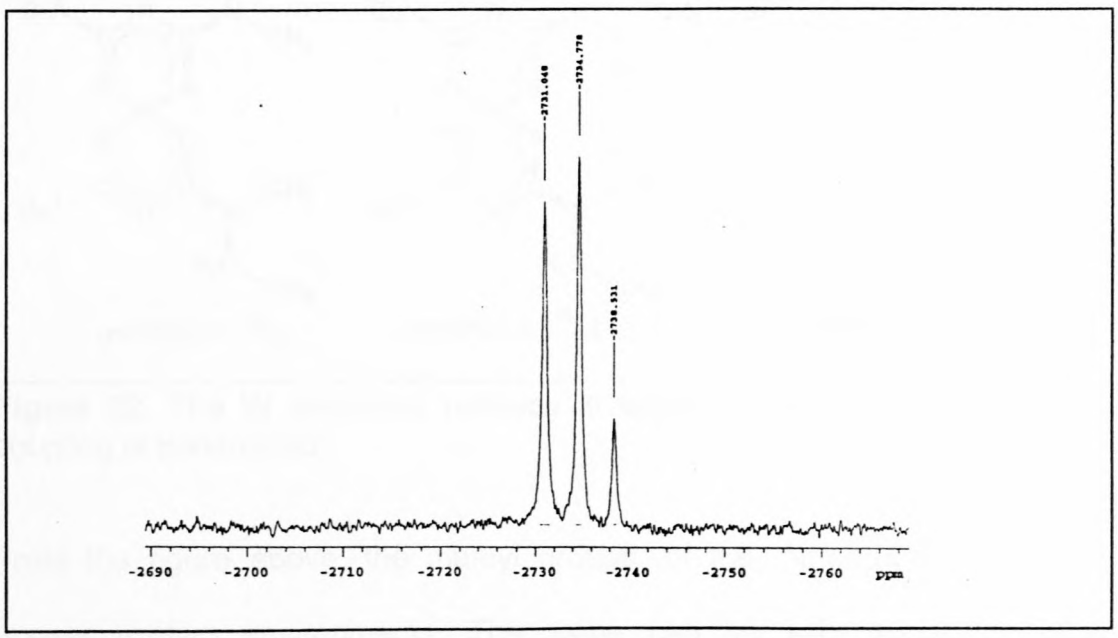

Figure 21: A $^{195}Pt\{^1H\}$ NMR spectrum of *cis*-[Pt(L^{15}-*S,O*)$_2$], with the *Z,Z*; *E,Z* and *E,E* isomers resonating at -2731, -2735 and -2739 ppm respectively.

Since these complexes are chromatographically equivalent (have the same R_f value in different organic solvents), an alternative means of assigning them was devised. The assignment of the peaks as to which is *E,E*; *E,Z* and *Z,Z* is by no means trivial. Full structural elucidation of the complexes is carried out using high field ^{1}H-(^{13}C)-^{195}Pt correlation NMR spectroscopy, which is described below.

It is known that the platinum nucleus couples to carbon in a **W** pathway as this is a favourable electronic pathway in which coupling can be transmitted. **Figure 22** shows the favoured electronic pathway that transmits platinum-carbon coupling in bold.

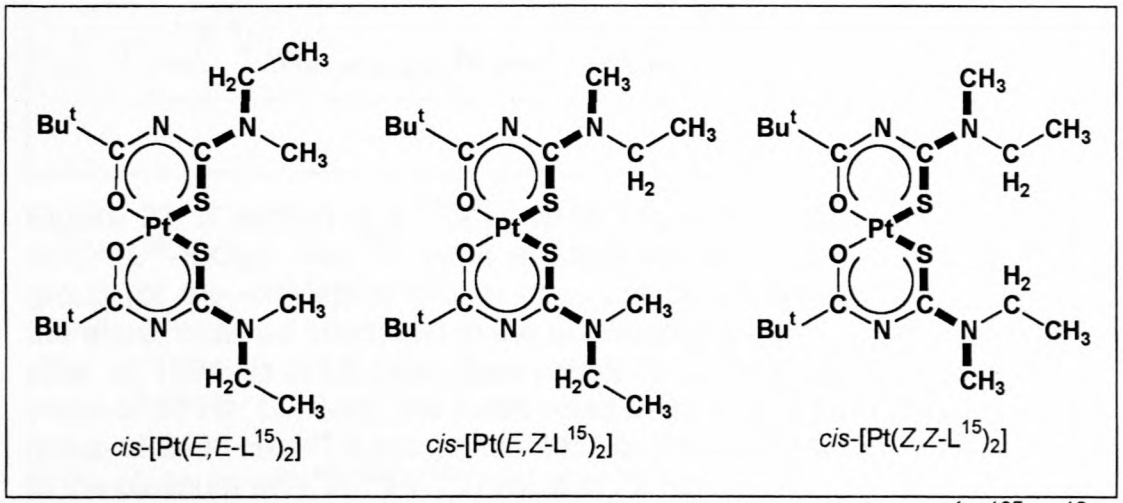

Figure 22: The **W** electronic pathway in which the four-bond $^{4}J(^{195}Pt$-$^{13}C)$ coupling is transmitted.

From the figure above, the methyl groups (of the **-N(Me)(Et)** group) can appear in two environments. The same can be said about the ethyl substituents. In two of the three isomers, both the ethyl and methyl substituents are positioned in either the favoured electronic pathway for

platinum coupling or the unfavoured path. This is evident from the $^{13}C\{^{1}H\}$ NMR spectrum (**figure 23**), which reveals two sets of peaks for the methyl carbons and two sets of peaks for the ethyl carbons.

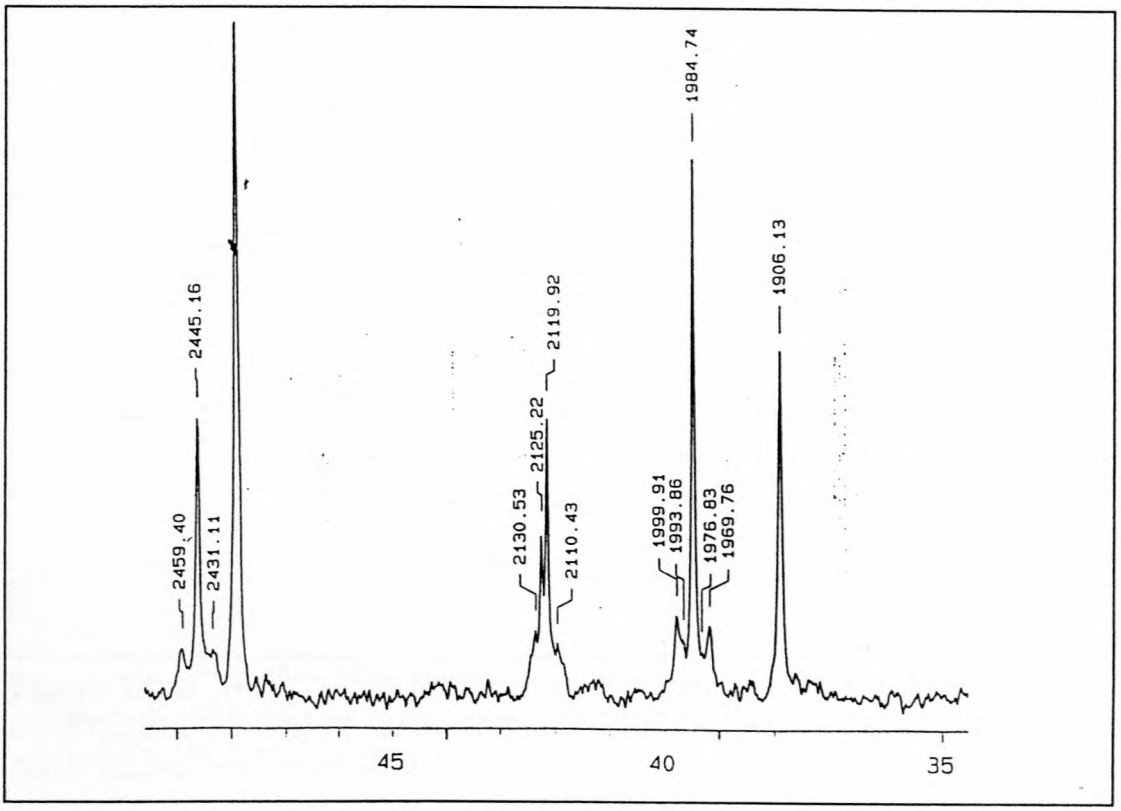

Figure 23: A section of a $^{13}C\{^{1}H\}$ NMR spectrum of the platinum(II) chelate *cis*-[Pt(L^{15}-*S,O*)$_2$]. The ^{13}C peak at 1906 Hz (37.9 ppm) due to the methyl group (of the **-N(Me)(Et)** group) does not couple to the platinum nucleus, therefore, must be orientated in the unfavoured electronic pathway, while the other at 1984 Hz (39.5 ppm) does couple to the platinum with a $^{4}J(^{195}Pt\text{-}^{13}C)$ value of 30 Hz. Similarly, the same could be said about the CH_2's of the ethyl group at 2408 Hz (47.9 ppm) and 2445 Hz (48.6 ppm) with the latter coupling to the platinum with $^{4}J(^{195}Pt\text{-}^{13}C)$ value of 28 Hz.

Due to the insensitivity of the carbon nucleus in NMR spectroscopy and the expected broadness of the $^{195}Pt\text{-}^{13}C$ satellites due to chemical anisotropy broadening at high field, the platinum nucleus could not be directly correlated to these carbons even though they are in a favourable pathway. Instead, the highly sensitive protons, attached to these $^{195}Pt\text{-}^{13}C$ coupled carbons were correlated to platinum, achieving a $^{1}H\text{-}(^{13}C)\text{-}^{195}Pt$ NMR correlation spectrum.

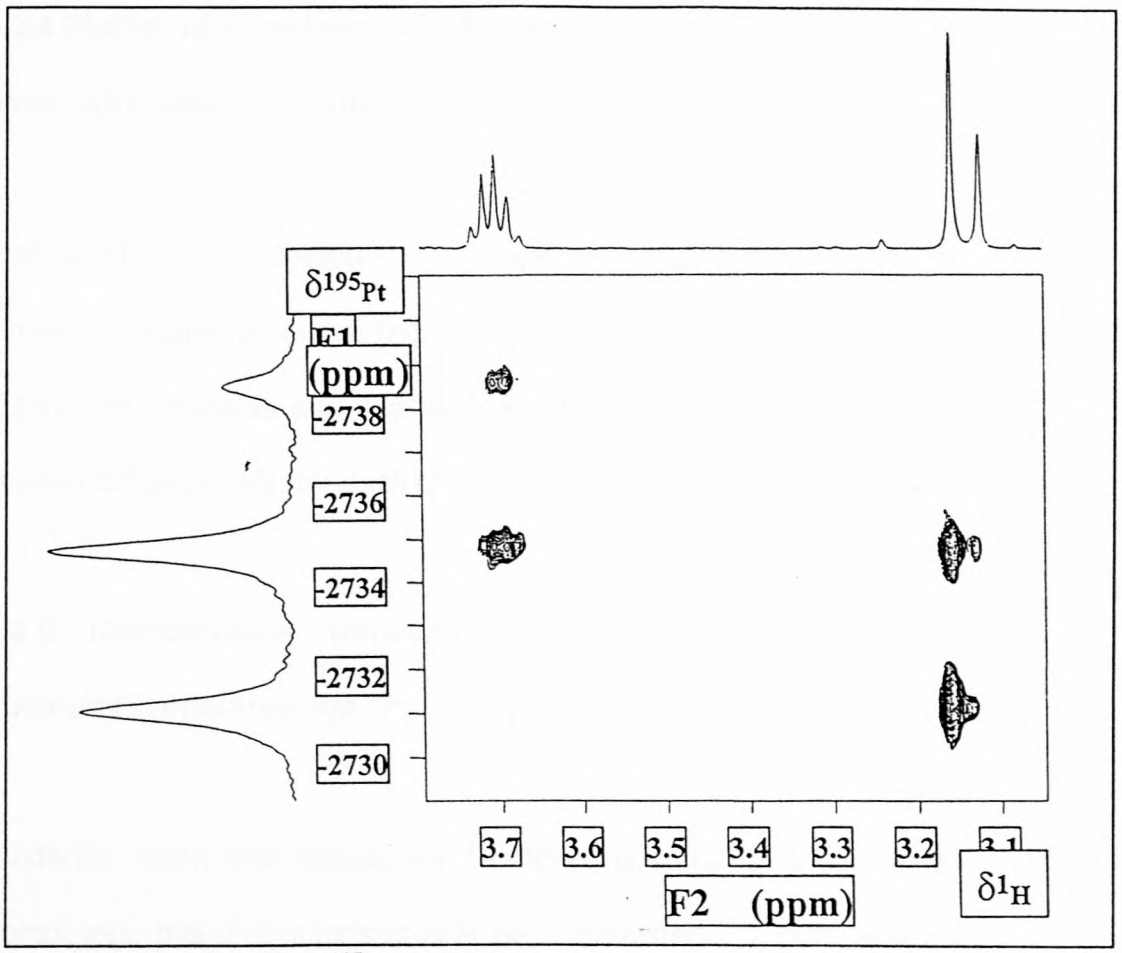

Figure 24: A ^{1}H-(^{13}C)-^{195}Pt NMR correlation spectrum for the assignments of *cis*-[Pt(*E,E*-L^{15}-*S,O*)$_2$] at -2739 ppm, *cis*-[Pt(*E,Z*-L^{15}-*S,O*)$_2$] at -2735 ppm and *cis*-[Pt(*Z,Z*-L^{15}-*S,O*)$_2$] at -2731 ppm.

The peak at *ca* 3.2 ppm is due to hydrogen atoms attached to the **methyl group** and these are correlated to the most deshielded isomer, therefore, they must be due to *cis*-[Pt(*Z,Z*-L^{15}-*S,O*)$_2$]. The middle peak in the platinum spectrum is correlated to both the methyl protons as well as the CH_2 protons of the ethyl group at *ca* 3.7 ppm, this must be the *cis*-[Pt(*E,Z*-L^{15}-*S,O*)$_2$]. The most shielded peak in the ^{195}Pt{^{1}H} NMR spectrum correlates only to the hydrogen atoms of the CH_2 group of the ethyl substituent and, hence, is assigned to *cis*-[Pt(*E,E*-L^{15}-*S,O*)$_2$].

3.3.4 Platinum(II) chelates with *N*-2-methylpyrrolidine-*N'*-2,2-dimethylpropanoylthiourea, HL^{13}

Platinum(II) chelates with *N*-2-methylpyrrolidine-*N'*-2,2-dimethylpropanoylthiourea (HL^{13}) were synthesised in a similar way as other platinum(II) chelates and characterised by means of elemental analysis (see section **2.7** page **57**), but lack of time precluded a more in-depth study.

3.3.5 Comparisons between the asymmetric ligands and their platinum(II) chelates, *cis*-[Pt(L-*S,O*)$_2$]

Evidently, from the respective ^{1}H NMR spectra of the ligands and the complexes, the characteristic N-H peak (between 7.2 ppm and 7.9 ppm) for the ligands disappear in the complexes. One striking feature in the $^{13}C\{^1H\}$ NMR spectra of the complexes is that the C(O) peak appears downfield compared to the C(S) peak and this is reversed in the unbound ligands. The $^{13}C\{^1H\}$ NMR spectra of the $HL^{13,15}$ ligands showed that the *E* isomer is the major isomer and *N*-tert-butyl-*N*-methyl-*N'*-2,2-dimethylpropanoylthiourea (HL^{14}), was produced exclusively as the *E* isomer. On complexation to the platinum(II) ion, the preferred orientation for the ligands is the *Z* configuration, which is rather counter-intuitive. It is not yet known what causes this reversal, but it may have to do with changes of the restricted rotation of the N-C(S) bond at elevated temperatures, as discussed in section **3.1.4**.

Chapter Four

Results and discussion of platinum(II) complexes of ligands closely related to *N*,*N*-diakyl-*N*'-acyl(aroyl)thioureas

4 RESULTS AND DISCUSSION OF PLATINUM(II) COMPLEXES OF LIGANDS CLOSELY RELATED TO *N,N*-DIALKYL-*N'*-ACYL(AROYL)THIOUREAS

4.1 PLATINUM(II) CHELATES WITH *N*-THIOPHOSPHORYLATED THIOAMIDE AND *N*-PHENYL-*N'*-THIOPHOSPHORYLATED THIOUREA AS LIGANDS

The platinum(II) chelates of *N*-diisopropoxythiophosphoryl thioamide (**I**)and *N*-diisopropoxythiophosphoryl-*N'*-phenylthiourea (**II**) were synthesised as described in **chapter 2** section **2.4**. They were fully characterised by means of multinuclear (^{1}H, ^{13}C, ^{31}P, ^{195}Pt) magnetic resonance spectroscopy, elemental analysis and by a crystal structure determination of the two *trans* platinum-ligand complexes. The platinum(II) chelate formed from **I** following Koch *et al*[50] synthetic route (see **synthesis scheme 1**) is a *trans*-isomer (**figure 26**), with a molecular structure closely resembling the palladium complex described by Zabirov *et al.*[25]

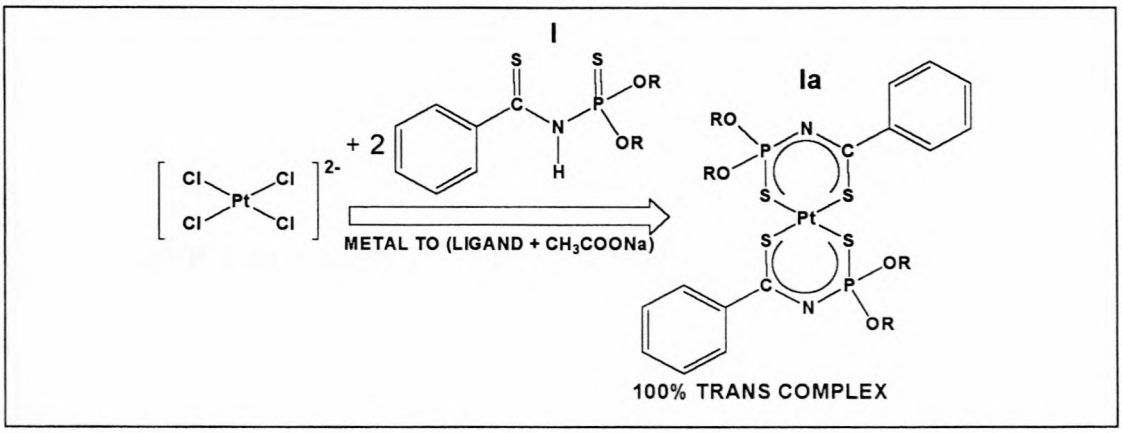

Synthesis scheme 1: Metal solution to the ligand solution in the synthesis of the platinum-ligand(**I**) chelate leads to the *trans*-complex exclusively.

The $^{31}P\{^{1}H\}$ NMR spectrum in $CDCl_3$ of this compound shows a ^{31}P peak at 42.6 ppm with a $^{2}J(^{195}Pt\text{-}^{31}P)$ coupling constant of 119 Hz. This is also confirmed by a triplet at -3923 ppm in the $^{195}Pt\{^{1}H\}$ NMR spectrum.

The coordination chemistry of **II** is subtly different from that of **I**. Following the same method of synthesis for Pt(II) complexes using ligand **II**, somewhat unexpectedly, a mixture of isomers is found. This is revealed by the $^{31}P\{^{1}H\}$ NMR spectrum, which shows two ^{31}P peaks at 43,6 ppm with a $^{2}J(^{195}Pt\text{-}^{31}P)$ value of 106 Hz and at 44.5 ppm with a $^{2}J(^{195}Pt\text{-}^{31}P)$ value of 101 Hz, suggesting two isomers (see **figure 25**). The presence of the two isomers is confirmed by two ^{195}Pt peaks at -3964 ppm and at -3956 ppm. The formation of a *cis*-isomer is the first of its kind to be reported, which is contrary to the report by Brus'ko *et al*,[33] who claims that these reactions only result in the *trans*-product.

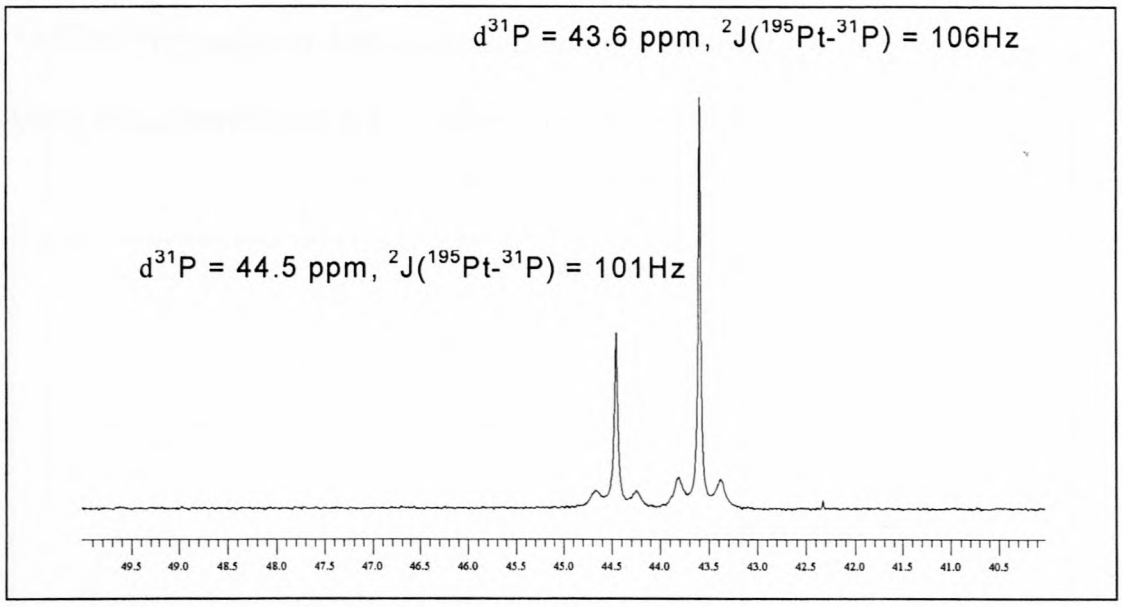

Figure 25: The $^{31}P\{^{1}H\}$ NMR spectrum of the platinum chelates when ligand **II** is used; a mixture of *cis* and *trans*-isomers result after adding the metal solution to the ligand solution.

At the time of measuring the spectrum, there was no trivial way of knowing which peak belonged to which isomer and attempts of separating the two were carried out. On thin layer chromatography (TLC) plates, (layer 0.2 mm silica gel with fluorescent indicator), with various organic solvents and solvent mixtures, it was observed that the R_f values of these compounds, though different, were too close to separate them by chromatographic means.

A different mode of synthesising the Pt(II) complex was followed by simply reversing the order of addition of the reactants. By adding the ligand solution to the $[PtCl_4]^{2-}$ solution, the $[PtCl_4]^{2-}$ would remain in relative excess during the progress of the reaction. Recrystallising the crude product in a mixed solvent system of acetonitrile and chloroform, gave single crystals of the *trans*-isomer, which were analysed by means of X-ray diffraction. Measuring the $^{31}P\{^{1}H\}$ NMR spectrum of this compound, a single ^{31}P peak at 43.6 ppm with a

$^{2}J(^{195}Pt\text{-}^{31}P)$ value of 106 Hz was observed (see **figure 26**), so establishing the stereochemistry of the complex which gave rise to this resonance.

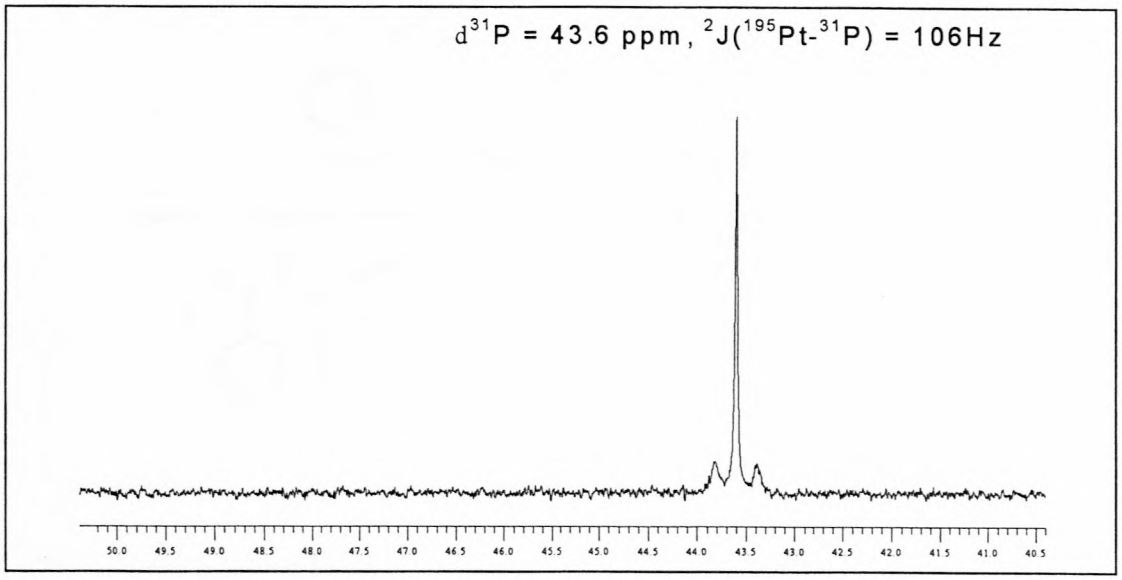

Figure 26: $^{31}P\{^{1}H\}$ NMR spectrum shows that the *trans*-complex resonates at 43.6 ppm with $^{2}J(^{195}Pt\text{-}^{31}P)$ value of 106 Hz.

The presence of only one isomer is confirmed by a triplet at -3964 ppm in the $^{195}Pt\{^{1}H\}$ NMR spectrum of this compound. The isolation of the *trans*-isomer makes it easy to unambiguously assign both the phosphorus and the platinum spectra of the mixture.

Thus, interestingly, depending on the mode of the reaction synthesis, the platinum(II) chelates formed are found to be either mainly the *trans*-complex (**IIa**) or a mixture of *trans* (**IIa**) and *cis* (**IIb**) isomers.

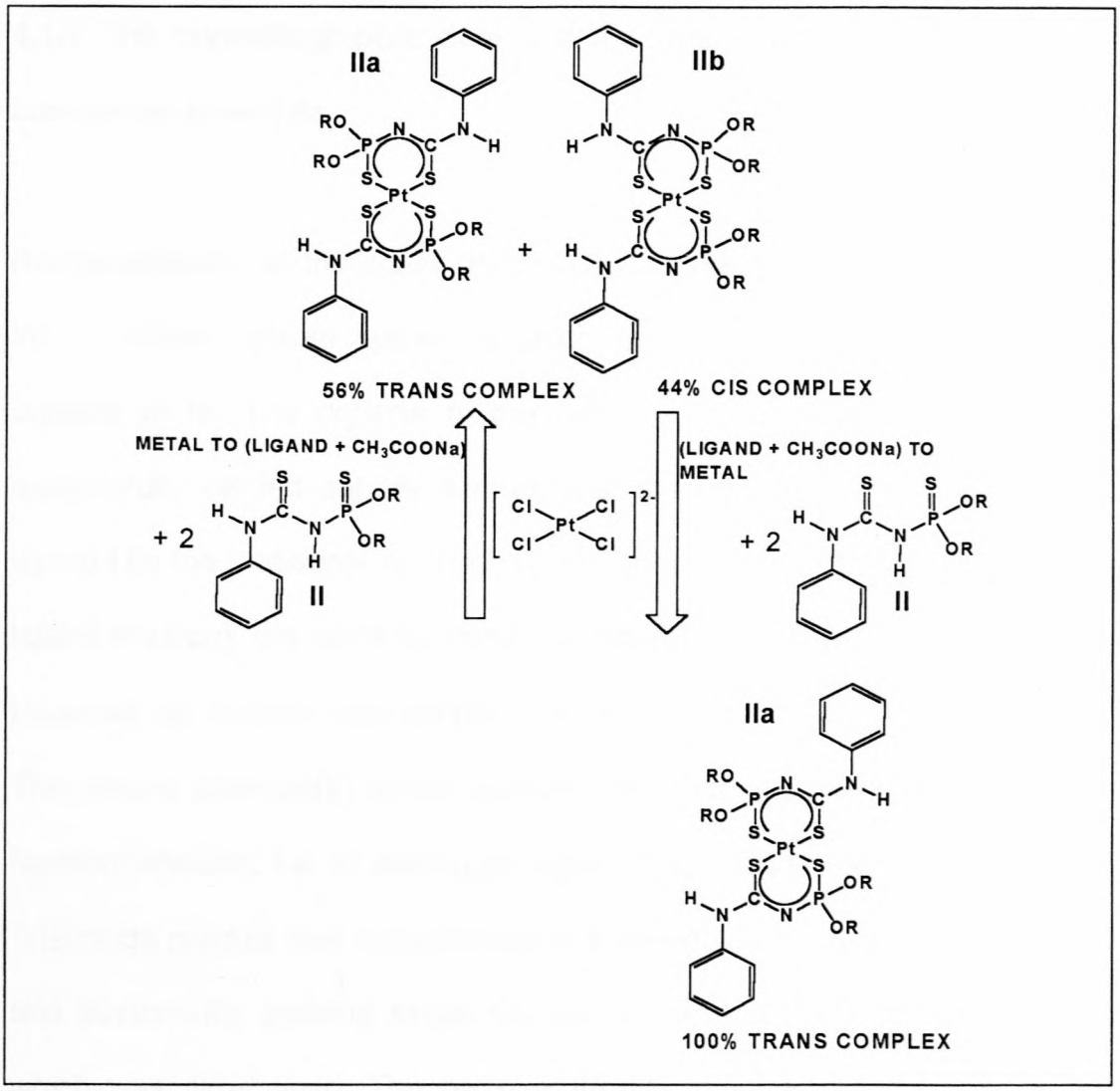

Synthesis scheme 2: Different reaction modes for the synthesis of the platinum-ligand(**II**) chelates lead to different isomer distribution

The relative amounts of isomers (56% *trans* and 44% *cis*) obtained from the $[PtCl_4]^{2-}$ to ligand synthesis described in **synthesis scheme 2** were obtained from the peak integrals of the $^{31}P\{^1H\}$ NMR spectrum.

4.1.1 The crystallographic data and the molecular structures of *trans* complexes Ia and IIa

Recrystallisation of the crude $[Pt(L^{I}\text{-}S,S)_2]$.chelate synthesised from ligand **I** from a mixed solvent system of chloroform and acetonitrile, gave single crystals of **Ia**. The crystals of the complex **Ia** are stable in air. Having successfully carried out the synthesis of the first platinum(II) chelate with ligand **I** by the traditional synthetic route[50] (adding the $[PtCl_4]^{2-}$ solution to the ligand solution), the same synthetic procedure was employed using ligand **II**. However, no crystals could be grown after recrystallising in the same manner. The second platinum(II) chelate was only isolated after reversing the order of reactant addition, i.e. by adding the ligand **II** solution to the $[PtCl_4]^{2-}$ solution. The crude product was recrystallised in a mixed solvent system of chloroform and acetonitrile, yielding single crystals of **IIa**, and the crystal structure of which was determined. The complex **IIa** was observed to discolour in few hours out of the mother liquor. This necessitated the sealing of crystals of **IIa** with paratone oil prior to X-ray diffraction data collection. The crystal lattice of **IIa** was observed to contain acetonitrile solvent molecules and its disintegration when out of the mother liquor was caused by the escape of these non-coordinating solvent molecules from the crystal lattice. Both compounds **Ia** and **IIa** crystallised in the monoclinic system, with **IIa** having two acetonitrile solvent molecules in its crystal lattice. The crystallographic data of the two complexes is presented in **table 18**. Only the important bond lengths and bond angles are accompanying the molecular structures. **Tables**

3 and 4 in the appendix **3** contain all other (bond lengths, bond angles) and torsion angles for **Ia**, while **tables 5 and 6** in appendix **4** contain data for **IIa**.

Table 18: The crystal data and structure refinement for complexes **Ia** and **IIa**.

	Ia	**IIa**
Molecular formula	$PtP_2C_{26}H_{38}N_2S_4O_4$	$PtP_2C_{26}H_{40}N_4S_4O_4{\cdot}2CH_3CN$
M	827.89	940.03
T/K	173(2)	173(2)
Crystal system	Monoclinic	Monoclinic
Space group	$2P_1/c$	$2P_1/n$
a/Å	13.1450(10)	9.6570(2)
b/Å	8.0377(5)	9.0520(1)
c/Å	15.5770(10)	22.491(2)
α/°	90	90
β/°	93.145(2)	97.459(1)
γ/°	90	90
V/Å^3	1643.32(19)	1949.4(3)
μ/mm^{-1}	4.654	3.936
Reflections collected/unique	3553/3553	10446/4463
Final R1, wR2[I>2σI]	0.0243, 0.0595	0.0207, 0.0421
(all data)	0.0319, 0.0629	0.0310, 0.0448

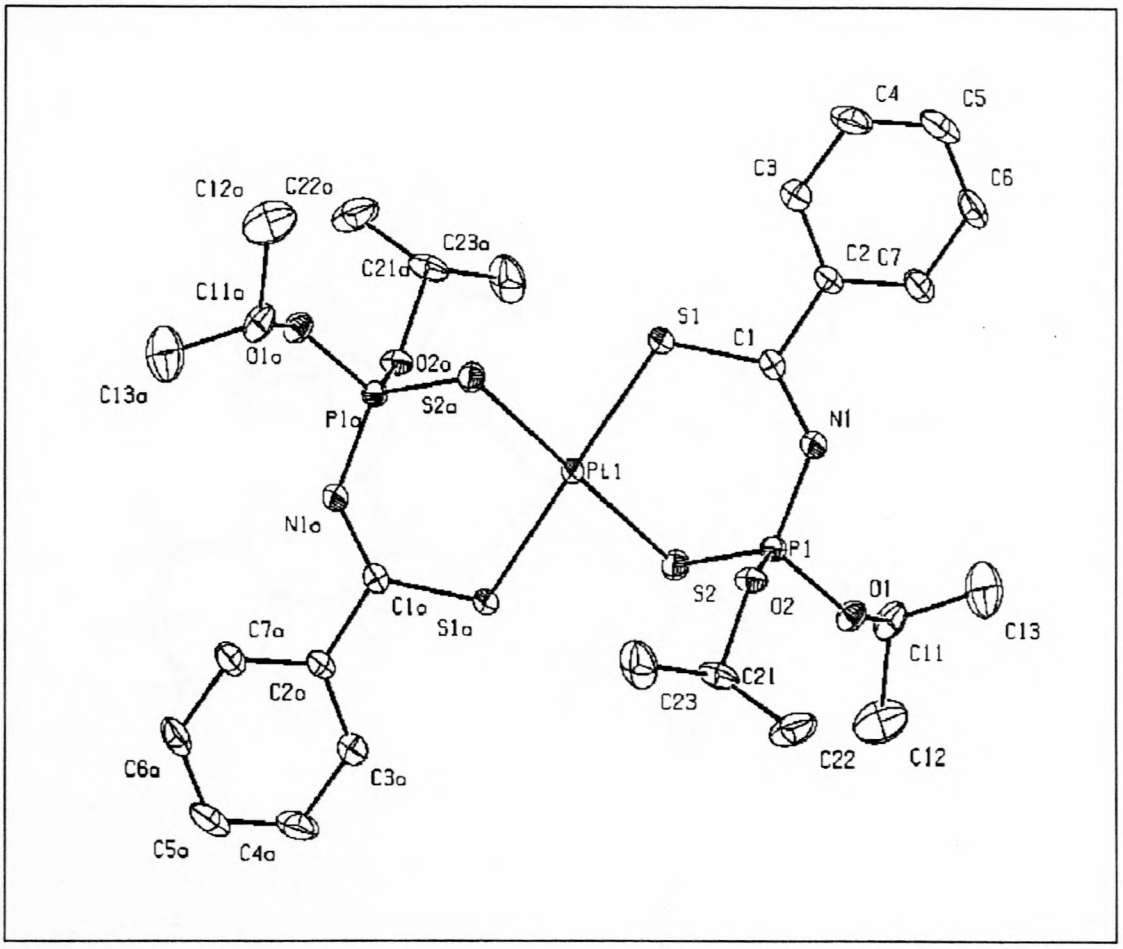

Figure 27: The molecular structure of **Ia**, with selected bond lengths (Å) and bond angles (°) within the coordination sphere of the Pt(II) atom. Pt(1)-S(1) 2.3034(7), Pt(1)-S(2) 2.3367(7), C(1)-S(1) 1.718(3), P(1)-S(2) 1.9994(10), P(1)-N(1) 1.608(2), N(1)-C(1) 1.307(4); S(1)-Pt(1)-S(1)a 180.0, S(1)-Pt(1)-S(2) 96.96(3), S(1)-Pt(1)-S(2)a 83.04(3), S(2)-Pt(1)-S(2)a 180.0

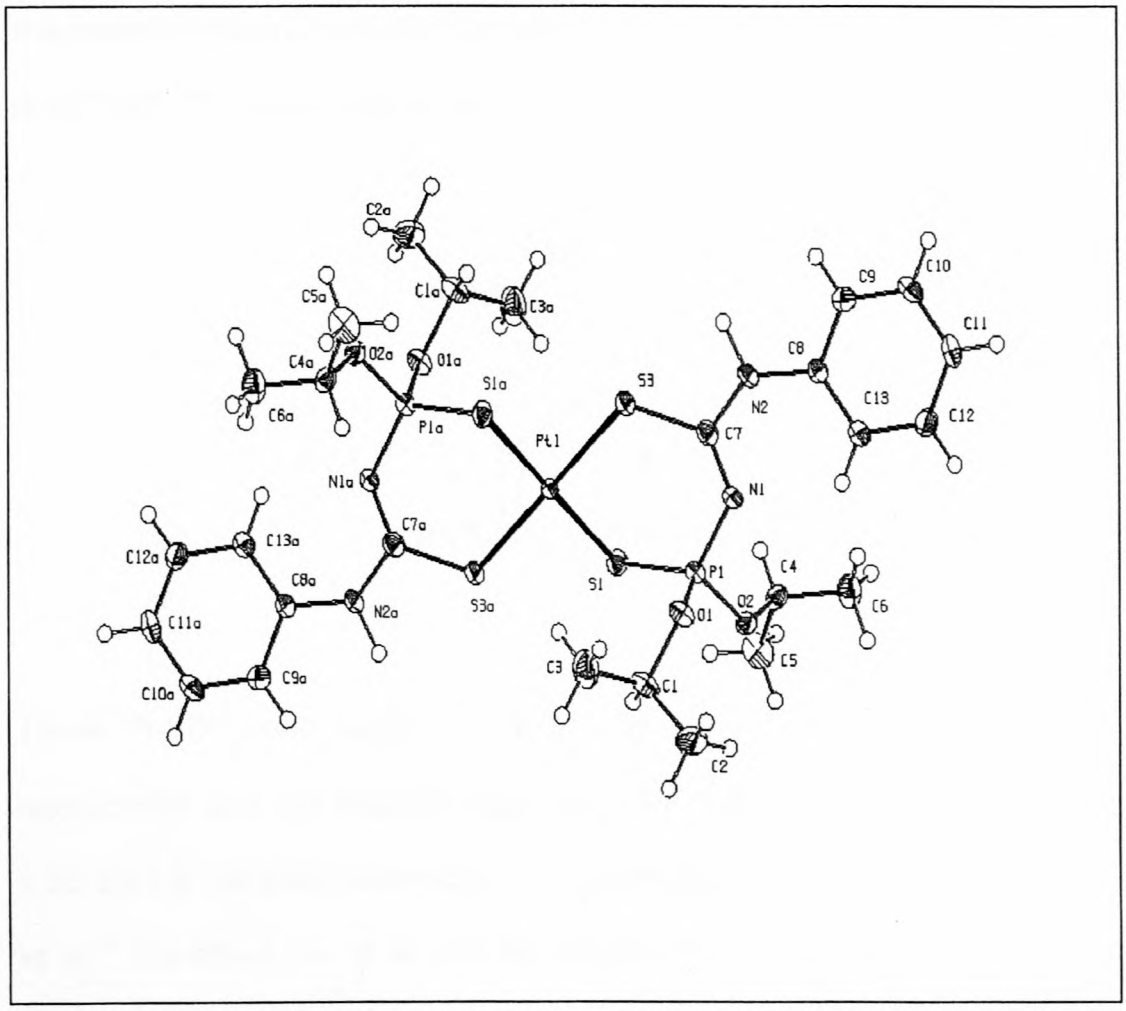

Figure 28: The molecular structure of **IIa**, with selected bond lengths (Å) and bond angles (°) within the coordination sphere of the Pt(II) atom. Pt(1)-S(3) 2.3070(7), Pt(1)-S(1) 2.3242(7), C(7)-S(3) 1.749(2), P(1)-S(1) 2.0033(9), P(1)-N(1) 1.5992(19), N(1)-C(7) 1.305(3); S(3)-Pt(1)-S(3)a 180.000(10), S(3)-Pt(1)-S(1) 81.54(3), S(3)-Pt(1)-S(1)a 98.46(3) S(1)-Pt(1)-S(1)a 180.0

Both molecules, **Ia** and **IIa** are virtually planar and centrosymmetric. The coordination sphere of each Pt(II) atom distorted from the ideal square planarity, as seen from the significant deviations of the S-Pt-S angles from 90°: S(2)-Pt(1)-S(1)a, 83.04(3)°; S(1)-Pt(1)-S(2), 96.96(3)° for **Ia** and S(1)-Pt(1)-S(3)a, 98.46(3)°; S(1)-Pt(1)-S(3); 81.54(3)° for **IIa**. The S-Pt-S bite angle in **IIa**, S(1)-Pt(1)-S(3); 81.54(3)° is smaller in than that of **Ia**, S(1)-Pt(1)-S(2), 96.96(3)°. The Pt-S(P) bond lengths for **Ia** and **IIa** are 2.3367(7) Å and 2.3242(7) Å respectively, which are comparable to the platinum complex of

the related monoanionic bidentate ligand, shown below, reported by Cupertino *et al*,[60] with Pt-S bond lengths of 2.334(2) Å.

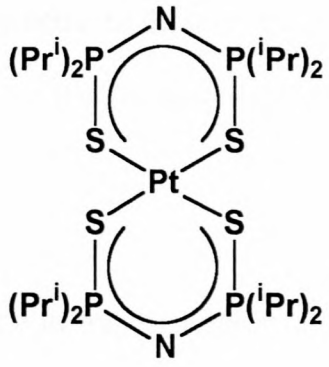

These Pt-S(P) bond lengths for **Ia** and **IIa** are 2.3367(7) Å and 2.3242 Å, respectively and are slightly longer than the two Pt-S(C), 2.3034(7) Å and 2.3070(7) Å. As also observed for the palladium complex reported by Zabirov *et al*,[25] the structures of **Ia** and **IIa** indicate that the thiophosphoryl sulphur atom coordinates relatively weaker than the thiocarbonyl sulphur atom does to the Pt(II) centre. The bond lengths of P(1)-S(2) 1.9994(10) Å and C(1)-S(1) 1.718(3) Å in **Ia** are lengthened as compared to the molecular structure of the unbound ligand studied by Solov've *et al*,[61] which are P-(S) 1.912(1) Å and C-(S) 1.635(4) Å. The bond lengths P(1)-S(2) 1.9994(10) Å and C(1)-S(1) 1.718(3) Å in the complex correspond more closely to partial single bonds, while those in the unbound ligand are double bonds.

4.1.2 The multinuclear magnetic resonance data of the platinum(II) chelates

The ^{1}H and $^{13}C\{^{1}H\}$ NMR spectra of the complexes (**Ia**, **IIa** and **IIb**) will not be discussed in detail except for the notable differences which distinguish them from each other.

The most notable difference in the ^{1}H NMR spectra of the complexes is the disappearance N-H peak (characteristic of the unbound ligands), which appear at 8.1 and 9.7 ppm for **I** and **II**, respectively. This clearly shows that the ligand becomes deprotonated on coordination to the platinum(II) ion. The $^{31}P\{^{1}H\}$ NMR spectra are most informative about the Pt(II) complexes formed. The chemical shifts, $\delta(^{31}P)$ of the complexes and those of the unbound ligands are compared in **table 19**. Included in the table is the difference, Δ, between the chemical shifts of the complexes and that of the unbound ligands, $\Delta = \delta(^{31}P)_{complex} - \delta(^{31}P)_{unbound\ ligand}$.

Table 19: The comparison of $\delta(^{31}P)$ chemical shifts of complexes with those of unbound ligands.

LIGAND	$\delta(^{31}P)$/ppm	COMPLEX	$\delta(^{31}P)$/ppm	Δ/ppm
I	57.9	**Ia**	42.6	-15.3
II	53.2	**IIa**	43.6	-9.6
		IIb	44.5	-8.6

Data in **table 19** show an upfield displacement of the $\delta(^{31}P)$ shift of *ca* 8-15 ppm of the ligand on coordination to the platinum(II) ion. This is consistent with an upfield shift (4-9 ppm) noted by Mashkina *et al*,[51] for palladium(II) and platinum(II) complexes of **I** and related ligands. A plausible rationale behind this upfield shift is that in the **(S)CNP(S)** chelate ring, electrons are delocalised, consequently, shielding the phosphorus atoms of the complexes. Another difference between the $^{31}P\{^{1}H\}$ resonance's of the complexes and the ligands is that the unbound ligands appear as singlet peaks, while in the complexes we see a singlet peak (corresponding to $[Pt\text{-}L^{I/II}\text{-}S,S)_2]$ molecule with non magnetically active Pt isotopes) flanked by $^{1}J(^{195}Pt\text{-}^{31}P)$ coupling satellites corresponding to the complexes containing the ^{195}Pt isotopes at ca 33.8% natural abundance.

A pictorial representation for **IIa/IIb** and the comparison of some of their coupling constants are shown in **table 20**.

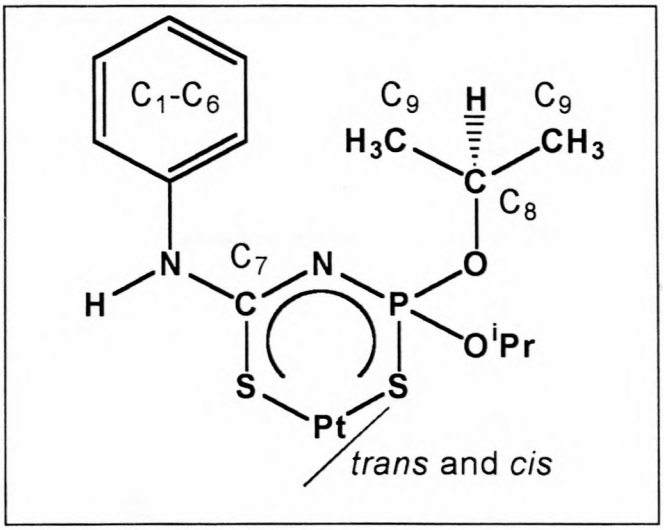

Table 20: Comparison of important coupling constants for the *trans* (**IIa**) and *cis* (**IIb**) complexes

Coupling constant/Hz	**IIa**	**IIb**
$^{2}J(^{195}Pt\text{-}^{31}P)$	106	101
$^{1}J(^{13}C_9\text{-}^{1}H_9)$	127	127
$^{3}J(^{31}P\text{-}^{1}H_8)$	10.4	10.3
$^{3}J(^{1}H_8\text{-}^{1}H_9)$	6.6	6.6
$^{4}J(^{31}P\text{-}^{1}H_9)$	11.3	6.4

The accurate values of $^{3}J(^{31}P\text{-}^{1}H_8)$ and $^{4}J(^{31}P\text{-}^{1}H_9)$ of the two complexes are achieved by selective homonuclear decoupling of H_8 to H_9 and *vice versa*. This effectively collapses the multiplets at 1.36 and 4.87 ppm into simple doublets, which can be attributed to phosphorus coupling to H_9 and H_8 respectively. The following two figures **29** and **30** serve as an example of a homonuclear decoupling experiment.

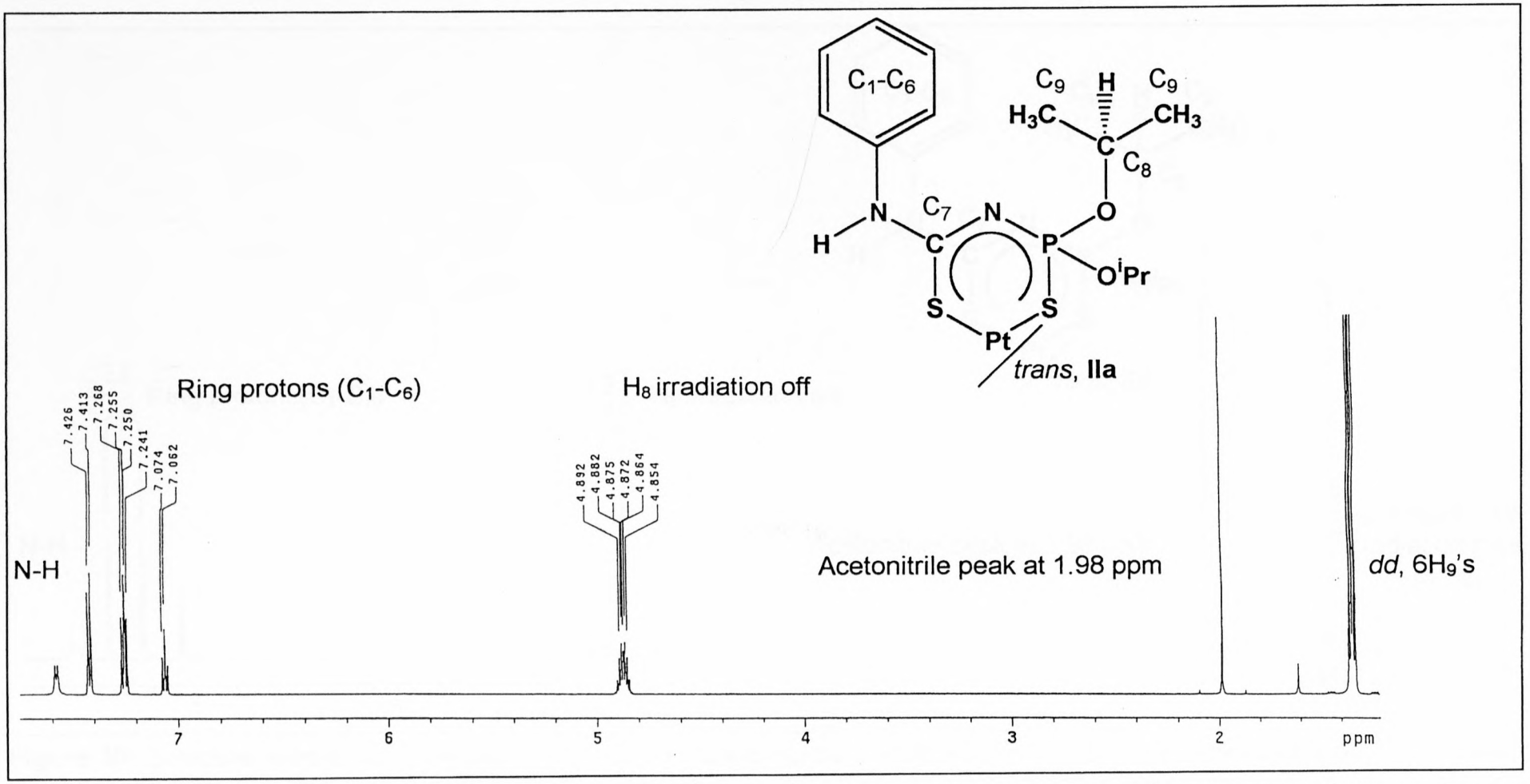

Figure 29: A fully coupled ^{1}H NMR spectrum of **IIa**, with H_8 resonating as a multiplet at 4.87 ppm since it couples to the protons at C_9 as well as to the phosphorus atom three bonds away.

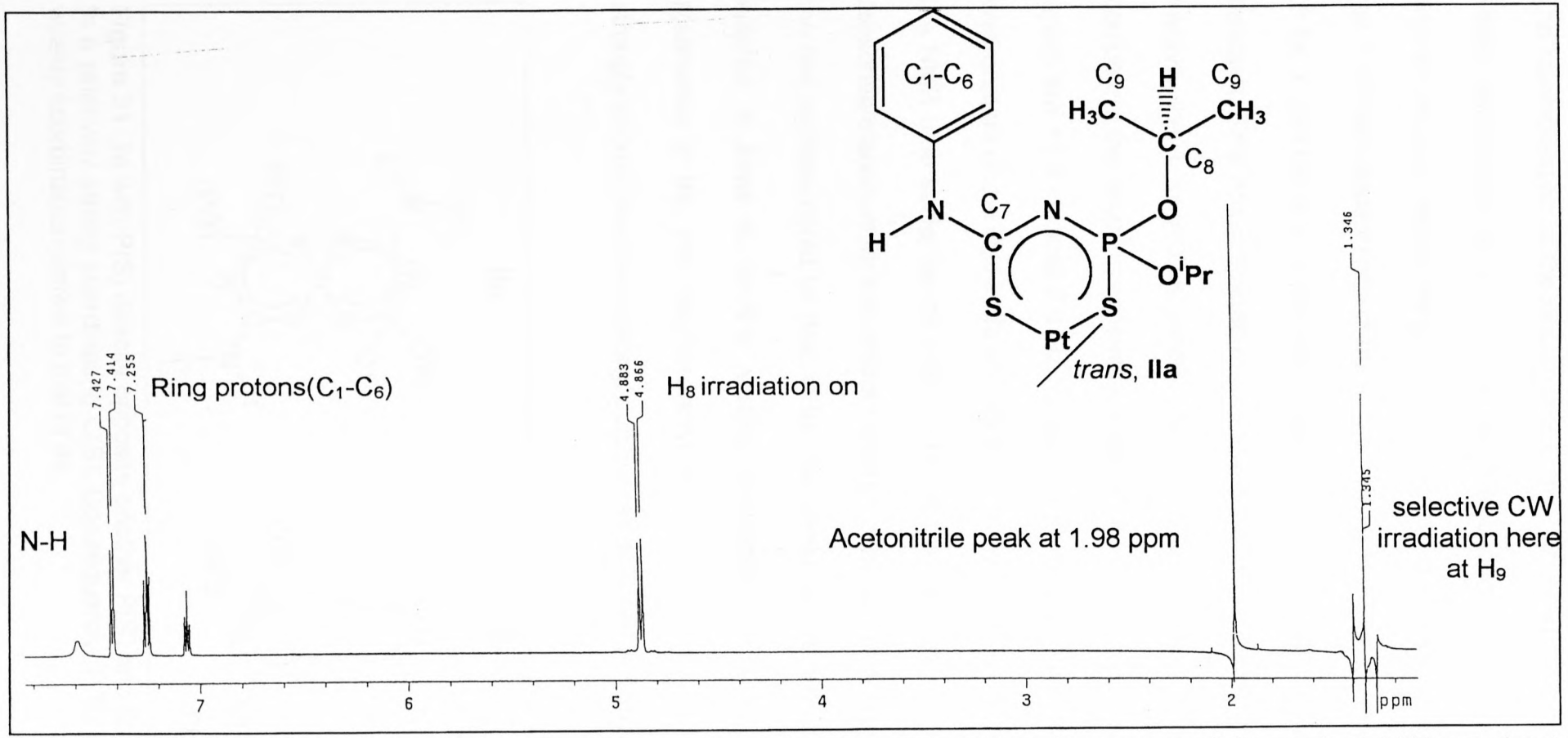

Figure 30: Selective irradiation of the peak at 1.34 ppm (due to H_9) decouples H_9's to H_8, as a result the peak at 4.87 ppm due to H_8 collapses from a multiplet to a simple doublet, as shown in the spectrum. This particular experiment allows one to obtain a precise value of $^{3}J(^{31}P\text{-}^{1}H_8)$, which is about 10.4 Hz for **IIa**.

The rationalisation of the assignment of the $^{n}J(^{31}P\text{-}^{1}H)$ values, n = 3 and 4 in these complexes is thought to be dependent on different electronic environments in which the phosphorus atoms are in the two isomers. From the downfield appearance of **IIb**, in the $^{31}P\{^{1}H\}$ NMR spectrum by comparison to **IIa**, it can be argued that the phosphorus atom in **IIb** is relatively electron deficient. This has predictable consequences in the coupling constants that involve the phosphorus atoms. An example of this is observed when comparing the coupling constants in **table 20**, in particular that of $^{4}J(^{31}P\text{-}^{1}H_9)$, which are 11.3 Hz and 6.4 Hz for **IIa** and **IIb** respectively. Due to a similar environment of the H_8's in **IIa** and **IIb** occur, they are chemically equivalent on the NMR time scale, hence their $^{3}J(^{1}H_8\text{-}^{1}H_9)$ values 6.6 Hz are the same. A reasonable account for the different environments of the phosphorus atoms of the two isomers could be that, in **IIa**, the weakly coordinated thiophosphoryl sulphur is *trans* to another weakly coordinated thiophosphoryl sulphur. Meanwhile in **IIb**, the thiophosphoryl sulphur is *trans* to a relatively more strongly coordinated thiocarbonyl sulphur, as depicted in **figure 31**.

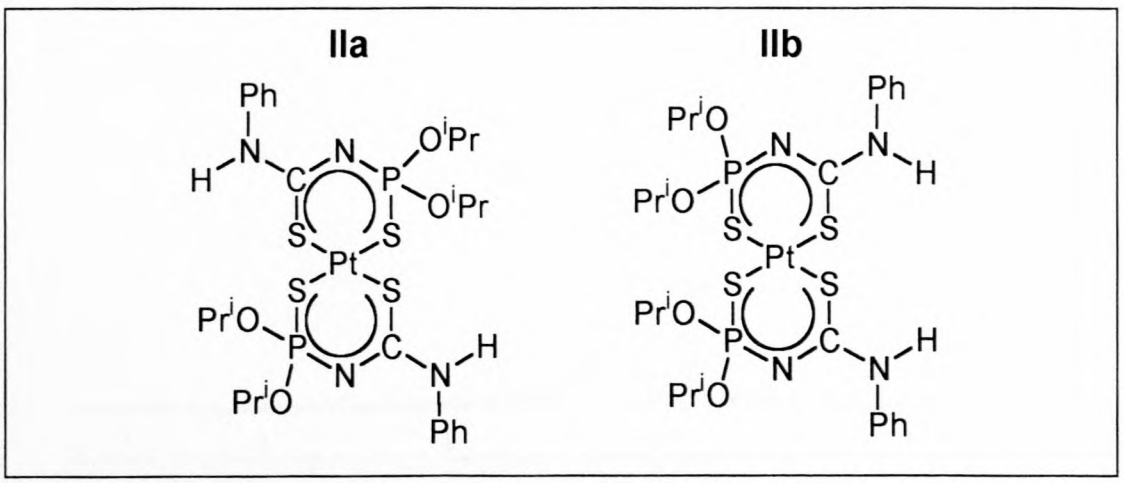

Figure 31: **IIa** with P(S) directly opposite another P(S) and **IIb** with P(S) *trans* to a relatively strong coordinating C(S). Consequently, P(S) in **IIb** should be weakly coordinated relative to that of **IIa**.

From the molecular structure of **IIa** in **figure 28**, the Pt-S(P) bond length is 2.3242(7) Å and that of Pt-S(C) is 2.3070(7) Å, hence it is known that C(S) is relatively strongly coordinating than P(C). In **IIb** the weakly coordinating P(S) *trans* to a relatively more strongly coordinating C(S), hence it is expected to be the weaker coordinated P(S) of the two complexes. The electronic differences in the phosphorus atoms then influence all the coupling constants that involve the phosphorus atoms.

4.2 THE KINETIC STUDY OF THE ISOMERISATION OF PLATINUM(II) CHELATE, *trans*-[Pt(L^{II}-*S,S*)$_2$]

Having isolated a small amount (*ca* 6 mg) of the *cis*-[Pt(L^{II}-*S,S*)$_2$], **IIb**, its $^{31}P\{^1H\}$ NMR spectrum was run in $CDCl_3$ solution. The spectrum showed a ^{31}P peak at 44.5 ppm with small traces of the *trans*-isomer at 43.6 ppm (see **figure 32**).

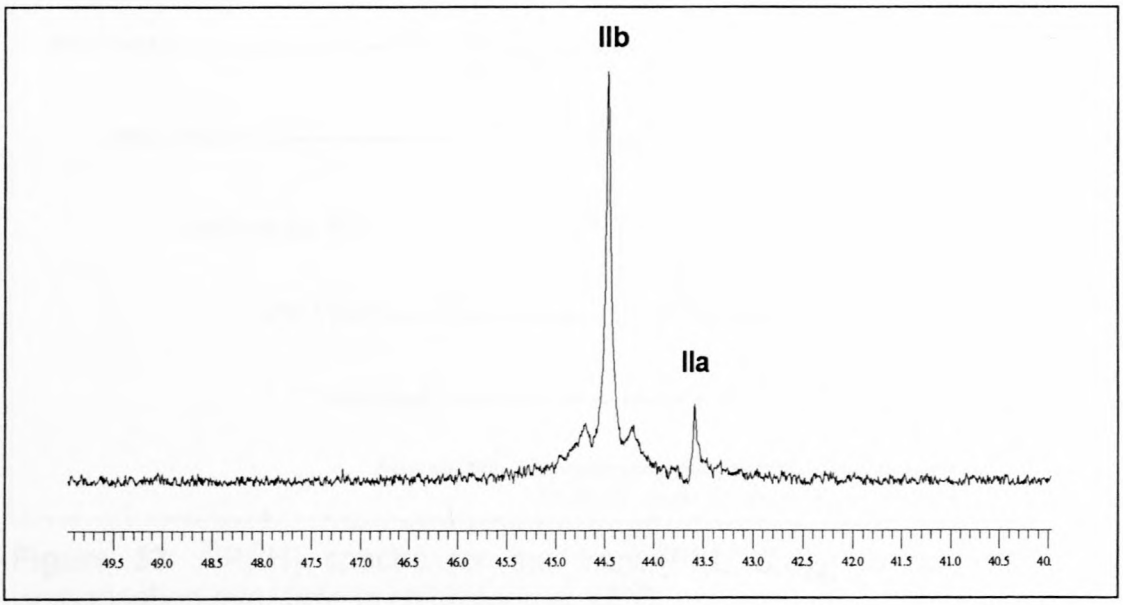

Figure 32: A $^{31}P\{^1H\}$ NMR spectrum of the *cis*-isomer with traces of the *trans*-isomer.

A week later, the $^{195}Pt\{^{1}H\}$ NMR spectrum of the same sample was run and surprisingly, it showed two ^{195}Pt peaks of almost equal intensities at -3964 ppm and at -3956 ppm. The pure *cis*-isomer (**IIb**) had isomerised over this time to produce a mixture of **IIa** and **IIb**.

To follow the isomerisation of *cis*-[Pt(L^{II}-*S,S*)$_2$] to the *trans*-[Pt(L^{II}-*S,S*)$_2$] over time, the following experiment was carried out. A sample of pure *trans*-[Pt(L^{II}-*S,S*)$_2$] was freshly dissolved in $CDCl_3$ and left to stand, with the $^{31}P\{^{1}H\}$ NMR spectra of this sample measured over a period of six weeks. It was discovered that this rare chelate isomerisation occurs for both the *cis*-isomer as well as for the pure *trans*-isomer. This kind of isomerism has been reported only in a few cases[52, 53, 54] and prompted further investigation.

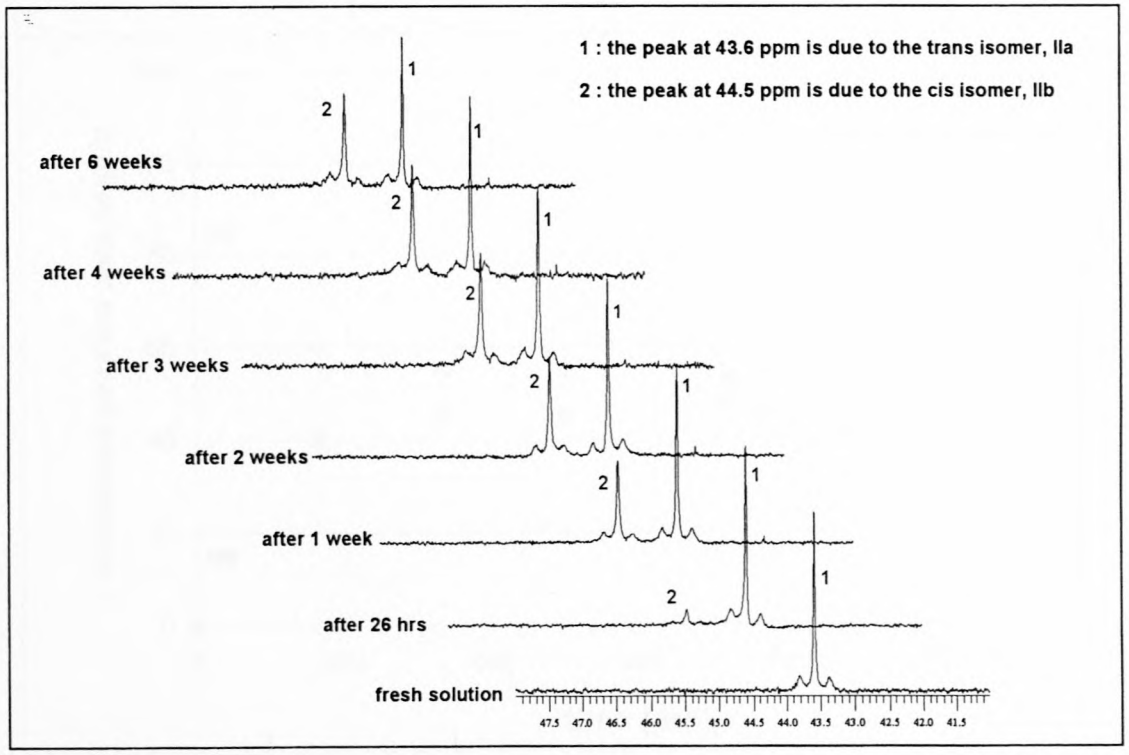

Figure 33: $^{31}P\{^{1}H\}$ spectra for the *trans*-[Pt(L^{II}-*S,S*)$_2$] to *cis*-[Pt(L^{II}-*S,S*)$_2$] isomerisation over time in chloroform at 25°C.

As can be seen in **figure 33**, over time, the concentration of the *cis*-isomer gradually grows at the expense of the *trans*-isomer from 0% to 44%. This 56:44 *trans*:*cis* isomer distribution is the same as the one obtained in the reaction mode where the metal solution is added to the ligand solution (see **synthesis scheme 2**). This suggests that a true equilibrium between *trans* and *cis* complexes has been reached at 25°C in $CDCl_3$.

The following plot shows the slow kinetics of the isomerisation. The *trans*-[Pt(L^{II}-*S,S*)$_2$] to *cis*-[Pt(L^{II}-*S,S*)$_2$] isomerisation equilibrates in no less than 300 hours with a K_e = *cis*-[Pt(L^{II}-*S,S*)$_2$]/*trans*-[Pt(L^{II}-*S,S*)$_2$] value of about 8.52×10^{-1} at 25°C. The detailed calculations for the weighted peak heights are included in appendix **5**, **table 7**.

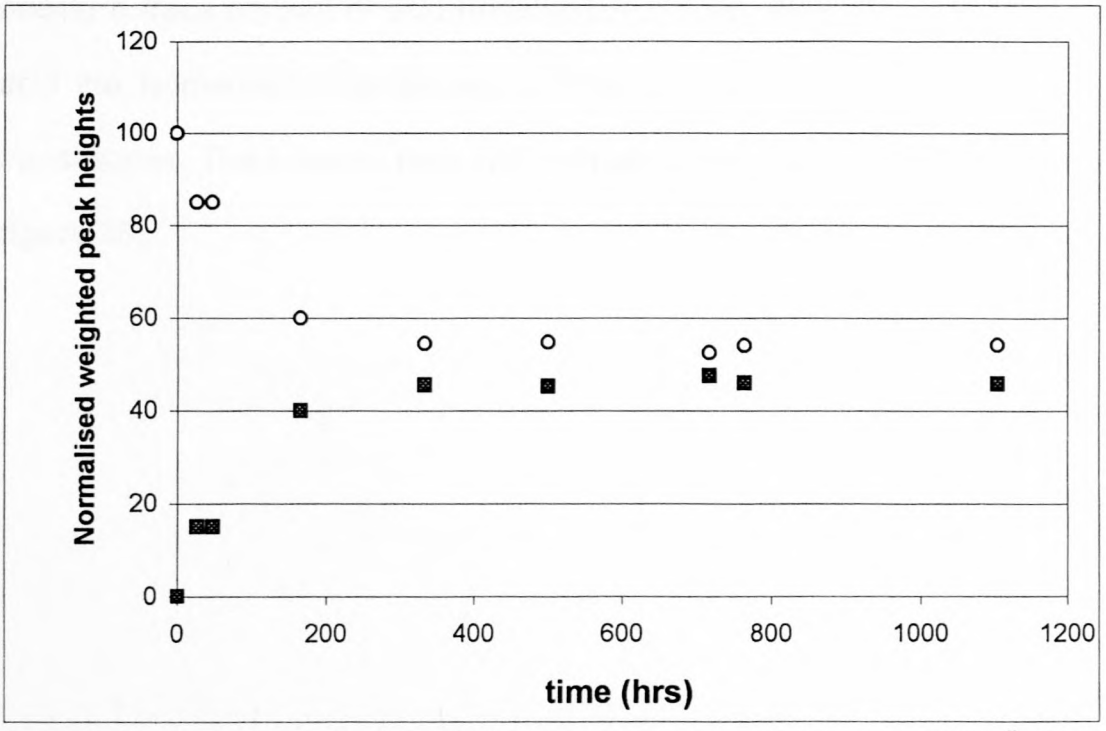

Figure 34: Reaction kinetics of the isomerisation of the *trans*-[Pt(L^{II}-*S,S*)$_2$] complex (**IIa**) (○) to form the *cis*-[Pt(L^{II}-*S,S*)$_2$] complex (**IIb**) (■) in chloroform. **IIa** remains in excess of **IIb** at equilibrium.

The progress of the isomerisation reaction is very slow, presumably due to unstrained stable six membered chelates and the complementary soft-soft acid-base pairs of the platinum(II) ion and the sulphur donors.

The aim of this investigation was to determine what triggers this isomerism, what is the dependence on the polarity of the solvent and to follow the kinetics of this phenomenon.

In a much more polar solvent like dimethylformamide (DMF) no isomerisation took place even after three weeks of standing. Quite surprisingly, in the least polar solvent, benzene, the isomerisation, though significantly slower than in chloroform, did take place. The isomerisation in benzene stops at 97.5:2.5 *trans:cis* after one week. The reaction was then accelerated by deliberately adding a trace amount of acid (trifluoroacetic acid). After the addition of the acid the isomerisation continues until the *cis*-isomer slightly outgrows the *trans*-isomer. The *trans:cis* ratio after thirteen weeks stands at 49.6:50.4 (see **figure 35**).

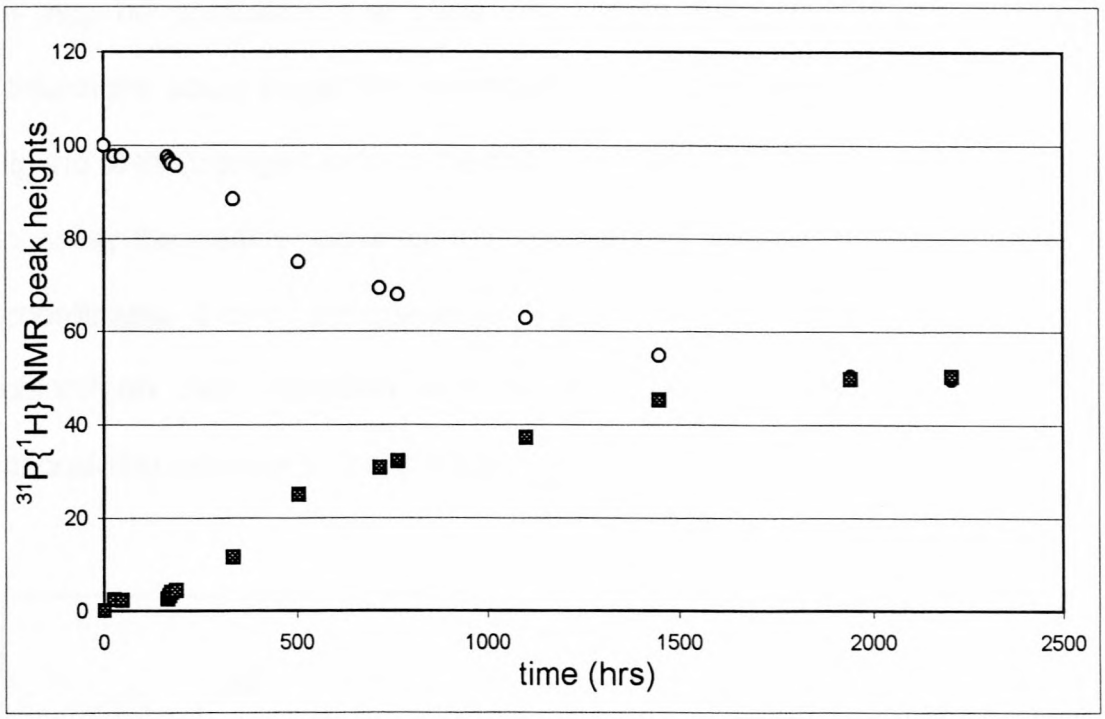

Figure 35: Reaction kinetics of the isomerisation of the *trans*-complex (**IIa**) (○) to form the *cis*-complex (**IIb**) (■) in benzene. The reaction is accelerated by addition of acid after it had ceased after a week. **IIa** is outgrown by **IIb** from the 12th week.

The other effect of the solvent was on the phosphorus chemical shift of the compounds. However, the chemical shift differences have no significance in the isomerism itself. Below is a table of solvent polarity with the chemical shifts of the *trans*-isomer.

Table 21: Measured phosphorus chemical shifts of **IIa** in solvents of different polarity (relative permittivity or dielectric constant).

solvent	relative permittivity, D^{56}	**IIa** $\delta(^{31}P)$/ppm
C_6D_6	2.27	44.6
$CDCl_3$	4.70	43.6
DMF-d_7	36.7	47.1

It may be postulated that trace amounts of acid (HCl) in the deuterated chloroform could trigger the isomerism. The acid is believed to protonate the ligand at the nitrogen atom of the chelate. This initiates a Pt-S bond cleavage, possibly the weakly coordinated thiophosphoryl sulphur. When the ligand re-coordinates, it forms the *cis*-isomer, which is favoured in a polar solvent like chloroform (see **reaction scheme 6**). The isomerisation occurs at a decreasing rate due to mass action.

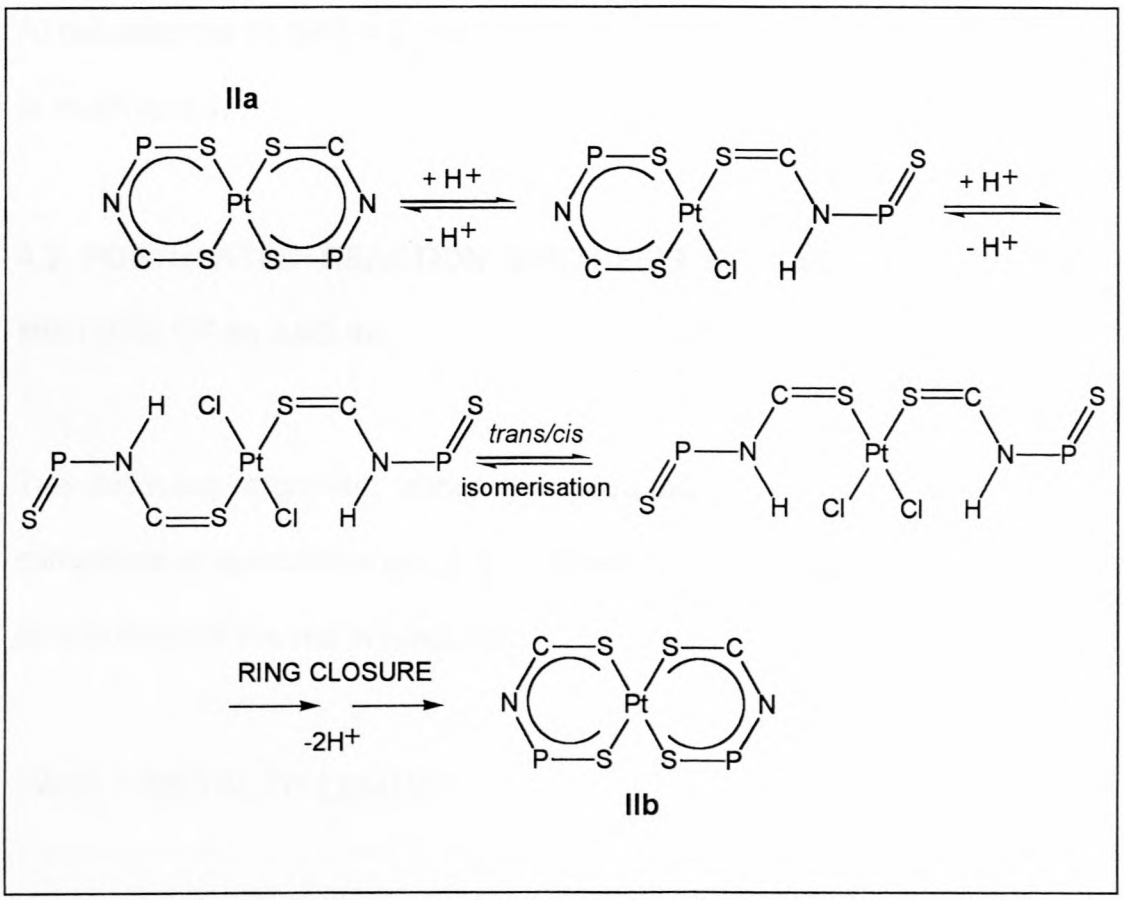

Reaction scheme 6: Postulated acid catalysed reaction mechanism for the isomerisation of *trans*-[Pt(L^{II}-*S,S*)$_2$] (**IIa**) to *cis*-[Pt(L^{II}-*S,S*)$_2$] (**IIb**) in $CDCl_3$ at 25°C. For clarity, the atoms not in the chelate ring are omitted.

Examples of the *cis/trans* isomerisation in **reaction scheme 6** are reported by Koch *et al*,[14] with *cis*- and *trans*-[Pt(H_2L-*S*)$_2Cl_2$] complexes as well as by Chatt and Wilkinson,[34] with *cis*- and *trans*-[Pt(PR_3)$_2Cl_2$] complexes.

In support of this postulate is the fact that when the isomerisation stopped after a week in benzene, it was promoted by addition of trace amounts of trifluoroacetic acid.

The occurrence of this rare chelate isomerism in the case of **IIa/IIb** may well be explained by the very small difference (0.0172 Å) between the Pt-S(P) = 2.3242(7) Å and Pt-S(C) = 2.3070(7) Å bond lengths in the complex **IIa**. This isomerisation phenomenon in **Ia**, is not observed where the difference (0.0333 Å) between the Pt-S(P) = 2.3367(7) Å and Pt-S(C) = 2.3034(7) Å bond lengths is much larger.

4.3 POSTULATED REACTION SYNTHESIS OF EXCLUSIVE IIa AND A MIXTURE OF IIa AND IIb.

The following argument about the postulated reaction synthesis of the complexes is speculative and it is an attempt to rationalise the different isomer distributions of the two procedures.

CASE 1: METAL TO LIGAND

From the crystal structure data of **Ia** and **IIa** as well as in the palladium complex reported by Zabirov *et al*,[25] it is evident that the thiocarbonyl sulphur, C(S), coordinates much stronger than the thiophosphoryl sulphur, P(S). The first step in the synthesis is thought to involve the displacement of the first chloride ion by C(S) of the first ligand (step 1 in **reaction scheme 7**).

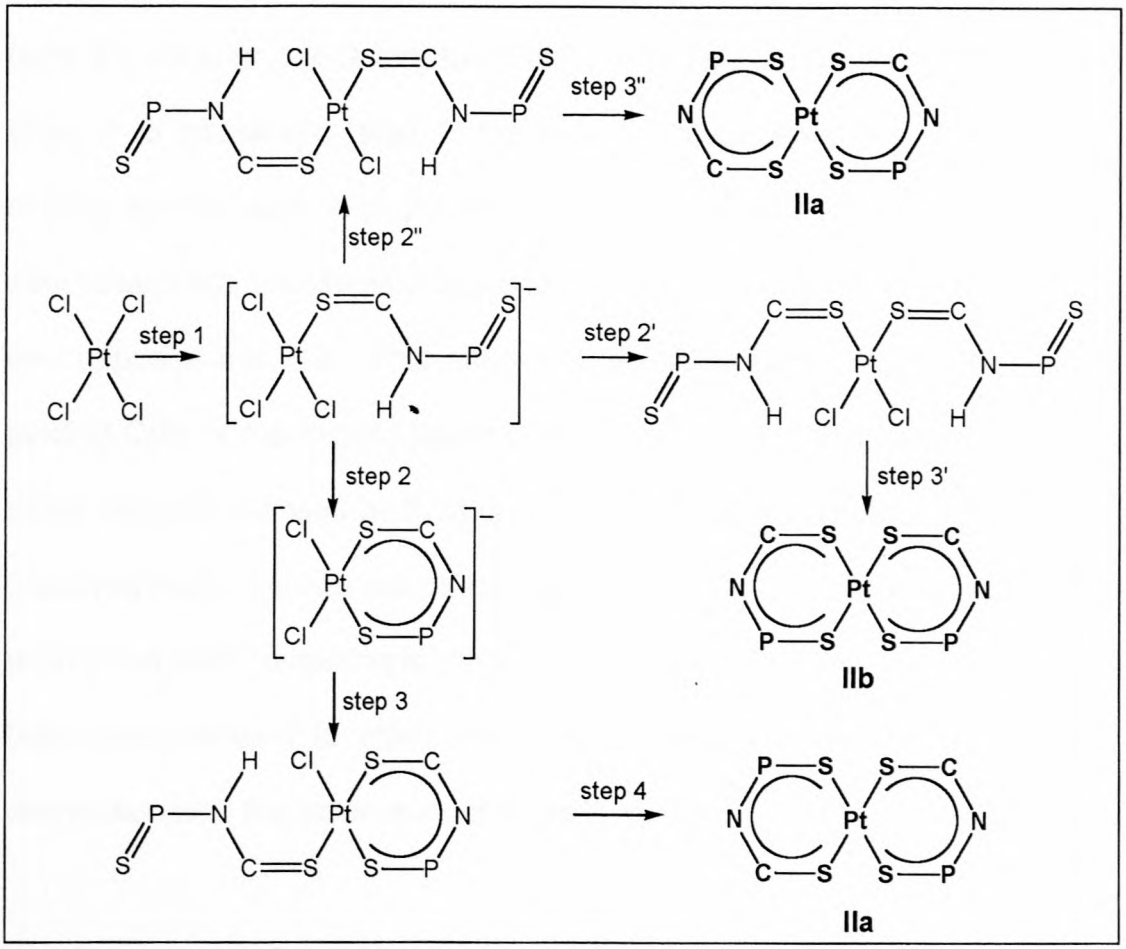

Reaction scheme 7: Postulated reaction scheme for the two modes of synthesis (metal to ligand and the reverse). For clarity, only the atoms in the chelate ring are shown.

The next step involves the displacement of the second chloride ion by C(S) of the second ligand. There are three positions of displacement, two are *cis* to the already coordinated C(S) of the first ligand and one *trans* C(S) (steps 2' and 2"). Statistically, this implies that it is two times more likely for the strongly coordinated C(S) of the two ligands to be in a *cis* orientation to each other. The next step then involves the coordination of the P(S) of each ligand (steps 3' and 3"). This ideally, would lead to a 2:1 mixture with the *cis*-isomer being favoured. However, this is not the case, for mainly two reasons. The first one is that the substitution of the most labile chloride ion by C(S) of the second ligand is favoured (step 2") compared to substitution of the *cis* chloride ions

(step 2'). Another one is that the proximity of the P(S) of the first ligand may allow it to coordinate (step 2) before the coordination of the C(S) of the second ligand (steps 2' or 2"). From step 2, since C(S) has a stronger *trans* effect than P(S), the chlorine opposite the former is much more labile than the one opposite the P(S). This effectively allows once again for the strongly binding C(S) of the second ligand to bind first where the chloride ion is most labile (step 3), followed by P(S) (step 4). From **reaction scheme 7**, it can be observed that there are two paths that produce the *trans*-product while there is only one path competing to produce the *cis*-product. Experimentally this has been demonstrated to effectively produce an approximately 54:46 isomer distribution with the *trans*-product being favoured.

CASE 2: LIGAND TO METAL

In this case, where the metal is in large excess, the first ligand will coordinate fully with minimal competition from the second ligand (step 2). The most labile chloride ion is the one *trans* to C(S), therefore the coordination of the second ligand will start at that point. For the reasons stated previously, C(S) coordinates first (step 3) then P(S) follows, leading to exclusive *trans*-product (step 4). Other pathways are excluded (steps 2' and 2") since the metal is in large excess.

Although this postulated reaction scheme seems to roughly explain the occurrence of the isomer distributions for the two cases, it might be difficult to demonstrate it, experimentally!

4.4 REACTIONS OF *cis*-[Pt(P^nBu_3)$_2Cl_2$] WITH *N*-THIOPHOSPHORYLATED THIOAMIDE AND *N,N*-THIOPHOSPHENYLTHIOUREA

As part of the study, the reaction of *N*-diisopropoxythiophosphoryl thioamide (**I**) and *N*-diisopropoxythiophosphoryl-*N'*-phenylthiourea (**II**) with *cis*-[Pt(PBu_3)$_2Cl_2$] in the presence of a base (triethylamine) was investigated. This was to examine the postulate that this reaction might be similar to the reaction of *N,N*-dialkyl-*N'*-acyl(aroyl)thioureas discussed in **chapter 3**. In section **4.1**, it was demonstrated that the thiophosphoryl sulphur is subtly different from the thiocarbonyl sulphur and it should be interesting to see how these differences are reflected in these reactions. In the anticipated reaction scheme below, one might be able to see long-range $^3J(^{31}P\text{-}^{31}P)$ coupling constants between the phosphine and P(S) atom for complexes **A** and **B**.

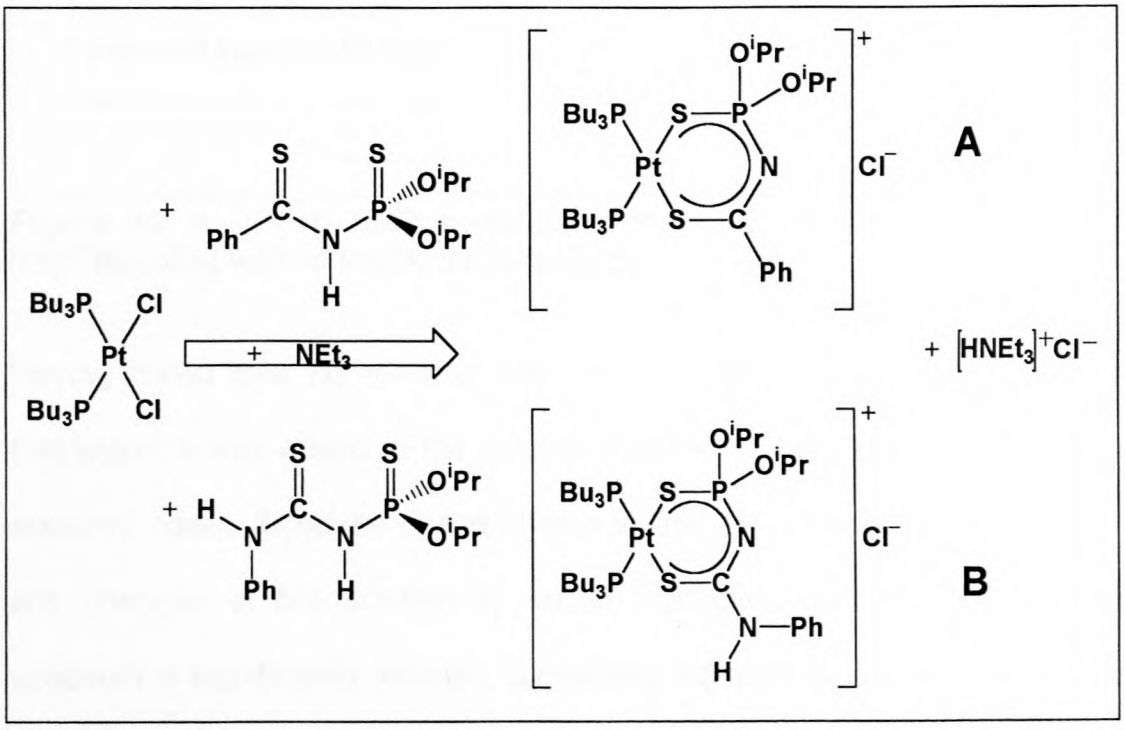

Anticipated reaction scheme 1: The platinum-ligand complexes formed when ligands **I** and **II** react with *cis*-[Pt(P^nBu_3)$_2Cl_2$] in the presence of a base.

4.4.1 Reaction of *cis*-[Pt(P^nBu_3)$_2Cl_2$] with *N*-diisopropoxythiophosphoryl thioamide, I

A 0.1 molar solution of *cis*-[Pt(PBu_3)$_2Cl_2$] was prepared by dissolving the appropriate amount of the solid in one millilitre of $CDCl_3$. An equimolar amount of ligand **I**, dissolved in $CDCl_3$ was added to the *cis*-[Pt(PBu_3)$_2Cl_2$] solution. The $^{31}P\{^1H\}$ NMR spectrum of this mixture was then measured. Two ^{31}P peaks at 1.7 ppm and at 57.9 ppm corresponding to the *cis*-[Pt(PBu_3)$_2Cl_2$] complex and ligand **I** respectively were observed.

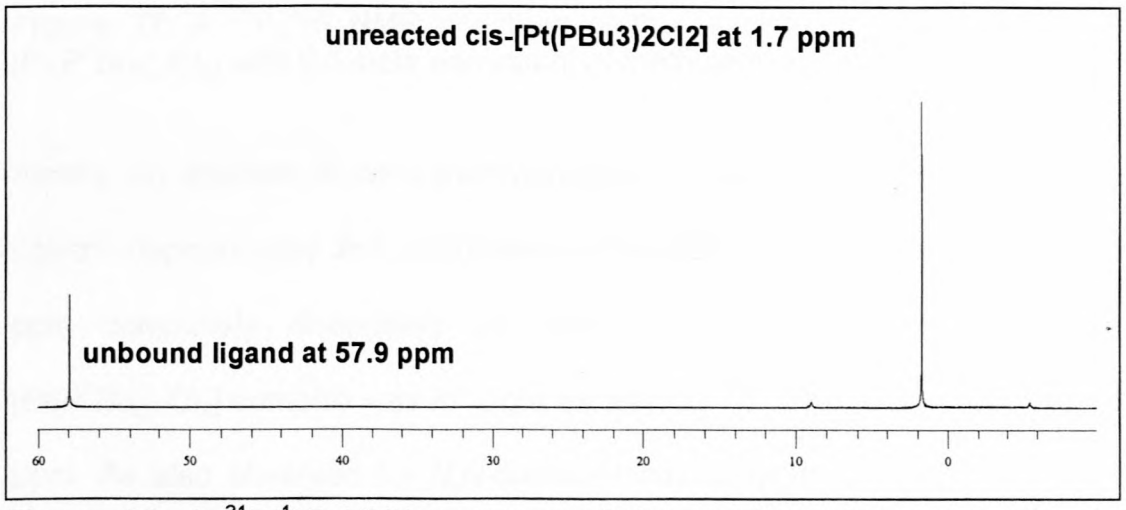

Figure 36: A $^{31}P\{^1H\}$ NMR spectrum of the reaction of ligand **I** with *cis*-[Pt(P^nBu_3)$_2Cl_2$] with no triethylamine added.

Having noted that no reaction has taken place, 0.5 mole equivalent of triethylamine was added to the solution and the $^{31}P\{^1H\}$ NMR spectrum was acquired again. Since the ligand **I** has a yellow colour, it is not easy to note any changes in the solution by visual inspection but the $^{31}P\{^1H\}$ NMR spectrum is significantly different. Since only 0.5 mole equivalent of the base has been added, not all the ligand is activated for coordination, hence the ^{31}P

peak for the unbound ligand and the *cis*-[Pt(P^nBu_3)$_2Cl_2$] still appear in the $^{31}P\{^1H\}$ NMR spectrum, see **figure 37**.

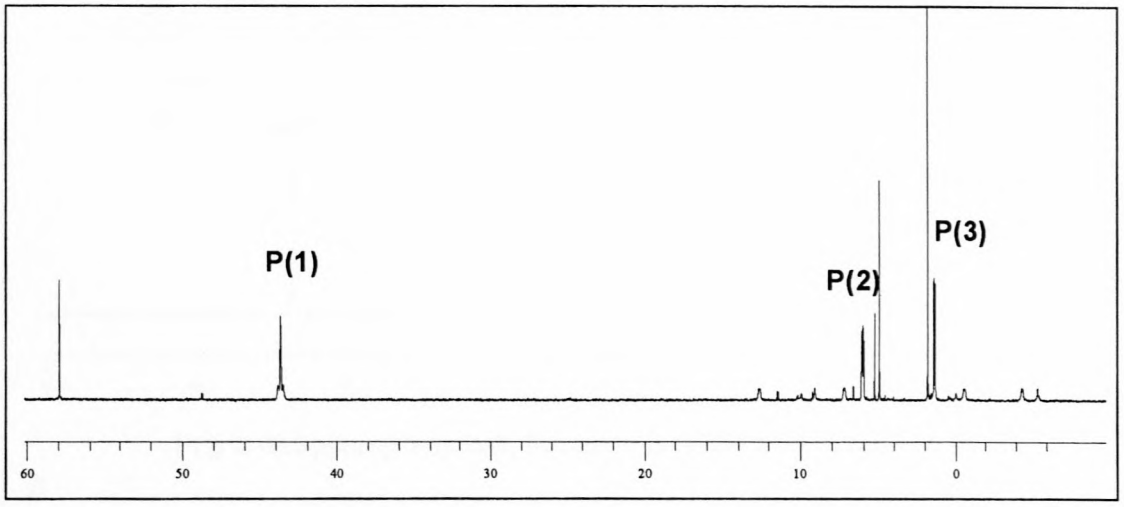

Figure 37: A $^{31}P\{^1H\}$ NMR spectrum of the reaction of ligand **I** with *cis*-[Pt(P^nBu_3)$_2Cl_2$] with 0.5 mole equivalent of triethylamine added.

Finally, on addition of more triethylamine (1.0 mole equivalent), with all the ligand **I** deprotonated and coordinated to the platinum(II) ion, the peak at 57.9 ppm completely disappears as **figure 38** illustrates. Since the *cis*-[Pt(P^nBu_3)$_2Cl_2$] complex was in slight excess, its ^{31}P peak still appears at 1.7 ppm. As also observed for *N,N*-dialkyl-*N'*-acyl(aroyl)thioureas in **chapter 3** section **3.2**, without triethylamine, no reaction takes place between ligand **I** and *cis*-[Pt(P^nBu_3)$_2Cl_2$]. Evidently, ligand **I** is deprotonated at the weakly acidic amido proton of the **-(S)CNHP(S)-** moiety and thus rapidly coordinates to the platinum(II) ion, displacing the two Cl^- ions from *cis*-[Pt(P^nBu_3)$_2Cl_2$].

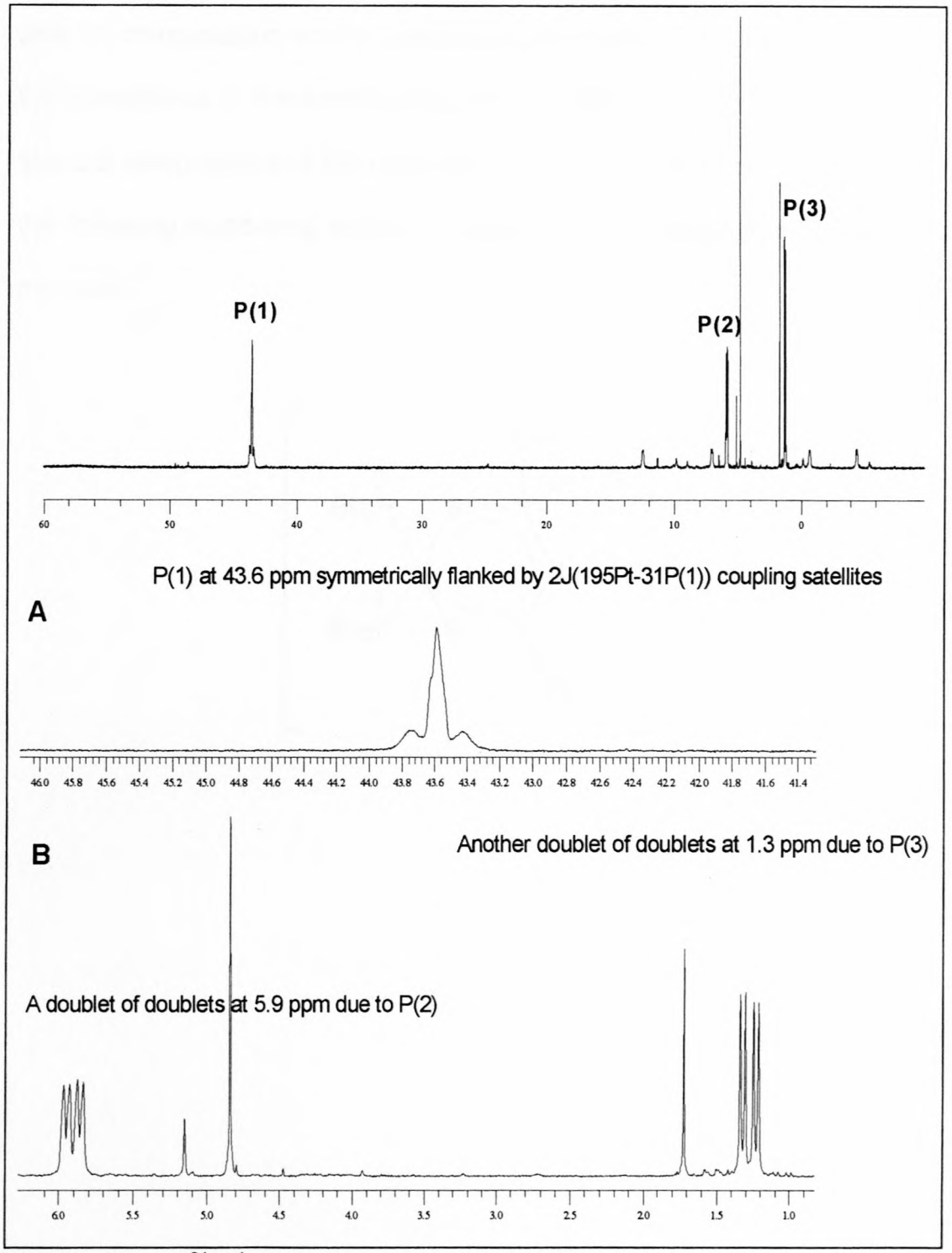

Figure 38: A $^{31}P\{^{1}H\}$ NMR spectrum of the reaction of ligand **I** with *cis*-$[Pt(P^{n}Bu_3)_2Cl_2]$ with one mole equivalence of triethylamine added. Expansion **A** shows the fine structure of P(1) while **B** shows the fine structures of the parent peaks of P(2) and P(3).

From the $^{31}P\{^{1}H\}$ NMR spectrum in **figure 37**, it is observed that the phosphorus of the coordinated ligand experiences an upfield shift of about 14.3 ppm by comparison to the unbound ligand. This is an expected upfield

shift on complexation as the delocalised electrons in the chelate ring shield the phosphorus of the coordinating ligand. **Table 22** shows the $^{31}P\{^{1}H\}$ NMR spectral assignments of the resulting mixed ligand platinum(II) complex with the following numbering scheme adopted for the phosphorus atoms of the complex:

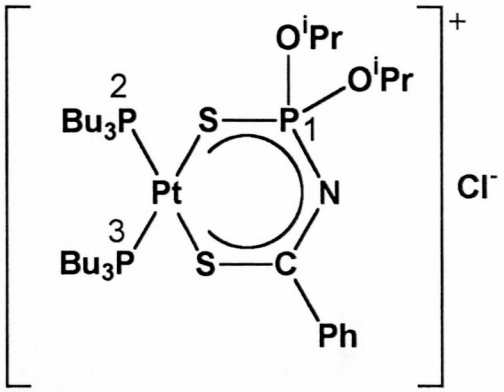

Table 22: The assignments of the phosphorus spectrum of the complex resulting from the reaction of *cis*-[Pt(P^nBu_3)$_2Cl_2$] with **I** in the presence of triethylamine.

Compound	δ^{31}P/ppm and multiplicity	$^1J(^{195}Pt-^{31}P)$ /Hz	$^2J(^{195}Pt-^{31}P)$ /Hz	$^2J(^{31}P(2)-^{31}P(3))$ /Hz	$^3J(^{31}P(1)-^{31}P)$ /Hz
cis-[Pt(P^nBu_3)$_2Cl_2$]	1.7, *s*	3515			
PhC(S)NHP(S)(O^iPr)$_2$	57.9, *s*				
Unbound ligand **I**					
[Pt(P^nBu_3)$_2$(L^I-*S*,*S*)]+	P(1) 43.6, *s*		76.7		
A					
	P(2) 5.9, *dd*	2811		22.3	8.2
	P(3) 1.3, *dd*	2849		22.1	9.5

s and *dd* in the table mean 'singlet' and 'doublet of doublets' respectively

Due to two-bond coupling of P(1) to the platinum nucleus, P(1) appears as a singlet symmetrically flanked by $^{2}J(^{195}Pt\text{-}^{31}P(1))$ coupling satellites. The $^{2}J(^{195}Pt\text{-}^{31}P(1))$ coupling constant is 76.7 Hz. This parent peak for P(1) is still very broad ($W_{1/2}$ = 22.1 Hz) and long-range $^{3}J(^{31}P\text{-}^{31}P)$ couplings due to P(2) and P(3) are not observed. Fortunately, this information is not totally lost since both $^{3}J(^{31}P(2)\text{-}^{31}P(1))$ = 8.2 Hz and $^{3}J(^{31}P(3)\text{-}^{31}P(1))$ = 9.5 Hz coupling constants are observed when looking at the parent peaks of P(2) and P(3), respectively. The $^{31}P\{^{1}H\}$ NMR spectrum in **figure 38** shows the expected doublet of doublets for the main ^{31}P peaks for P(2) and P(3), but their $^{1}J(^{195}Pt\text{-}^{31}P)$ coupling satellites do not reveal such fine structure. On high field instruments, such as 600 MHz, which was used in the investigation of this reaction, the $^{1}J(^{195}Pt\text{-}^{31}P)$ coupling satellites are very broad due to chemical shift anisotropy (CSA)[62] broadening and tend to lose such fine structure.

The subtle differences between the thiocarbonyl sulphur and the thiophosphoryl sulphur are reflected by different $^{1}J(^{195}Pt\text{-}^{31}P(2))$ = 2811 Hz and $^{1}J(^{195}Pt\text{-}^{31}P(3))$ = 2849 Hz values. As has been discussed earlier, the *trans influence* for the two donor sulphur atoms are quite different, hence, the phosphine groups bonded *trans* to them are expected to have different coupling constants. The $^{3}J(^{31}P(2)\text{-}^{31}P(1))$ = 8.2 Hz value is relatively smaller than that of $^{3}J(^{31}P(3)\text{-}^{31}P(1))$ = 9.5 Hz. Since P(2) is *cis* orientated to P(1) it is expected to have a smaller $^{3}J(^{31}P(2)\text{-}^{31}P(1))$ value than $^{3}J(^{31}P(3)\text{-}^{31}P(1))$ with P(3) *trans* orientated to P(1). The two-bond coupling $^{2}J(^{31}P(3)\text{-}^{31}P(2))$ of about 22 Hz is comparable to the phosphorus-phosphorus two-bond coupling of 24

Hz observed in complexes resulting from a reaction of *cis*-$[Pt(P^nBu_3)_2Cl_2]$ with *N,N*-dialkyl-*N'*-acyl(aroyl)thioureas reported in **chapter 3**.

4.4.2 Unexpected species resulting from the reaction of *cis*-$[Pt(P^nBu_3)_2Cl_2]$ with *N*-diisopropoxythiophosphoryl thioamide, I

The coordination chemistry of this ligand seems to be not limited to the expected complex (**A**), but another species develops after a while. This is quite unexpected and thus far, without further study, it is still very difficult to explain what might be happening in solution of these complexes (see **figures 39** and **40**)

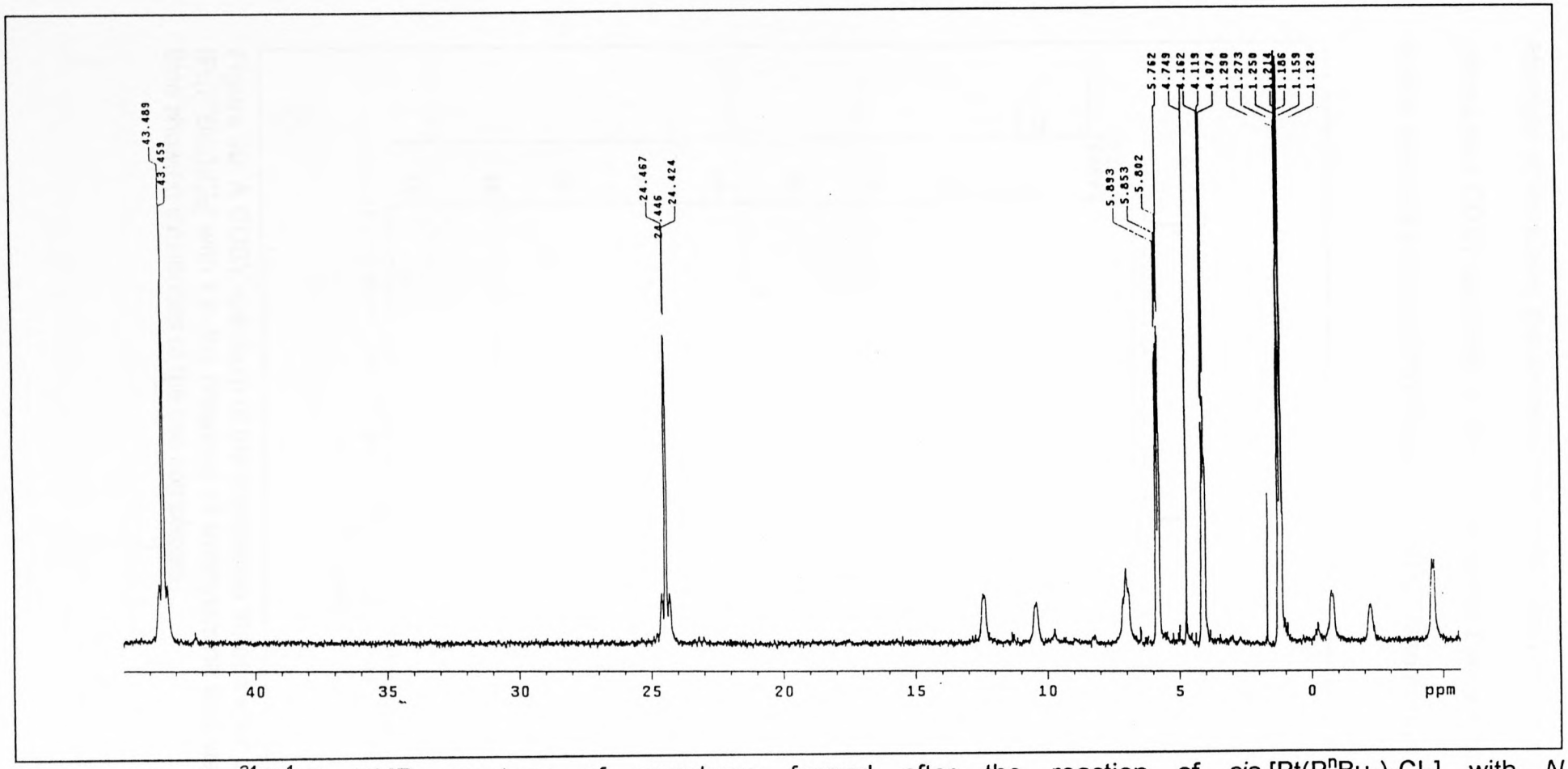

Figure 39: A $^{31}P\{^{1}H\}$ NMR spectrum of complexes formed after the reaction of *cis*-$[Pt(P^{n}Bu_3)_2Cl_2]$ with *N*-diisopropoxythiophosphoryl thioamide in the presence of triethylamine and standing for some time. Three of the six peaks have been identified to belong to $[Pt(P^{n}Bu_3)_2(L\text{-}S,S)]^{+}Cl^{-}$, the species where the ligand displaces two chloride ions with the sulphur donors. The other three at 24.4 ppm, 4.1 ppm and at 1.2 ppm are believed to belong to the new species, not as yet identified.

Attempts of identifying the second compound were not successful but from a phosphorus COSY spectrum, it could be said that the new species may have similar structure to the *cis*-$[Pt(P^nBu_3)_2(L^1\text{-}S,S)]^+Cl^-$ (see **figure 40**).

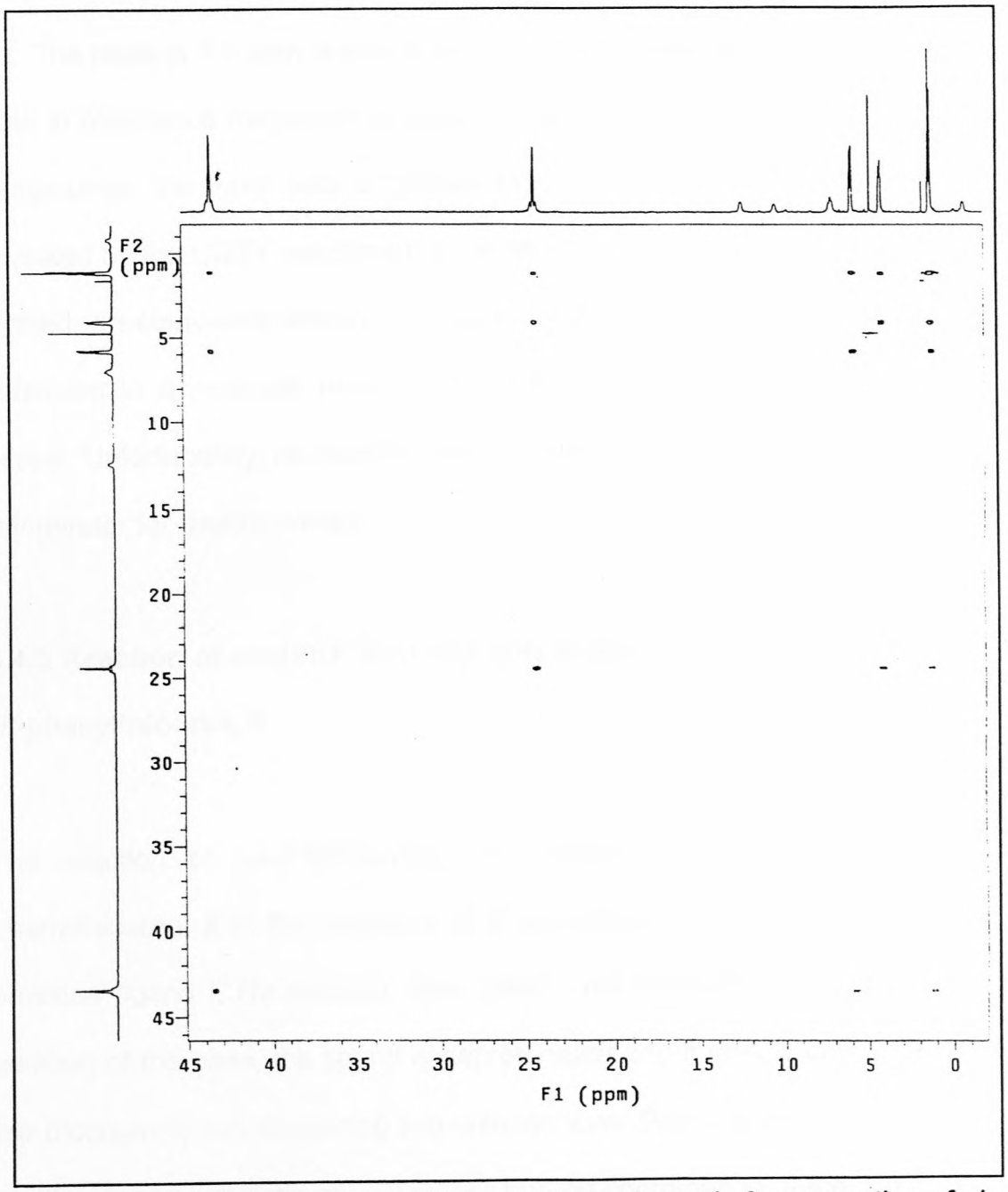

Figure 40: A COSY spectrum of the complexes formed after a reaction of *cis*-$[Pt(P^nBu_3)_2Cl_2]$ with I^- in the presence of triethylamine and standing for some time showing similarities of the two complexes.

The COSY spectrum on these complexes shows that the two complexes are very similar in nature, with the new peak at 24.1 ppm closely resembling the one at 43.6 ppm. Both peaks have platinum $^{2}J(^{195}Pt\text{-}^{31}P)$ coupling satellites with comparable coupling constants, one being 74.8 Hz while the other is 76.7 Hz. The peak at 4.1 ppm is similar to P(2) while the one at 1.2 ppm is similar both in resonance frequency as well as in coupling constant to P(3). In both compounds, the three sets of phosphorus atoms couple to each other as revealed by the COSY experiment. In an attempt to crystallise the compounds formed, an equivalent amount of ammonium hexaflourophosphate (NH_4PF_6), dissolved in a minimum amount of acetonitrile was added to the reaction vessel. Unfortunately, no crystals grew after leaving the reaction vessel in the refrigerator for several weeks.

4.4.3 Reaction of *cis*-[Pt(P^nBu_3)$_2Cl_2$] with *N*-diisopropoxythiophosphoryl-*N'*-phenylthiourea, II

The reaction of *cis*-[Pt(P^nBu_3)$_2Cl_2$] with *N*-diisopropoxythiophosphoryl-*N'*-phenylthiourea, **II** in the presence of a base follows the same route as the previous ligand **I**. No reaction takes place until triethylamine is added. On addition of the base, the ligand is deprotonated and it rapidly coordinates to the platinum(II) ion, displacing two chloride ions. Both the *cis*-[Pt(P^nBu_3)$_2Cl_2$] and the ligand solutions are colourless but, on coordination of the ligand, the solution becomes slightly yellow. **Table 23** serves to show the assignments of the peaks in the $^{31}P\{^{1}H\}$ NMR spectra of the complexes resulting from the reaction of *cis*-[Pt(P^nBu_3)$_2Cl_2$] with ligand **II**. The phosphorus atoms in the

$^{31}P\{^{1}H\}$ NMR spectrum have been arbitrarily named P(1), P(2) and P(3) according to the pictorial representation of the mixed ligand-platinum(II) complex:

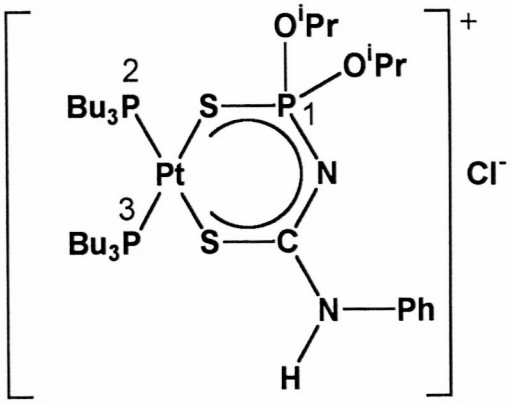

Table 23: The assignments of the phosphorus spectrum of the complex resulting from the reaction of *cis*-[Pt(P^nBu_3)$_2$$Cl_2$] with **II** in the presence of triethylamine.

Compound	δ^{31}P/ppm and multiplicity	$^1J(^{195}Pt-^{31}P)$ /Hz	$^2J(^{195}Pt-^{31}P)$ /Hz	$^2J(^{31}P(2)-^{31}P(3))$ /Hz	$^3J(^{31}P(1)-^{31}P)$ /Hz
cis-[Pt(P^nBu_3)$_2$$Cl_2$]	1.7, *s*	3515			
PhNHC(S)NHP(S)(O^iPr)$_2$	53.2, *s*				
Unbound ligand **II**					
[Pt(P^nBu_3)$_2$(L^{II}-*S,S*)]+	P(1) 45.1, *s*		*		
B					
	P(2) 7.5, *s*	3158		*	*
	P(3) 1.0, *dd*	2887		22.1	14.7

s and *dd* in the table mean 'singlet' and 'doublet of doublets' respectively
* refers to values expected to be observed, but were not observed due to broadness of the peaks

The chemical shift trends are very similar to the case previously described. The expected up field-shift for P(1) is reproduced on coordination of ligand **II**, however, here it is only 8.1 ppm, unlike in the previous case where it was 14.3 ppm. The ^{31}P peak for P(1) in this case is so broad such that the expected platinum $^{2}J(^{195}Pt\text{-}^{31}P)$ coupling satellites are not observed at all, unlike in the previous case. Once again, the broadness of peaks is noted on P(2) when **II** is used. Instead of resonating as a doublet of doublets, this peak appears as a singlet, losing the valuable information about the $^{3}J(^{31}P(2)\text{-}^{31}P(1))$ value. This value is of course expected to be much smaller than $^{3}J(^{31}P(3)\text{-}^{31}P(1))$ since P(2) is in a *cis* orientation to P(1) and P(3) is in a *trans* orientation to P(1). The $^{2}J(^{31}P(3)\text{-}^{31}P(2))$ = 22 Hz coupling constant is not a surprise and is consistent with the value obtained in the previous case. In this reaction, some peaks were unidentified and therefore the reaction deserves further investigation. The attempt of isolating any resulting complex was not successful when the method of using PF_6^- (in the form of NH_4PF_6) as a large counter anion was added to the mixed ligand-platinum(II) complex.

4.4.4 Comparison of the mixed ligand platinum(II) complexes resulting from the reactions of *cis*-[Pt(P^nBu_3)$_2$Cl$_2$] with ligands of the type *N,N*-dialkyl-*N'*-acyl(aroyl)thioureas, *N*-diisopropoxythiophosphoryl thioamide and *N*-diisopropoxythiophosphoryl-*N'*-phenylthiourea

Following all the reactions of *cis*-[Pt(P^nBu_3)$_2$Cl$_2$] with ligands by means of $^{31}P\{^{1}H\}$ NMR spectroscopy, it is observed that no reaction takes place until triethylamine is added to the solution of *cis*-[Pt(P^nBu_3)$_2$Cl$_2$] and the ligands. On

coordination, the ligands would displace two Cl^- ions of *cis*-$[Pt(P^nBu_3)_2Cl_2]$, resulting in charged species of the type *cis*-$[Pt(P^nBu_3)_2L]^+Cl^-$, where L represents a coordinated ligand

While **I** and **II** are sulphur-sulphur donors the *N,N*-dialkyl-*N'*-acyl(aroyl)thioureas are sulphur-oxygen donors. This difference manifests itself notably in the $^1J(^{195}Pt-^{31}P)$ coupling constants of the resulting mixed ligand-platinum(II) complexes. The $^1J(^{195}Pt-^{31}P)$ coupling constants for the phosphines opposite the oxygen donors are about 3550 Hz while the phosphines opposite the sulphur donors about 3000 Hz for *N,N*-dialkyl-*N'*-acyl(aroyl)thioureas and ranging from 2800 Hz to 3100 Hz for **I** and **II**. Judging from the $^1J(^{195}Pt-^{31}P)$ coupling constants, the C(S) donors seem to coordinate in a comparable manner, regardless in what type of molecules they exist. Other comparable features about these mixed ligand-platinum(II) complexes is that, for those resulting from **I** and **II**, the value of the $^2J(^{31}P-^{31}P)$ coupling constant between the phosphines is 22 Hz and for those resulting from *N,N*-dialkyl-*N'*-acyl(aroyl)thioureas, this value is 24 Hz.

The reaction between the *N,N*-dialkyl-*N'*-acyl(aroyl)thioureas and *cis*-$[Pt(P^nBu_3)_2Cl_2]$ occurs with no other species developing over time, accept for the expected one. The extra peaks in the $^{31}P\{^1H\}$ NMR spectra obtained when reacting *cis*-$[Pt(P^nBu_3)_2Cl_2]$ with **I** and **II** indicate some other species (are still to be determined) which develop over time (compare **figures 38** and **39**).

Chapter Five

Concluding remarks

5 CONCLUDING REMARKS

5.1 The coordination chemistry of *N,N*-dialkyl-*N'*-acyl(aroyl)thioureas

Ligands of the type *N,N*-dialkyl-*N'*-acyl(aroyl)thiourea, **R"C(O)NHC(S)NRR'** were synthesised in high yield from relatively inexpensive starting materials, in two steps, for the purpose of evaluating the relative donicities of *S* and *O* donor atoms. In solution, the asymmetrically disubstituted *N,N*-dialkyl-*N'*-acylthioureas HL^{13} and HL^{15} exist in two configurational isomers, the *E* and the *Z* with respect to the partial double bond character of the **-(S)C-NRR'** bond. The isomer distribution for HL^{13} and HL^{15} favours the *E* isomer, while HL^{14} (also asymmetrically disubstituted) only occurs as the *E* isomer. In general, the ligands are stable in air and will remain in their solid form for long period of time with the exception of *N*-tert-butyl-*N*-methyl-*N'*-2,2-dimethylpropanoylthiourea, which turns into a liquid at room temperature after standing for several weeks.

While evaluating the relative donicities of sulphur and oxygen of the *N,N*-dialkyl-*N'*-acyl(aroyl)thioureas, it was concluded from the coupling constant $^1J(^{195}Pt\text{-}^{31}P_O)$ = 3537 Hz, that the oxygen donor becomes less "hard" in HL^7, with two ortho substituted methoxy groups, which are electron releasing. The $\delta(^{195}Pt)$ chemical shift values of the resultant mixed ligand-platinum(II) complexes show an upfield shift as the *N,N*-dialkyl-*N'*-aroylthiourea changes from having an electron withdrawing group to having an electron donating

group, indicating an overall increase in the relative donicities of the *O* and *S* donor atoms.

Comparing the *N,N*-dialkyl-*N'*-acylthioureas with each other, there is an interesting dependence of the $^{1}J(^{195}Pt\text{-}^{31}P_S)$ values as the **R/R'** groups are varied, but these could not be correlated to the relative basicity of the amine substituents. The *E/Z* isomerism in the asymmetrically disubstituted *N,N*-dialkyl-*N'*-acylthioureas, HL^{13} and HL^{15} was carried through to the resulting mixed ligand-platinum(II) complexes as observed by means of $^{31}P\{^{1}H\}$ and $^{195}Pt\{^{1}H\}$ NMR spectroscopy.

Even though some information has been gathered about the relative donor properties of *S* and *O* of the ligands in terms of the $^{1}J(^{195}Pt\text{-}^{31}P)$ variations, it is difficult to make any definite conclusions since the differences in these NMR parameters are too small to be reliably interpreted.

The synthesis of platinum(II) chelates using the asymmetrically disubstituted *N,N*-dialkyl-*N'*-acylthioureas, HL^{13}, HL^{14} and HL^{15} was carried out successfully at elevated temperatures (60°C). The platinum(II) chelates that are obtained with HL^{15} as a ligand occur as three configurational isomers, *cis*-[Pt(*EE*-L^{15}-*S,O*)$_2$], *cis*-[Pt(*EZ*-L^{15}-*S,O*)$_2$] and *cis*-[Pt(*ZZ*-L^{15}-*S,O*)$_2$]. Three well resolved singlets in the $^{195}Pt\{^{1}H\}$ NMR spectrum of the chelates occur at -2739 ppm, -2735 ppm and -2731 ppm respectively. These isomers are chromatographically equivalent, therefore, could not be separated by chromatographic means. The assignment of these ^{195}Pt peaks as to which

belongs to which isomer was achieved by means of high field ^{1}H-(^{13}C)-^{195}Pt correlation NMR spectroscopy.

The platinum(II) chelate with HL^{14} was exclusively the *cis*-[Pt(*ZZ*-L^{14}-*S,O*)$_2$], as revealed by a single ^{195}Pt peak at -2733 ppm, which is consistent with ^{1}H and $^{13}C\{^{1}H\}$ NMR spectra. The ^{1}H and $^{13}C\{^{1}H\}$ NMR spectra of the platinum(II) chelate formed with HL^{13} seem to suggest that more than one complex is formed, which is intuitively sound since the ligand to start with exists as *E* and *Z* isomers, however, lack of time precluded further investigation.

5.2 The coordination chemistry of *N*-diisopropoxythiophosphoryl thiobenzamide and *N'*-diisopropoxythiophosphoryl-*N*-phenylthiourea

Platinum(II) chelates of *N*-diisopropoxythiophosphoryl thiobenzamide (**I**) and *N'*-diisopropoxythiophosphoryl-*N*-phenylthiourea (**II**) are predominantly formed as *trans*-[Pt(L-*S,S*)$_2$] complexes, unlike those of *N,N*-dialkyl-*N'*-acyl(aroyl)thioureas. The coordination of **II** is however, different to that of **I** since the chelates formed from this ligand are either exclusively *trans*-[Pt(L^{II}-*S,S*)$_2$] (**IIa**) or a mixture of *cis*-[Pt(L^{II}-*S,S*)$_2$] (**IIb**) and *trans*-[Pt(L^{II}-*S,S*)$_2$] (**IIa**) isomers, depending on the method of synthesis. The existence of the two isomers, **IIa** and **IIb**, is evident from the $^{31}P\{^{1}H\}$ NMR spectrum with ^{31}P peaks at 43.6 ppm and 44.5 ppm, respectively as well as with the $^{195}Pt\{^{1}H\}$ NMR spectrum with ^{195}Pt peaks at -3956 ppm and -3964 ppm, respectively.

In solution, it was observed that the chelates formed from **II** isomerise to form a mixture of isomers. Following the *trans*-[Pt(L^{II}-*S,S*)$_2$]-*cis*-[Pt(L^{II}-*S,S*)$_2$] isomerisation, in chloroform by means of $^{31}P\{^1H\}$ NMR spectroscopy, the equilibrium constant, K_e = *cis*-[Pt(L^{II}-*S,S*)$_2$]/*trans*-[Pt(L^{II}-*S,S*)$_2$] was determined to be $8.53x10^{-1}$ at 25°C. Equilibrium is reached after a relatively long period (in no less than 300 hours), indicating some stability of the complimentary soft-soft acid/base pairs of the sulphur donors and the platinum(II) ion. It is not yet known with certainty what triggers the isomerisation but acid catalysis and solvent polarity as a possible reason cannot be excluded.

Indirectly evaluating the sulphur-sulphur donor properties of **I** and **II** by reacting these ligands with equimolar amounts of *cis*-[Pt(P^nBu_3)$_2$Cl$_2$] in chloroform and looking at their $^1J(^{195}Pt\text{-}^{31}P)$ values was carried out directly in the NMR tube. It was observed that even though the donors are the same atom, sulphur, for both ligands, the donors are sufficiently different to influence the coordination of the phosphines bonded *trans* to them in different ways, thereby easily distinguishing them unambiguously.

5.3 Future work

For mixed ligand-platinum(II) complexes, it will be interesting to relate the Pt-S and Pt-O bond lengths with the information obtained in this study about the sulphur and oxygen donor properties of the ligands. Suitable counter ions to the large resultant cations, *cis*-[Pt(P^nBu_3)$_2$(L-*S,O*)]$^+$, will be necessary to obtain the desired complexes in a crystalline form.

To complete the study of the platinum(II) chelates of asymmetrically disubstituted *N,N*-dialkyl-*N'*-acylthioureas, the number of isomers of the platinum(II) chelates resulting from *N-2*-methylpyrrolidyl-*N'-2,2*-dimethylpropanoylthioureas (HL^{13}) still need to be fully resolved.

Finally, for completion, the molecular structure of the *cis*-[$Pt(L^{II}$-*S,S*$)_2$] isomer needs to be isolated and compared with that of the *trans*-[$Pt(L^{II}$-*S,S*$)_2$] isomer. This should be possible since related complexes of nickel(II) chelates with *N*-thioacylthiourea have been isolated in both *cis* and *trans* isomers.[54] The *trans/cis* chelate isomerism is an interesting phenomenon with questions that still need to be answered, such as the mechanism of isomerisation and what triggers the isomerisation. With regards to the latter question, experimental evidence, thus far, suggest acid catalysis but further studies still need to be carried out to verify this. The most plausible mechanism is thought to be via a platinum-sulphur bond break. In an attempt to demonstrate this, the isomerisation study could be carried out in a strongly coordinating solvent, or in chloroform (where it is known with certainty that this phenomenon does occur) with fluorophosphate anion, PF_6^- present in the solution, in the hope of trapping possible intermediates.

6 References

6 REFERENCES

1. *Kirk Othmer Encyclopedia of Chemical Technology*, 4th Edition, 19, 347-375, John Wiley & Son, 1996.
2. Cowley, A. (Ed.) *Platinum 2000*, Johnson Matthey PLC, London 2000, p. 20.
3. Cowley, A. and Steel, M. (Ed.) *Platinum 2001*, Johnson Matthey PLC, London 2001, p. 48.
4. Pearson, R. G., *J. Chem. Ed.*, 1968, **45**, no 9, 581.
5. Cotton, F. A. and Wilkinson, G., *Advanced Inorganic Chemistry* 5th Ed, John Wiley, 1988, p 64 and 918.
6. Edwards, R. I., Bird, A. J. and Berfeld, G. J., *Gmelin Handbook of Inorganic Chemistry*, vol. A1, 18th Ed., Springer, 1986, p. 30.
7. Venanzi, L. M., *Chem. Brit.*, 1968, **4**, 162.
8. Tolman, C. A., *Chem. Rev.*, 1977, **77**, 313.
9. Cobley, C. J. and Pringle, P. G., *Inorg. Chim. Acta.*, 1997, **265**, 107.
10. Fischer, E. O., Louis, E. and Kreiter, C. G., *Angew. Chem., Int. Ed. Eng.*, 1969, **8**, 377.
11. Huheey, J. E., *Inorganic Chemistry: Principles of Structure and Reactivity* 2nd Ed., 1978, Harper & Row, New York, p 490.
12. Douglass, I. B. and Dain, F. B., *J. Ame. Chem. Soc.*, 1934, **56**, 719.
13. (a) Schuster, M. *Fresenius Z. Anal. Chem.*, 1992, **342**, 791. (b) König, K-H., Schuster, M., Steinbrech, B., Schneeweis, G and Schlodder, R. *Fresenius Z. Anal. Chem.*, 1985, **321**, 457. (c) Vest. P., Schuster, M.

and König, K-H., *Fresenius Z. Anal. Chem.*, 1989, **335**, 759. (d) Vest. P., Schuster, M. and König, K-H., *Fresenius Z. Anal. Chem.*, 1991, **339**, 142.

14. Koch, K. R., Grimmbacher, T. and Sacht, C., *Polyhedron*, 1998, **17**, 267.
15. Koch, K. R., Sacht, C. and Bourne, S., *Inorg. Chim. Acta.*, 1995, **232**, 109.
16. Kurnakow, N., *J. Prakt. Chem.*, 1898, **50**, 234.
17. Koch, K. R., *Coord. Chem. Rev.*, 2001, **216-217**, 473.
18. (a) König, K-H., Schuster, M., Steinbrech, B., Schneeweis, G. and Steinbrech, B., *Fresenius Z. Anal. Chem.*, 1984, **319**, 66. (b) Schuster, M. *Fresenius Z. Anal. Chem.*, 1992, **342**, 791.
19. Schuster, M. and Unterreitmaier, E., *Fresenius Z. Anal. Chem.*, 1993, **346**, 360.
20. Schuster, M. and Sador, M., *Fresenius Z. Anal. Chem.*, 1996, **356**, 326.
21. Unterreitmaier, E. and Schuster, M., *Anal. Chim. Acta*, 1995, **309**, 339.
22. Mautjana, A. N., MSc dissertation, University of Cape Town, 2000.
23. Bhattacharyya, P., Novosad, J., Phillips, J. R., Slawin, A. M. Z., Williams, D. J. and Woollins, J. D., *J. Chem. Soc., Dalton Trans.*, 1995, 1607.
24. Zimin, M. G., Kamalov, R. M., Cherkasov, R. A. and Pudovik, A. N., *Phosphorus Sulfur*, 1982, **13**, 371.

25. Zabirov, N. G., Litvinov, I. A., Kataeva, O. N., Khashevarov, S. V., Sokolov, F. D. and Cherkasov, R. A., *Russ. J. Gen. Chem.* 1998, **68**, *no.* 9, 1408.

26. Kon'kin, A. L., Shtyrlin, V. G., Zabirov, N. G., Aganov, A. V., Zapechel'nyuk, L. E., Kashevarov, S. V. and Zakharov, A. V., *Zh. Neorg. Khim.*, 1996, **41**, 1156.

27. Kon'kin, A. L., Shtyrlin, V. G., Zabirov, N. G., Aganov, A. V., Rakhmatullin, A. I., Kashevarov, S. V. and Zakharov, A. V., *Russ. J. Gen. Chem.,*1996, **66**, 512.

28. Toropova, V. F., Lazareva, G. A., Batyrshina, F. M. and Zimin, M. G., *Zh. Anal. Khim.*, 1982, **37**, 1739.

29. Zimin, M. G., Lazareva, G. A., Savel'eva, N. I, Islamov, R. G., Zabirov, N. G., Toropova, V. F. and Pudovic, A. N., *Zh. Obshch. Khim.*, 1982, **52**, 1776.

30. Solov'ev, V. N., Chekhlov, A. N., Zabirov, N. G. and Martynov, I. V., *Dokl. Ross. Akad. Nauk.*, 1995, **341**, 502.

31. Zabirov, N. G., Solov'ev, V. N., Shamsevaleev, F. M., Cherkasov, R. A. and Martynov, I. V., *Zh. Obshch. Khim.*, 1991, **61**, 1748.

32. Zabirov, N. G., Solov'ev, V. N., Shamsevaleev, F. M., Cherkasov, R. A., Cheklov, A.N., Tsifarkin, A.G. and Martynov, I. V., *Zh. Obshch. Khim.*, 1991, **61**, 657.

33. Brus'ko, V. V., Sokolov, F. D. Zabirov, N. G., Cherkasov, R. A., Rakhmatullin, A. I. and Verat, Yu. A., *Russ. J. Gen. Chem.*, 1999, **69**, 664.

34. (a) Chatt, J. and Wilkinson, R.G., *J. Chem. Soc.*, 1952, 4300. (b) Chatt, J. and Wilkinson, R.G., *J. Chem. Soc.,*1953, 70. (c) Chatt, J. and Wilkinson, R.G., *J. Chem. Soc.*,1956, 525.

35. Harris, R. K. and Mann, B. E., NMR *and the Periodic Table*, New York Academic Press, 1978.

36. Günther, H., NMR *Spectroscopy: An Introduction*, Wiley, New York, 1980.

37. Derome, A. E., *Modern* NMR *Techniques for Chemistry Research*, New York, Pergamon Press, 1987.

38. Pople, J. A. and Santry, *Mol. Phys.*, 1964, **8**, 1.

39. Mather, G. G., Pidcock, A. and Rapsey, G. J. N., *J. Chem. Soc., Dalton Trans.*, 1973, 2095.

40. (a) Pregosin, P. S. and Kunz, R. W. ^{31}P *and* ^{13}C NMR *of Transition Metal Complexes*, Springer, New York, 1979. (b) Pregosin, P. S., *Coord. Chem. Rev.,* 1982, **44**, 247.

41. Pesek, J. J. and Mason, W. R., *J. Magn. Reson.*, 1977, **25**, 519.

42. Abel, E. W., Orrell, K. and Platt, A. W. G., *J. Chem. Soc., Dalton Tans.*, 1983, 2345.

43. Miller, J., PhD thesis, University of Cape Town, 2000.

44. "Collect" data software, Nonius B. V. Deft, The Netherlands, 1999.

45. Otwinowski, Z. and Minor, W., Processing of X-ray Diffraction Data Collected in Oscillation Mode", Method in Enzymology, 276: Macromolecular Crystallography, part A, 307-326, 1997, Carter C. W., Jr. and Sweet Eds, R. M., Academic Press.

46. Sheldrick, B. M., SHELXL97, Program for the refinement of Crystal Structures, University of Gőttingen, Germany, 1997.

47. Burnett, M. N. and Johnson, C. K., *ORTEP-III*, Oak Ridge Thermal Ellipsoid Program for Crystal Structure Illustrations, Oak Ridge National Lab. Report ORNL-6895, 1996.

48. Spek, A. L., *PLATON*, University of Utrecht, The Netherlands,1997.

49. Kauffman, G. B. and Teler, L. A., *Inorg. Synth.*, 1963, **7**, 239.

50. Koch, K. R. and Matoetoe, M. C., *Magn. Res. Chem.*, 1991, **29**, 1158.

51. Mashkina, S. V., Pestova, N. Yu., Ulakhovic, N. A. and Zabirov, N. G., *Russ. J. Gen. Chem.* 1996, **66**, 515.

52. Real, J., Prat, E., Polo, A., Alvarez-Larena, A. and Piniella, F. J., *Inorg. Chem. Comm.* 2000, **3**, 221.

53. Mikhailov, V. O., *Trans. Met. Chem.*, 1994, **19**, 387.

54. (a) Sieler, J., Richter, R., Braun, U., Beyer, L., Lindqvist, O. and Andersen, L., *Z. Anorg. Allg. Chem.*, 1985, **528**, 107. (b) Sieler, J., Richter, R., Hoyer, E., Beyer, L., and Köhler, R., *Z. Anorg. Allg. Chem.*, 1991, **603**, 25.

55. Dago, A., Shepelev, Yu., Fajardo, F., Alvarez, F. and Ponies, R., *Acta. Crystallogr. Sect. C.*, 1989, 45, 1992.

56. Koch, K. R., Sacht, C., Grimmbacher, T. and Bourne, S., *S. Afr. J. Chem.*, 1995, **48**, 71.

57. CRC Handbook of Chemistry and Physics, 64th Ed. Weast, R. C., CRC Press, Boca Raton, Florida, 1983, p. F-171.

58. Koch, K. R., Wang, Y. and Coetzee, A., *J. Chem. Soc., Dalton Trans.*, 1999, 1013.

59. Koch, K. R., du Toit, J., Caira, M. R. and Sacht, C., *J. Chem. Soc. Dalton Trans.*, 1994, 785.

60. Cupertino, D., Keyte, R., Slawin, A. M. Z., Woollins, J. D. and Williams, D. J., *Polyhedron*, 1996, 4441.

61. Solov've, V. N., Chekhlov, A. N., Zabirov, N. G., Cherkasov, R. A. and Martynov, I. V., *Zh. Strukt. Khim.*, 1990, **31**, 103.

62. Sanders, J. K. M. and Hunter, B. K., *Modern* NMR *Spectroscopy: A Guide for Chemists*, Oxford University Press, 1987, Oxford, p 217.

7 Appendices

APPENDIX 1 Crystallographic data of *N,N*-diethyl-*N'-4*-nitrobenzoylthiourea, HL^4

Table 1: Bond lengths (Å) and angles (°) for *N,N*-diethyl-*N'-4*-nitrobenzoylthiourea, HL^4

BOND	LENGTH	ANGLE	DEGREES
S(1)-C(8)	1.663(2)	C(8)-N(3)-C(11)	120.79(19)
O(3)-C(7)	1.230(2)	C(8)-N(3)-C(9)	123.73(19)
N(3)-C(8)	1.324(3)	C(11)-N(3)-C(9)	115.5(2)
N(3)-C(11)	1.469(3)	C(7)-N(2)-C(8)	121.22(16)
N(3)-C(9)	1.478(3)	N(3)-C(8)-N(2)	114.3(2)
N(2)-C(7)	1.344(2)	N(3)-C(8)-S(1)	126.62(17)
N(2)-C(8)	1.430(3)	N(2)-C(8)-S(1)	119.1(2)
C(4)-C(3)	1.386(3)	C(3)-C(4)-C(5)	119.0(2)
C(4)-C(5)	1.398(3)	C(3)-C(4)-C(7)	117.15(16)
C(4)-C(7)	1.496(3)	C(5)-C(4)-C(7)	123.70(17)
N(1)-O(2)	1.208(2)	O(2)-N(1)-O(1)	122.8(2)
N(1)-O(1)	1.222(2)	O(2)-N(1)-C(1)	118.53(19)
N(1)-C(1)	1.467(3)	O(1)-N(1)-C(1)	118.68(18)
C(3)-C(2)	1.375(3)	C(2)-C(3)-C(4)	120.80(18)
C(5)-C(6)	1.374(3)	C(6)-C(5)-C(4)	120.38(18)
C(1)-C(2)	1.375(3)	O(3)-C(7)-N(2)	120.7(2)
C(1)-C(6)	1.376(3)	O(3)-C(7)-C(4)	121.21(18)
C(11)-C(12)	1.505(3)	N(2)-C(7)-C(4)	118.01(16)
C(9)-C(10)	1.510(3)	C(2)-C(1)-C(6)	121.9(2)
		C(2)-C(1)-N(1)	118.60(19)
		C(6)-C(1)-N(1)	119.43(18)
		C(3)-C(2)-C(1)	118.85(19)
		C(5)-C(6)-C(1)	118.99(17)
		N(3)-C(11)-C(12)	111.98(18)
		N(3)-C(9)-C(10)	112.62(18)

Table 2: Torsion angles (°) for *N,N*-diethyl-*N'*-*4*-nitrobenzoylthiourea, HL^4

TORSION ANGLE	DEGREES
C(11)-N(3)-C(8)-N(2)	-177.76(15)
C(9)-N(3)-C(8)-N(2)	0.8(2)
C(11)-N(3)-C(8)-S(1)	2.0(3)
C(9)-N(3)-C(8)-S(1)	-179.52(14)
C(7)-N(2)-C(8)-N(3)	-89.6(2)
C(7)-N(2)-C(8)-S(1)	90.7(2)
C(5)-C(4)-C(3)-C(2)	-0.7(4)
C(7)-C(4)-C(3)-C(2)	175.7(2)
C(3)-C(4)-C(5)-C(6)	0.7(3)
C(7)-C(4)-C(5)-C(6)	-175.4(2)
C(8)-N(2)-C(7)-O(3)	4.2(3)
C(8)-N(2)-C(7)-C(4)	-178.7(2)
C(3)-C(4)-C(7)-O(3)	-3.6(3)
C(3)-C(4)-C(7)-N(2)	172.6(2)
C(3)-C(4)-C(7)-N(2)	179.4(2)
C(5)-C(4)-C(7)-N(2)	-4.4(3)
O(2)-N(1)-C(1)-C(2)	-177.1(2)
O(1)-N(1)-C(1)-C(2)	2.2(3)
O(2)-N(1)-C(1)-C(6)	4.7(3)
O(1)-N(1)-C(1)-C(6)	-175.9(2)
C(4)-C(3)-C(2)-C(1)	0.1(4)
C(6)-C(1)-C(2)-C(3)	0.4(3)
N(1)-C(1)-C(2)-C(3)	-177.7(2)
C(4)-C(5)-C(6)-C(1)	0.2(3)
C(2)-C(1)-C(6)-C(5)	-0.3(4)
N(1)-C(1)-C(6)-C(5)	177.8(2)
C(8)-N(3)-C(11)-C(12)	-96.6(2)
C(9)-N(3)-C(11)-C(12)	84.7(2)
C(8)-N(3)-C(9)-C(10)	-84.2(3)
C(11)-N(3)-C(9)-C(10)	94.3(2)

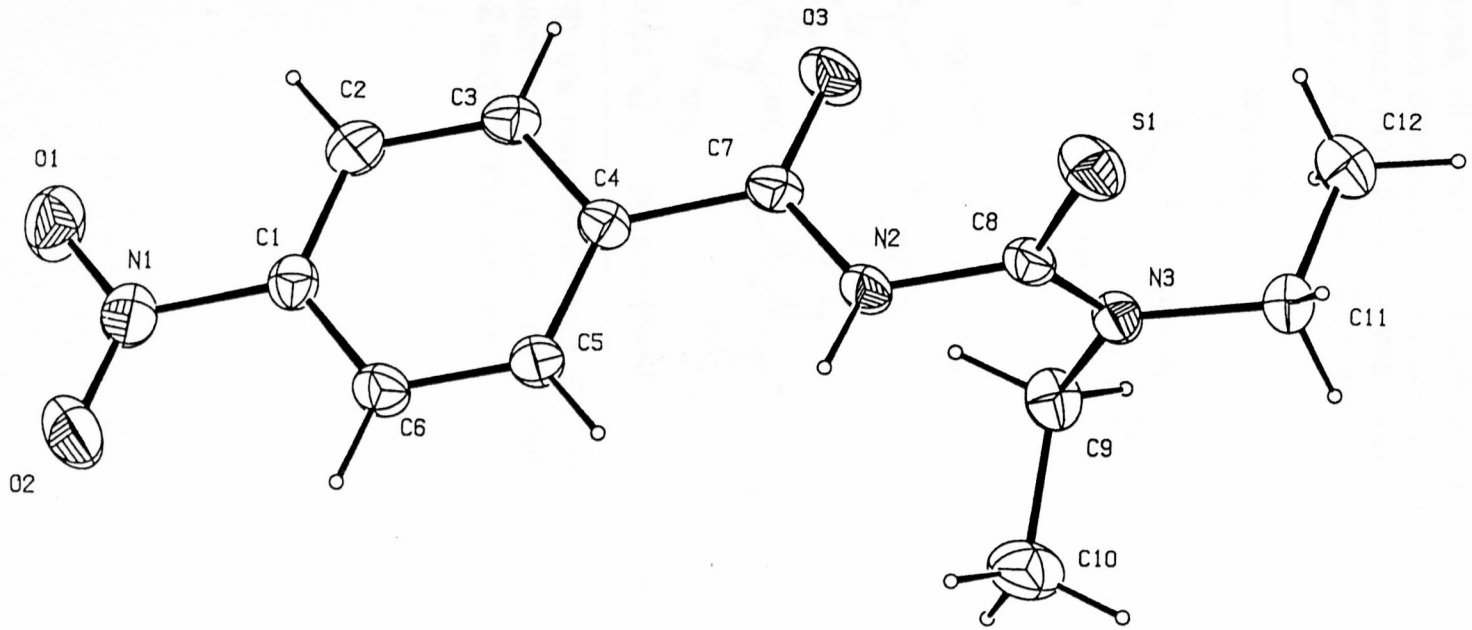
O3
S1
C12
C2
C3
O1
C7
C4
C8
N2
C1
N3
N1
C11
C5
C6
C9
O2
C10

APPENDIX 2 Statistical algorithm of mixtures

Claim: Given that the E/Z isomers of the ligand *N*-ethyl-*N*-methyl-*N'*-2,2-dimethylpropanoylthiourea, HL^{15}, are in 3:1 distribution (in favour of the *E* isomer) then, the expected distribution of the configurational isomers of the Pt(II) *bis* complexes formed from these ligands should be 5:2:1 or 62.5%: 25.0%: 12.5% for *E,E*:*E,Z*:*Z,Z* complexes. See figure below for illustration.

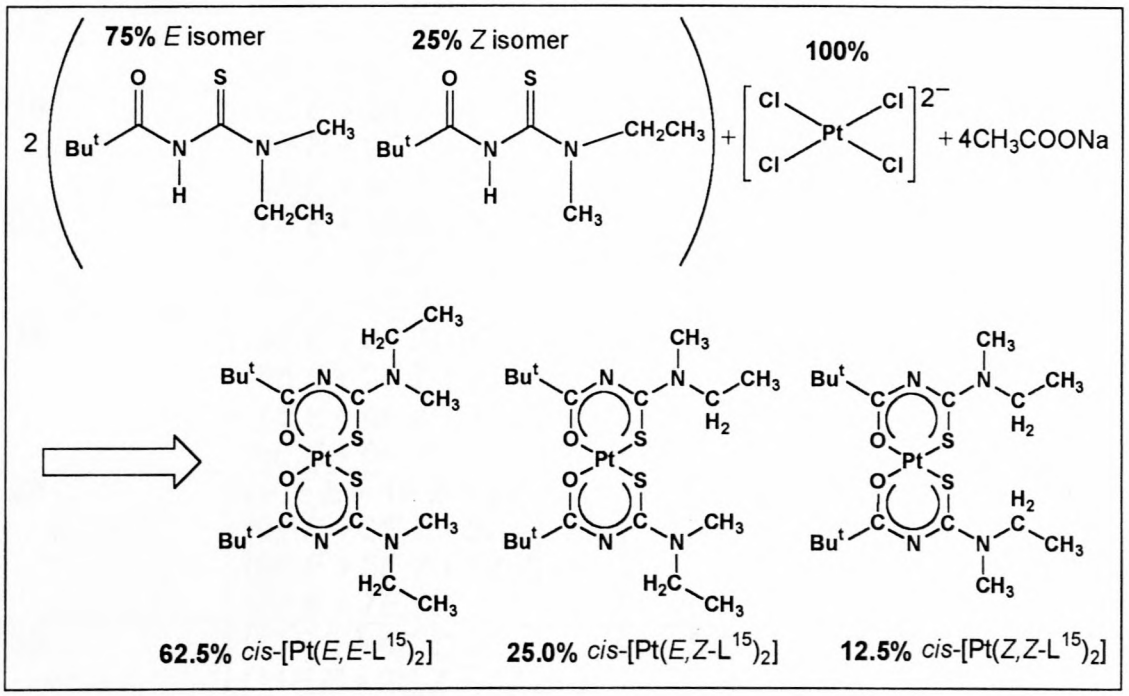

The formation of Pt(II) bis complexes from *E*/*Z* isomers of ligand HL^{15}, assuming that in solution or during complex formation the ligands do not interconvert from *E* to *Z* isomers and vice versa.

7 Appendices

Proof:

Number of ligands at the beginning of the reaction	Ways of combining the ligands in the complexes and retain the 3:1 ratio of *E*:*Z* isomers	*E,E*:*E,Z*:*Z,Z* ratio	*E,E*:*E,Z*:*Z,Z* ratio in percentage
4	(*E,E* + *E,Z*)	1:1:0	50%:50%:0%
8	(3*E,E* + *Z,Z*) or (2*E,E* + 2*E,Z*)	5:2:1	62.5%:25.0%:12.5%
12	(4*E,E* + 1*E,Z* +1*Z,Z*) or (3*E,E* + 3*Z,Z*)	7:4:1	58.3%:33.3%:8.3%
16	(6*E,E* + 2*Z,Z*) or (5*E,E* + 2*E,Z* + *Z,Z*) or (4*E,E* + 4*E,Z*)	5:2:1	62.5%:25.0%:12.5%
20	(7*E,E* + 1*E,Z* + 2*Z,Z*) or (6*E,E* + 3,*EZ* + 1*Z,Z*) or (5*E,E* + 5*E,Z*)	6:3:1	60.0%:30.0%:10.0%
24	(9*E,E* + 3*Z,Z*) or (8*E,E* + 2*E,Z* + 2*Z,Z*) or (7*E,E* + 4*E,Z* + 1*Z,Z*) or (6*E,E* + 6*E,Z*)	5:2:1	62.5%:25.0%:12.5%
28	(10*E,E* + 1*E,Z* + 3*Z,Z*) or (9*E,E* + 3*E,Z* + 2*Z,Z*) or (8*E,E* + 5*E,Z* + 1*Z,Z*) or (7*E,E* + 7*E,Z*)	17:8:3	60.7%:28.6%:10.7%
32	(12*E,E* + 4*Z,Z*) or (11*E,E* + 2*E,Z* + 3*Z,Z*) or (10*E,E* + 4*E,Z* + 2*Z,Z*) or (9*E,E* + 6*E,Z* + 1*Z,Z*) or (8*E,E* + 8*E,Z*)	5:2:1	62.5%:25.0%:12.5%

The calculation of the *E,E*:*E,Z*:*Z,Z* ratio, with 28 ligands at the beginning of the reaction for example, is done as follows:

E,E = (10*1/4 + 9*1/4 + 8*1/4 + 7*1/4)/14 = 0.607
E,Z = (1*1/4 + 3*1/4 + 5*1/4 + 7*1/4)/14 = 0.286
Z,Z = (3*1/4 + 2*1/4 + 1*1/4 + 0*1/4)/14 = 0.107

For many ligands, the *E,E*:*E,Z*:*Z,Z* ratio approaches 5:2:1 or 62.5%:25.0%:12.5%. Clearly, since this theoretical ratio is not obtained, it stands to reason that the ligands interconvert from *E* to *Z* isomers and *vice versa* during the complex formation under those reaction conditions. In support of this argument, the $^{13}C\{^{1}H\}$ NMR spectrum of the unbound ligand, HL^{15} at elevated temperature (50°C) was different to the $^{13}C\{^{1}H\}$ NMR spectrum at 25°C (see **figure 12** on page 68).

APPENDIX 3 Crystallographic data of *trans*-[Pt{$C_6H_5C(S)NP(S)(O^iPr)_2$}$_2$], **Ia**

Table 3: Bond lengths (Å) and angles (°) for **Ia**

BOND	LENGTH	ANGLE	DEGREES
Pt(1)-S(1)	2.3034(7)	S(1)-Pt(1)-S(1)a	180.0
Pt(1)-S(1)a	2.3034(7)	S(1)-Pt(1)-S(2)	96.96(3)
Pt(1)-S(2)	2.3367(7)	S(1)a-Pt(1)-S(2)	83.04(3)
Pt(1)-S(2)a	2.3367(7)	S(1)-Pt(1)-S(2)a	83.04(3)
S(1)-C(1)	1.718(3)	S(1)a-Pt(1)-S(2)a	96.96(3)
P(1)-O(2)	1.5646(19)	S(2)-Pt(1)-S(2)a	180.0
P(1)-O(1)	1.5650(19)	C(1)-S(1)-Pt(1)	114.78(11)
P(1)-N(1)	1.608(2)	O(2)-P(1)-O(1)	102.79(11)
P(1)-S(2)	1.9994(10)	O(2)-P(1)-N(1)	105.11(11)
O(1)-C(11)	1.466(3)	O(1)-P(1)-N(1)	115.27(9)
N(1)-C(1)	1.307(4)	O(1)-P(1)-S(2)	108.44(8)
C(1)-C(2)	1.494(4)	N(1)-P(1)-S(2)	116.72(9)
O(2)-C(21)	1.472(3)	C(11)-O(1)-P(1)	124.06(19)
C(2)-C(3)	1.384(4)	C(1)-N(1)-P(1)	128.9(2)
C(2)-C(7)	1.411(5)	N(1)-C(1)-C(2)	116.1(3)
C(3)-C(4)	1.384(4)	N(1)-C(1)-S(1)	129.6(3)
C(4)-C(5)	1.373(5)	C(2)-C(1)-S(1)	114.3(2)
C(5)-C(6)	1.374(5)	P(1)-S(2)-Pt(1)	96.19(3)
C(6)-C(7)	1.384(5)	C(21)-O(2)-P(1)	121.85(17)
C(11)-C(13)	1.504(6)	C(3)-C(2)-C(7)	118.6(3)
C(11)-C(12)	1.507(5)	C(3)-C(2)-C(1)	122.4(3)
C(21)-C(23)	1.510(5)	C(7)-C(2)-C(1)	119.0(3)
C(21)-C(22)	1.513(5)	C(4)-C(3)-C(2)	120.5(3)
		C(5)-C(4)-C(3)	120.7(3)
		C(4)-C(5)-C(6)	119.6(3)
		C(5)-C(6)-C(7)	120.8(3)
		C(6)-C(7)-C(2)	119.8(3)
		O(1)-C(11)-C(13)	106.8(3)
		O(1)-C(11)-C(12)	106.8(3)
		C(13)-C(11)-C(12)	113.5(3)
		O(2)-C(21)-C(23)	107.1(3)
		O(2)-C(21)-C(22)	107.3(3)
		C(23)-C(21)-C(22)	113.1(3)

Symmetry transformations used to generate equivalent atoms : a, -x+1, -y+1, z+1

Table 4: Torsion angles (°) for **Ia**

TORSION ANGLE	DEGREES
S(1)a-Pt(1)-S(1)-C(1)	-36(100)
S(2)-Pt(1)-S(1)-C(1)	-30.54(11)
S(2)a-Pt(1)-S(1)-C(1)	149.46(11)
O(2)-P(1)-O(1)-C(11)	173.6(3)
N(1)-P(1)-O(1)-C(11)	-75.8(3)
S(2)-P(1)-O(1)-C(11)	51.1(3)
O(2)-P(1)-N(1)-C(1)	-89.0(3)
O(1)-P(1)-N(1)-C(1)	162.0(2)
S(2)-P(1)-N(1)-C(1)	40.1(3)
P(1)-N(1)-C(1)-C(2)	-179.6(2)
P(1)-N(1)-C(1)-S(1)	1.0(4)
Pt(1)-S(1)-C(1)-N(1)	-0.3(3)
O(2)-P(1)-S(2)-Pt(1)	-179.81(17)
O(1)-P(1)-S(2)-Pt(1)	58.47(8)
N(1)-P(1)-S(2)-Pt(1)	173.02(9)
S(1)-Pt(1)-S(2)-P(1)	-65.60(10)
S(1)a-Pt(1)-S(2)-P(1)	52.40(4)
S(2)a-Pt(1)-S(2)-P(1)	-127.60(4)
Pt(1)-S(3)-C(7)-N(2)	84(100)
O(1)-P(1)-O(2)-C(21)	-63.4(2)
N(1)-P(1)-O(2)-C(21)	-175.6(2)
S(2)-P(1)-O(2)-C(21)	54.4(2)
N(1)-C(1)-C(2)-C(3)	-156.6(3)
S(1)-C(1)-C(2)-C(3)	23.0(4)
N(1)-C(1)-C(2)-C(7)	21.9(4)
S(1)-C(1)-C(2)-C(7)	-158.6(2)
C(7)-C(2)-C(3)-C(4)	-1.3(5)
C(1)-C(2)-C(3)-C(4)	177.1(3)
C(2)-C(3)-C(4)-C(5)	1.1(5)
C(3)-C(4)-C(5)-C(6)	-0.6(5)
C(4)-C(5)-C(6)-C(7)	0.3(5)
C(5)-C(6)-C(7)-C(2)	-0.5(5)
C(3)-C(2)-C(7)-C(6)	1.0(5)
C(1)-C(2)-C(7)-C(6)	-177.5(3)
P(1)-O(1)-C(11)-C(13)	116.3(3)
P(1)-O(1)-C(11)-C(12)	-121.9(3)
P(1)-O(2)-C(21)-C(23)	-131.5(3)
P(1)-O(2)-C(21)-C(22)	106.9(3)

Symmetry transformations used to generate equivalent atoms : a, -x+1, -y+1, z+1

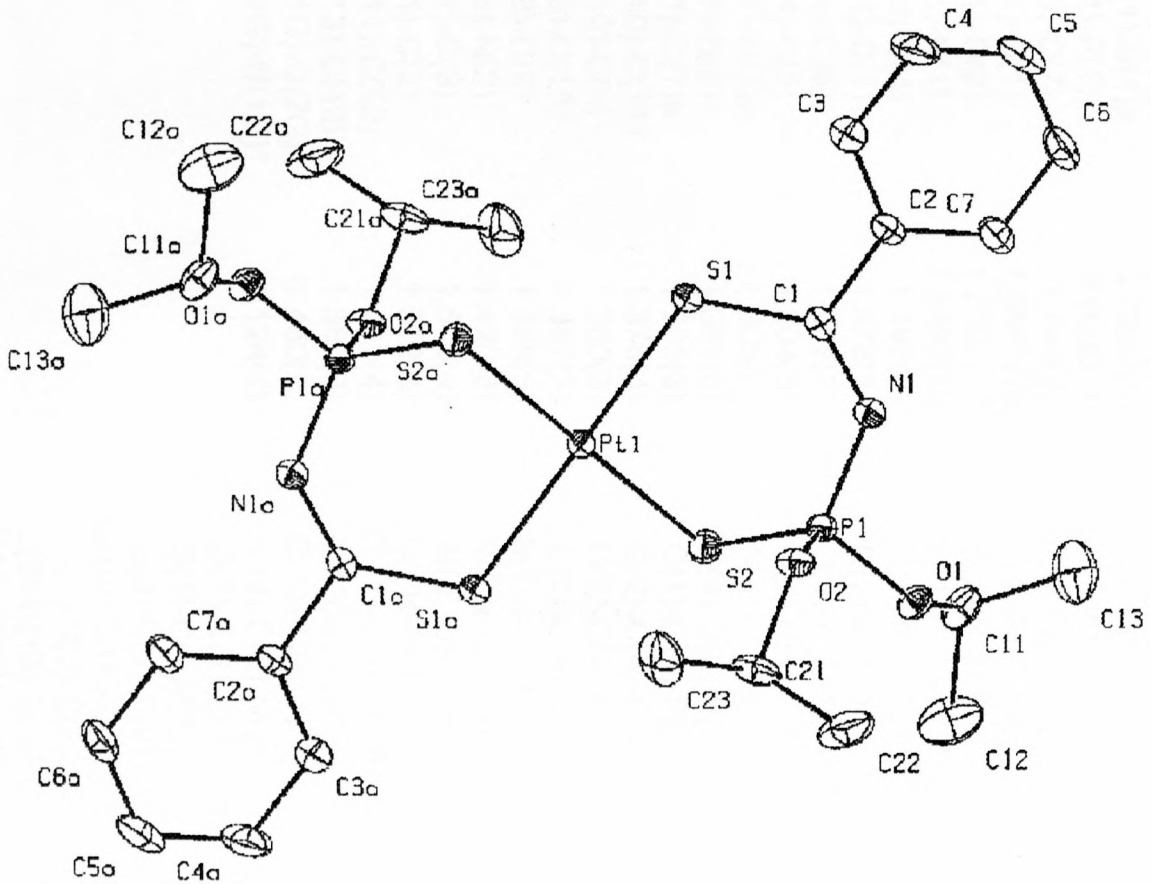
C4
C5
C3
C6
C12a
C22a
C23a
C21a
C2 C7
C11a
S1
C1
O1a
O2a
C13a
P1a
S2a
N1
Pt1
N1a
P1
C1a
S1a
S2
O2
O1
C13
C7a
C11
C2a
C21
C23
C22
C12
C6a
C3a
C5a
C4a

APPENDIX 4 Crystallographic data of *trans*-[Pt{$C_6H_5NHC(S)NP(S)(O^iPr)_2$}$_2$], **IIa**

Table 5: Bond lengths (Å) and angles (°) for **IIa**

BOND	LENGTH	ANGLE	DEGREES
Pt(1)-S(3)	2.3070(7)	S(3)-Pt(1)-S(3)a	180.000(10)
Pt(1)-S(3)a	2.3070(7)	S(3)-Pt(1)-S(1)	81.54(3)
Pt(1)-S(1)	2.3242(9)	S(3)a-Pt(1)-S(1)	98.46(3)
Pt(1)-S(1)a	2.3242(9)	S(3)-Pt(1)-S(1)a	98.46(3)
S(1)-P(1)	2.0033(9)	S(3)a-Pt(1)-S(1)a	81.54(3)
S(3)-C(7)	1.749(2)	S(1)-Pt(1)-S(1)a	180.0
P(1)-O(1)	1.5585(16)	P(1)-S(1)-Pt(1)	100.67(3)
P(1)-O(2)	1.5700(17)	C(7)-S(3)-Pt(1)	115.87(8)
P(1)-N(1)	1.5992(19)	O(1)-P(1)-O(2)	104.52(9)
O(2)-C(4)	1.483(3)	O(1)-P(1)-N(1)	105.77(10)
O(1)-C(1)	1.478(3)	O(2)-P(1)-N(1)	107.11(10)
C(4)-C(6)	1.502(3)	O(1)-P(1)-S(1)	114.59(7)
C(4)-C(5)	1.504(3)	O(2)-P(1)-S(1)	106.53(7)
C(7)-N(1)a	1.305(3)	N(1)-P(1)-S(1)	117.38(7)
C(7)-N(2)	1.361(3)	C(4)-O(2)-P(1)	119.91(14)
N(1)-C(7)a	1.305(3)	C(1)-O(1)-P(1)	124.88(14)
C(10)-C(11)	1.376(4)	O(2)-C(4)-C(6)	107.62(19)
C(10)-C(9)	1.380(3)	O(2)-C(4)-C(5)	108.0(2)
C(8)-C(13)	1.387(3)	C(6)-C(4)-C(5)	114.3(2)
C(8)-C(9)	1.388(3)	N(1)a-C(7)-N(2)	119.5(2)
C(8)-N(2)	1.420(3)	N(1)a-C(7)-S(3)	130.17(18)
C(1)-C(3)	1.505(4)	N(2)-C(7)-S(3)	110.36(17)
C(1)-C(2)	1.512(4)	C(7)a-N(1)-P(1)	128.82(17)
C(11)-C(12)	1.377(4)	C(11)-C(10)-C(9)	120.2(2)
C(13)-C(12)	1.387(3)	C(13)-C(8)-C(9)	119.4(2)
C(1G)-C(2G)*	1.450(5)	C(13)-C(8)-N(2)	124.4(2)
C(2G)-N(1G)*	1.124(4)	C(9)-C(8)-N(2)	116.2(2)
		O(1)-C(1)-C(3)	106.8(2)
		O(1)-C(1)-C(2)	106.7(2)
		C(3)-C(1)-C(2)	112.7(2)
		C(10)-C(11)-C(12)	119.3(2)
		C(7)-N(2)-C(8)	130.5(2)
		C(8)-C(13)-C(12)	119.2(2)
		C(11)-C(12)-C(13)	121.3(2)
		C(10)-C(9)-C(8)	120.6(2)
		N(1G)-C(2G)-C(1G)*	179.4(4)

Symmetry transformations used to generate equivalent atoms: a, -x+1, -y+1, z+1

* G here refers to the guest acetonitrile molecules

Table 6: Torsion angles (°) for **IIa**

TORSION ANGLE	DEGREES
S(3)-Pt(1)-S(1)-P(1)	136.18(3)
S(3)a-Pt(1)-S(1)-P(1)	-43.82(3)
S(1)a-Pt(1)-S(1)-P(1)	-70(38)
S(3)a-Pt(1)-S(3)-C(7)	83(100)
S(1)-Pt(1)-S(3)-C(7)	159.74(9)
S(1)a-Pt(1)-S(3)-C(7)	-20.26(9)
Pt(1)-S(1)-P(1)-O(1)	-64.06(8)
Pt(1)-S(1)-P(1)-O(2)	-179.11(7)
Pt(1)-S(1)-P(1)-N(1)	60.94(10)
O(1)-P(1)-O(2)-C(4)	173.61(16)
N(1)-P(1)-O(2)-C(4)	61.68(18)
S(1)-P(1)-O(2)-C(4)	-64.71(16)
O(2)-P(1)-O(1)-C(1)	70.02(19)
N(1)-P(1)-O(1)-C(1)	-177.09(18)
S(1)-P(1)-O(1)-C(1)	-46.2(2)
P(1)-O(2)-C(4)-C(6)	-117.82(18)
P(1)-O(2)-C(4)-C(5)	118.30(19)
Pt(1)-S(3)-C(7)-N(1)a	-6.1(3)
Pt(1)-S(3)-C(7)-N(2)	174.29(14)
O(1)-P(1)-N(1)-C(7)a	88.2(2)
O(2)-P(1)-N(1)-C(7)a	-160.7(2)
S(1)-P(1)-N(1)-C(7)a	-41.1(2)
P(1)-O(1)-C(1)-C(3)	118.6(2)
P(1)-O(1)-C(1)-C(2)	-120.7(2)
C(9)-C(10)-C(11)-C(12)	-1.2(4)
N(1)a-C(7)-N(2)-C(8)	4.8(4)
S(3)-C(7)-N(2)-C(8)	-175.6(2)
C(13)-C(8)-N(2)-C(7)	-19.3(4)
C(9)-C(8)-N(2)-C(7)	162.2(3)
C(9)-C(8)-C(13)-C(12)	-1.5(4)
N(2)-C(8)-C(13)-C(12)	-179.9(2)
C(10)-C(11)-C(12)-C(13)	1.4(4)
C(8)-C(13)-C(12)-C(11)	-0.1(4)
C(11)-C(10)-C(9)-C(8)	-0.4(4)
C(13)-C(8)-C(9)-C(10)	1.7(4)
N(2)-C(8)-C(9)-C(10)	-179.7(2)

Symmetry transformations used to generate equivalent atoms : a, -x+1, -y+1, z+1

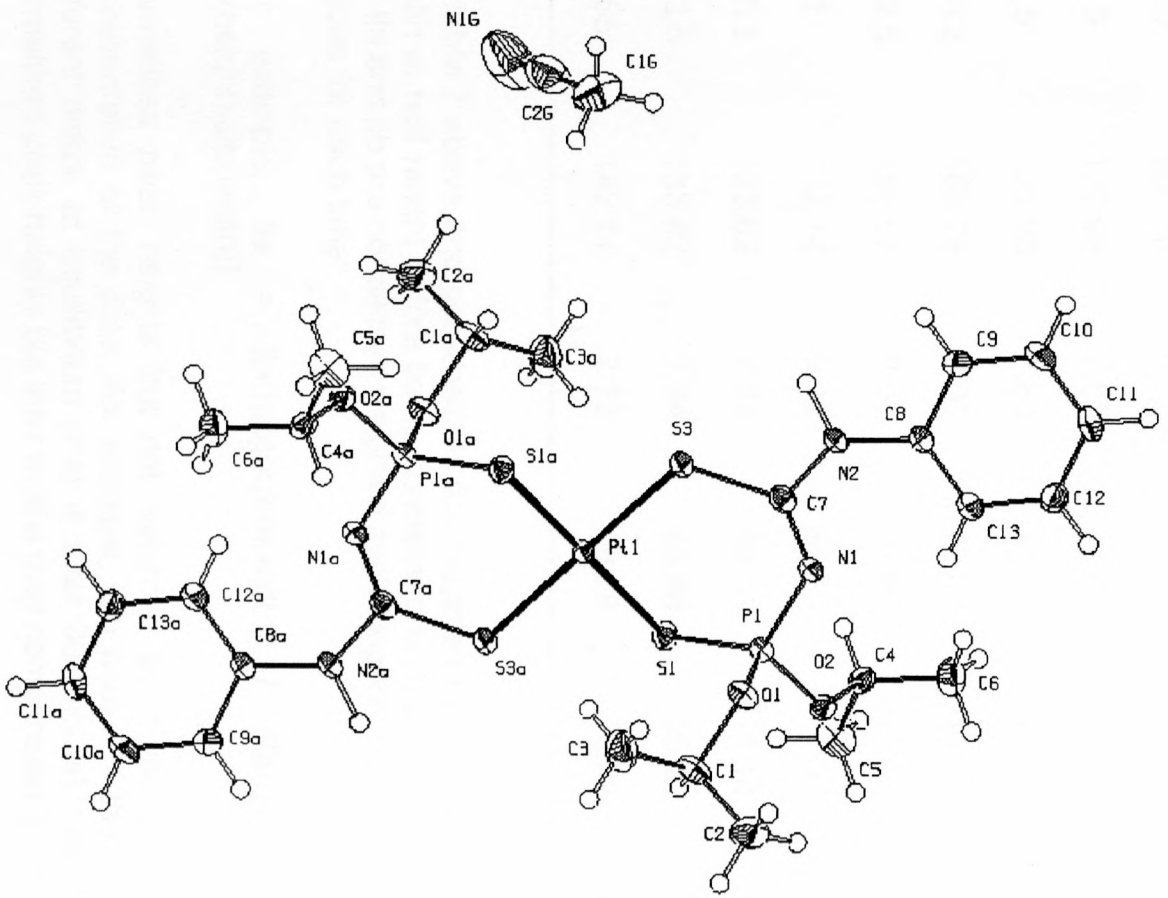
N1G
C1G
C2G
C2a
C5a
C1a
C3a
O2a
O1a
S3
C8
C9
C10
C11
C6a
C4a
P1a
S1a
N2
C7
C12
C13
Pt1
N1a
N1
C7a
C12a
C13a
P1
C8a
O2
C4
C6
N2a
S3a
S1
O1
C11a
C10a
C9a
C3
C1
C5
C2

APPENDIX 5 Calculations of the weighted ^{31}P peak heights of **IIa** and **IIb** isomers

Table 7: Variation of $^{31}P\{^{1}H\}$ NMR weighted peak heights of **IIa** and **IIb** over time in $CDCl_3$ solution.

time(hrs	IIa(height)/ (mm)	IIa(width)	IIb(height)/ (mm)	IIb(width)	**IIa**	**IIb**
0.25	106.70	10.05	0	0	100	0
26.5	122.99	7.65	11.89	13.95	85.01	14.99
46.5	122.98	7.65	11.89	13.95	85.01	14.99
165.2	156.75	8.06	73.68	11.43	60.02	39.98
332.5	158.57	8.07	91.87	11.66	54.45	45.55
501	142.14	9.12	89.80	11.91	54.81	45.19
716.5	133.82	7.84	84.91	11.16	52.54	47.46
763.5	133.82	7.84	85.86	10.40	54.03	45.97
1105	142.11	7.22	86.69	10.02	54.15	45.85

In **table 7** above, the peak heights are weighted by multiplying them by peak width at half height before being normalised to 100%. The last two columns for **IIa** and **IIb** are normalised weighted peak heights, each being calculated as follows for each time:

For example, **IIa** = **IIa**(height)x**IIa**(width) / {**IIa**(height)x**IIa**(width) + **IIb**(height)x**IIb**(width)}

Normalised peak heights but not weighted by peak widths will not be representative of the data. For example, two peaks of the same isomer at different times, at equilibrium (that is after 300 hours) may have different normalised peak heights but their widths may compensate for that difference!